Experimental and Numerical Study of Earth Pipe Cooling Performance in a Subtropical Climate



A Thesis

Submitted in the Fulfilment of the Requirements for the Degree of Doctor of Philosophy

By Shams Forruque Ahmed

School of Engineering and Technology Central Queensland University, Australia August, 2015

This thesis is dedicated to my parents, wife and our lovely son, Tahseen Ahmed

Declaration of Originality

I, Shams Forruque Ahmed, declare that the PhD thesis entitled "Experimental and Numerical Study of Earth Pipe Cooling Performance in a Subtropical Climate" has not been submitted for any publication, in whole or in part, for the award of any other scholastic degree or certificate. Except where due reference is made in the text, this thesis is my own particular work.

Shams Forruque Ahmed

Abstract

The energy crisis and environmental issues are the major obstacles for human development. There is ongoing research occurring in order to overcome these obstacles through energy saving initiatives and alternative energy options for a sustainable environment and economy. A passive air cooling strategy is seen as a viable option to save energy for all hot and humid subtropical climatic zones. An earth pipe cooling technique is one of them which utilises the earth's near constant underground temperature for cooling a space in a passive process without using any mechanical units, and thus saves energy in buildings with less or no environmental impact. It has mainly been used or studied in Europe and America and never been studied before in any subtropical climate of Australia.

The earth pipe cooling system involves long buried pipes in which intake air comes through one end and passes through buried underground pipes, then the air is cooled by the cold soil and finally the cooled air is released into the room through the outlet end. In this study, the buried pipes were aligned in horizontal and vertical trenches and thermal performance of the horizontal and vertical earth pipe cooling systems was investigated for a hot and humid climatic zone, Rockhampton, Australia using a new and novel approach with experimental and numerical modelling and parametric investigation.

The earth pipe cooling experiment was conducted on two rooms that were fabricated from two shipping containers and installed in the sustainable precinct of Central Queensland University, Rockhampton, Australia. One of the rooms was connected to a horizontal earth pipe cooling (HEPC) system and the other to a vertical earth pipe cooling (VEPC) system. Effects of air velocity, air temperature, relative humidity and soil temperature on room cooling performance were investigated through a series of experiments. An integrated thermal model was developed for both the horizontal and vertical earth pipe cooling systems using the simulation program ANSYS Fluent to compare and validate their cooling performance.

A temperature reduction of 1.13°C was found for the HEPC system while 1.87°C was obtained for the VEPC system. The temperature reductions saved an average

energy cost of \$122.82 (maximum of \$210.87) in 3 months of summer 2013-2014 using the HEPC system and \$131.84 (maximum of \$275.58) in 3 months of summer 2014-2015 using the VEPC system for a 27.23m³ room. These savings contributed to return the initial investment in 4.59 years and 4.27 years (payback period) for the HEPC and VEPC system respectively.

To measure the optimum efficiency of the earth pipe cooling system, a parametric analysis was carried out in ANSYS Fluent. The parameters affecting the earth pipe cooling performance, namely air velocity, pipe length, pipe diameter and thickness, pipe material, and pipe depth were taken into consideration for this analysis. Since the VEPC system exhibited better performance than the HEPC system, the effects of these parameters on the thermal performance of the earth pipe cooling system were examined and analysed using the VEPC model. The parametric study showed that the VEPC system is capable of reducing the room temperature by a further 3.50°C. The results and outcomes of this study provide new knowledge and information which will assist to develop optimum passive air cooling product guidelines and the product unit(s) for consumers and builders to design energy efficient buildings.

Acknowledgement

I would like to express my gratitude to almighty Allah who has provided me with the opportunity to complete this thesis. I express my deepest gratitude and sincere appreciation to my principal supervisor, Professor Masud Khan, for his willingness to accept me as a research student and give me an opportunity to do research under his supervision. I thank him for his constant guidance, encouragement, valuable suggestions and huge support at every stage of this work. I also express utmost gratitude to my associate supervisors Dr. Amanullah Maung Than Oo, Associate Professor Mohammad Golam Rasul, and Dr. Nur Md. Sayeed Hassan for their guidance, useful suggestions, constant encouragement and constructive comments throughout the study.

I gratefully acknowledge the support provided by Ergon Energy for supplying the earth pipe cooling system, measuring devices and funding the installation cost. I wish to thank the Central Queensland University, Australia for providing me an international postgraduate research award (IPRA) scholarship to support this study. I am thankful to Simon Cumming (Technical Officer, School of Engineering and Technology) and Mohammad Anwar (Lab Supervisor, School of Engineering and Technology) for their technical assistance.

Finally, I like to express my thanks and gratefulness to my family for their unmeasured sacrifices, patience, continuous inspiration and support. Especially, my deepest gratitude goes to my wife, Ashika Anjuman whose moral support, encouragement and assistance gave me the strength to complete this study.

Table of Contents

CHAPTER 1 : INTRODUCTION
1.1. Background of the Study1
1.2. Significance of the study7
1.3. Research Questions
1.4. Aims and Objectives9
1.5. Scopes and Limitations
1.6. Thesis Structure11
CHAPTER 2 : LITERATURE REVIEW
2.1. Introduction
2.2. Hot Humid Climate in Australia
2.3. Thermal Comfort and Theory
2.3.1. Thermal Comfort Factors
2.3.1.1. Environmental Factors
2.3.1.2. Personal Factors
2.3.2. Thermal comfort in Hot Humid Subtropical Climate
2.4. Passive Air Cooling Strategies
2.4.1. Natural Ventilation
2.4.2. Evaporative Cooling
2.4.3. High Thermal Mass
2.4.4. High Thermal Mass with Night Ventilation
2.4.5. Radiant Cooling
2.4.6. Wind Tower
2.4.7. Earth Pipe Cooling
2.4.7.1. Applications of Earth Pipe Cooling System
2.4.7.2. Factors Affecting Earth Pipe Cooling Performance
2.4.7.3. Heat Transfer Process in Earth Pipe Cooling System

2.4.7.4. Heat Flow within the Earth
2.5. Bioclimatic Chart for Passive Air Cooling Systems
2.6. Building Design Approach
2.6.1. Orientation of the Building
2.6.2. Materials, Colour and Texture
2.6.3. Shading and Vegetation
2.7. Thermal Modelling
2.8. Numerical Simulation in ANSYS Fluent
2.9. Conclusion
CHAPTER 3 : EXPERIMENTAL DESIGN AND MEASUREMENT
3.1. Introduction
3.2. Experimental Set Up
3.2.1. Earth Pipe Cooling Room Fitting61
3.2.2. Earth Pipe Cooling Pipe Installation
3.2.2.1. Blower (Fan) Selection
3.2.2.2. Horizontal Earth Pipe Cooling Pipe Installation
3.2.2.3. Vertical Earth Pipe Cooling Pipe Installation
3.2.2.4. Shading for Soil Covering67
3.3. Instrumentation and Data Collection
3.3.1. HOBO U23-001 Pro v2 Temperature/Relative Humidity Data Logger 72
3.3.2. HOBO U10-003 Temperature Relative Humidity Data Logger72
3.3.3. Lutron 12 Channels Temperature Recorder
3.3.4. Reed Vane Anemometer
3.3.5. G4400 BLACKBOX Fixed Power Quality Analyser75
3.4. Conclusion
CHAPTER 4 : P ERFORMANCE ANALYSIS OF HORIZONTAL EARTH PIPE
COOLING SYSTEM76

4.1. Introduction	
4.2. Soil Temperature Investigation in Summer 2013-201477	
4.3. Experimental Investigation for Horizontal Earth Pipe Cooling System	
4.4. Model Development for Horizontal Earth Pipe Cooling System	
4.4.1. Modelling Approaches	
4.4.1.1. Modelling Equations	
4.4.1.2. Geometry of the Model	
4.4.1.3. Mesh Generation	
4.4.1.4. Solver Approaches	
4.4.1.5. Grid Independence Study90	
4.4.2. Simulation Results and Discussion	
4.4.2.1. Simulation for HEPC Pipe Model	
4.4.2.2. Simulation for HEPC Room Model	
4.5. Energy Savings Using Horizontal Earth Pipe Cooling System	
4.6. Payback Period104	
4.7. Error Analysis	
4.8. Conclusion	
CHAPTER 5 : P ERFORMANCE ANALYSIS OF VERTICAL EARTH PIPE	
COOLING SYSTEM109	
5.1. Introduction	
5.2. Soil Temperature Investigation in Summer 2014-2015 110	
5.3. Experimental Investigation for Vertical Earth Pipe Cooling System	
5.4. Model Development for Vertical Earth Pipe Cooling System	
5.4.1. Modelling Approaches119	
5.4.1.1. Geometry of the Model	
5.4.1.2. Mesh Generation	
5.4.1.3. Grid Independence Study	

5.4.2. Simulation Results and Discussion	122
5.4.2.1. Simulation for VEPC Pipe Model	122
5.4.2.2. Simulation for VEPC Room Model	128
5.5. Energy Savings Using Vertical Earth Pipe Cooling System	
5.6. Payback Period	134
5.7. Error Analysis	
5.8. Performance comparison between VEPC and HEPC system	137
5.9. Conclusion	
CHAPTER 6 : PARAMETRIC STUDIES OF EARTH PIPE COOLING	SYSTEM
6.1. Introduction	
6.2. Air Velocity	140
6.3. Pipe Length	142
6.4. Pipe Diameter and Thickness	145
6.5. Pipe Material	146
6.6. Pipe Depth	148
6.7. Conclusion	149
CHAPTER 7 : CONCLUSIONS AND RECOMMENDATIONS	151
7.1. Major Findings and Conclusions	151
7.2. Recommendations	
References	
Appendices	

List of Figures

Figure 1.1: Global energy consumption (Data source: (EIA, 2013))1
Figure 1.2: World primary energy consumption by region (WEC, 2009)3
Figure 1.3: World population growth (Rosenberg, 2014)
Figure 1.4: World energy consumption for building sector (EIA, 2013)5
Figure 1.5: Total energy consumption of Australia by fuel (Data source: (DEWHA,
2008))
Figure 1.6: Total residential energy consumption by state7
Figure 1.7: Organisation of the thesis
Figure 2.1: Different weather in different climate zones in Australia (ATG, 2013). 14
Figure 2.2: Different climate zones in Australia (AG, 2013)14
Figure 2.3: Geographic position of Rockhampton on the Globe with longitude and
latitude (Google Earth, assessed on 17 March 2015)15
Figure 2.4: Climate of the subtropical zone Rockhampton, Queensland, Australia
(COT, 2014)16
Figure 2.5: Thermal comfort factors17
Figure 2.6: Natural ventilation strategy (Bhatia, 2012). (a) Cross-ventilation. (b)
Single-sided ventilation
Figure 2.7: Evaporative cooling system (REEA, 2012). (a) Direct evaporative
cooling. (b) Indirect evaporative cooling
Figure 2.8: Strategy of High thermal mass (ABSA, 2010). (a) During Day. (b)
During night25
Figure 2.9: High thermal mass with night ventilation system (CLEAR, 2013)26
Figure 2.10: Radiant cooling technology (Chenvidyakarn, 2007)27
Figure 2.11: Wind tower in a residence (DU, 2011)29
Figure 2.12: Earth pipe cooling system (Ahmed et al., 2014)
Figure 2.13: Earth pipe cooling strategies
Figure 2.14: Different types of closed loop system (MDH, 2010)
Figure 2.15: Heat conduction process through the earth pipe cooling room40
Figure 2.16: Convection through buried pipe in hot climate
Figure 2.17: Solar radiation to the ground surface
Figure 2.18: Earth structure showing Earth surface layers

Figure 2.19: Givoni's Bioclimatic chart for passive cooling strategies (Givoni, 1994).
Figure 2.20: Brown's Bioclimatic chart for passive cooling strategies (Brown, 1985).
Figure 2.21: Change in temperature and relative humidity in Queensland, Australia.
Figure 2.22: Temperature-humidity zone for Queensland, Australia
Figure 2.23: Passive cooling strategy selection
Figure 2.24: Compass card with different orientations (ECI, 2008)52
Figure 3.1: Flowchart of the general methodology applied in the study60
Figure 3.2: Experimental shed of the earth pipe cooling system61
Figure 3.3: Inside the shipping container before making an office room61
Figure 3.4: Number of layers of room walls62
Figure 3.5: Inside the shipping container after making an office room63
Figure 3.6: Air conditioning unit used in both the containers
Figure 3.7: Centrifugal in-line fan64
Figure 3.8: Excavated hole made for horizontal earth pipe cooling system65
Figure 3.9: Horizontal earth pipe cooling diagram65
Figure 3.10: Excavated hole made for vertical earth pipe cooling system
Figure 3.11: Manifold for vertical installation system
Figure 3.12: Four PVC tubes connected in a row of the manifold
Figure 3.13: Vertical earth pipe cooling diagram67
Figure 3.14: Plants covered the soil and buried pipes67
Figure 3.15: Auto irrigation system installed to maintain the plants
Figure 3.16: Two containers installed at same site in the sustainable precinct68
Figure 3.17: Excavated hole made for installing the buried pipes
Figure 3.18: Manifold fitted into the ground
Figure 3.19: PVC tubes set buried underground for connecting with the manifolds.69
Figure 3.20: Soil distributed to cover the PVC buried tubes
Figure 3.21: Small tress and grasses planted into the soil, which covered the PVC
buried tubes
Figure 3.22: Pipe outlet (inlet to the room)70
Figure 3.23: HOBO Pro v2 connected with optic base station (Onset, 2015b)72
Figure 3.24: HOBO U10-003 data logger (Onset, 2015a)73

Figure 3.25: Lutron 12 channels temperature recorder (Lutron, 2011)
Figure 3.26: Vane Anemometer data logger (MicroDAQ, 2015)74
Figure 3.27: Power quality analyser Blackbox
Figure 4.1: Hourly average soil temperature distribution during summer 2013-2014.
Figure 4.2: Temperature distribution of soil at 0.6 m depth and outdoor air78
Figure 4.3: Ground surface temperatures of grass covered soil and bare soil
Figure 4.4: Temperature fields in the horizontal earth pipe cooling and standard
room close to the wall, and outdoor
Figure 4.5: Relative humidity measured in the HEPC room, standard room and
outdoor
Figure 4.6: Temperature field at pipe inlet and outlet
Figure 4.7: Temperature profile at pipe inlet and outlet during hot pick hours
Figure 4.8: Trend of air velocity at pipe inlet and outlet
Figure 4.9: Mesh for HEPC pipe model. (a) Showing inlet. (b) Showing outlet (inlet
to the room)
Figure 4.10: Mesh pattern for HEPC room model
Figure 4.11: Pressure-based coupled algorithm
Figure 4.12: Temperature fields at the outlet of pipe model for different mesh size.91
Figure 4.13: Temperature fields at different heights of HEPC room for 3 mesh sizes.
Figure 4.14: Temperature fields throughout the pipes in HEPC system. (a)
Temperature magnitude. (b) Temperature vector
Figure 4.15: Temperature fields at the pipe inlet in HEPC system. (a) Temperature
magnitude. (b) Temperature vector
Figure 4.16: Temperature fields at the pipe outlet in HEPC system. (a) Temperature
magnitude. (b) Temperature vector
Figure 4.17: Velocity fields throughout the pipes in HEPC system. (a) Velocity
magnitude. (b) Velocity vector
Figure 4.18: Velocity fields at the pipe inlet in HEPC system. (a) Velocity magnitude.
(b) Velocity vector
Figure 4.19: Velocity fields at the pipe outlet in HEPC system. (a) Velocity
magnitude. (b) Velocity vector
Figure 4.20: Numerical data plotted against experimental data at the pipe outlet98

Figure 4.21: Temperature profiles in horizontal earth pipe cooling room (a)
Temperature magnitude. (b) Temperature vector
Figure 4.22: Velocity profiles in horizontal earth pipe cooling room. (a) Velocity
magnitude. (b) Velocity vector
Figure 4.23: Numerical data plotted against experimental data along middle of the
HEPC room
Figure 4.24: Energy consumption of HEPC and standard room102
Figure 4.25: Average savings cost in each month throughout the year using VEPC
system106
Figure 5.1: Soil temperature distribution during summer 2014-2015
Figure 5.2: Temperature distribution of soil at 1.10 m depth and outdoor air111
Figure 5.3: Temperature fields of the ground surface with grass covered and bare soil
during summer 2014-2015112
Figure 5.4: Temperature fields in the vertical earth pipe cooling and standard room
close to the wall, and outdoor during summer 2014-2015114
Figure 5.5: Relative humidity measured in the vertical earth pipe cooling, standard
room and outdoor115
Figure 5.6: Temperature field at pipe inlet and outlet in VEPC system
Figure 5.7: Temperature profile at pipe outlet during 10:00 am-5:00 pm in VEPC
system117
Figure 5.8: Velocity field at pipe inlet and outlet in VEPC system
Figure 5.9: Mesh for VEPC pipe model. (a) Showing inlet. (b) Showing outlet (inlet
to the room)
Figure 5.10: Mesh pattern for VEPC room model
Figure 5.11: Temperature fields at the outlet of pipe model for different mesh size.
Figure 5.12: Temperature field at different heights of VEPC room model for
different mesh size
Figure 5.13: Temperature fields throughout the pipes in VEPC system. (a)
Temperature magnitude. (b) Temperature velocity
Figure 5.14: Temperature fields at the pipe inlet in VEPC system. (a) Temperature
magnitude. (b) Temperature velocity124
Figure 5.15: Temperature fields at the pipe outlet in VEPC system. (a) Temperature
magnitude. (b) Temperature velocity

Figure 5.16: Velocity fields throughout the pipes in VEPC system. (a) Velocity
magnitude. (b) Velocity vector
Figure 5.17: Velocity fields at the pipe inlet in VEPC system. (a) Velocity magnitude.
(b) Velocity vector
Figure 5.18: Velocity fields at the pipe outlet in VEPC system. (a) Velocity
magnitude. (b) Velocity vector
Figure 5.19: Numerical data plotted against experimental data at the pipe outlet128
Figure 5.20: Temperature profile in VEPC room. (a) Temperature magnitude. (b)
Temperature vector
Figure 5.21: Velocity profile in VEPC room. (a) Velocity magnitude. (b) Velocity
vector
Figure 5.22: Numerical data plotted against experimental data along middle of the
VEPC room
Figure 5.23: Energy consumption of VEPC and standard room132
Figure 5.24: Average savings cost in each month throughout the year using VEPC
system
Figure 5.25: Air temperature in VEPC room, HEPC room and outside the room137
Figure 5.26: Relative humidity in HEPC room, VEPC room and outside the room.
Figure 6.1: Parametric study using four different air velocities141
Figure 6.2: Parametric study using four different pipe lengths142
Figure 6.3: Parametric study for different pipe sizes
Figure 6.4: Parametric study for various pipe materials
Figure 6.5: Parametric study for different depths

List of Tables

Table 1.1: Global energy consumption (quadrillion Btu) (EIA, 2013)2
Table 1.2: Regional energy use and growth 1990-2008 (Wikipedia, 2015)4
Table 2.1: Human reactions at different air speeds (Szokolay, 2008)
Table 2.2: Amount of energy released for different activities (Koenigsberger, 1975).
Table 2.3: Comparison between closed and open loop systems (Johnston, 2011)31
Table 2.4: List of earth pipe cooling studies applied to different climatic zones33
Table 2.5: List of earth pipe cooling optimal design applied to different climatic
zones
Table 2.6: Earth pipe cooling performance for different climatic zones. 34
Table 2.7: Effective orientation of a building facade (Ovacen, 2014)
Table 3.1: List of measured data and data logger locations71
Table 3.2: Measuring instruments used to log data in the experiment
Table 4.1: Air temperature and relative humidity in the HEPC and standard room82
Table 4.2: Different grid sizes for HEPC model
Table 4.3: Parameters used in boundary conditions of the HEPC pipe model93
Table 4.4: Comparison of temperature between experimental and numerical
(simulation) results at pipe outlet
(simulation) results at pipe outlet
Table 4.5: Parameters used in boundary conditions of the room model
Table 4.5: Parameters used in boundary conditions of the room model
Table 4.5: Parameters used in boundary conditions of the room model
Table 4.5: Parameters used in boundary conditions of the room model
Table 4.5: Parameters used in boundary conditions of the room model
Table 4.5: Parameters used in boundary conditions of the room model
Table 4.5: Parameters used in boundary conditions of the room model99Table 4.6: Comparison in room temperature between experimental and simulation.01(numerical) results of room model01Table 4.7: Hourly energy savings using horizontal earth pipe cooling technology.103Table 4.8: Energy costs for residential customers (EE, 2014)103Table 4.9: Average energy cost savings using horizontal earth pipe cooling system.01(costs in Australian Dollars (AUD))01
Table 4.5: Parameters used in boundary conditions of the room model99Table 4.6: Comparison in room temperature between experimental and simulation.101(numerical) results of room model101Table 4.7: Hourly energy savings using horizontal earth pipe cooling technology.103Table 4.8: Energy costs for residential customers (EE, 2014)103Table 4.9: Average energy cost savings using horizontal earth pipe cooling system.104Table 4.10: Predicted average energy cost savings during autumn, winter, and spring
Table 4.5: Parameters used in boundary conditions of the room model
Table 4.5: Parameters used in boundary conditions of the room model
Table 4.5: Parameters used in boundary conditions of the room model
Table 4.5: Parameters used in boundary conditions of the room model

Table 5.3: Parameters used in boundary conditions of the VEPC pipe model 123
Table 5.4: Comparison in temperature between experimental and numerical
(simulation) results at pipe outlet127
Table 5.5: Parameters used in boundary conditions of the VEPC room model128
Table 5.6: Comparison in room temperature between experimental and numerical
results of the room model130
Table 5.7: Hourly energy savings using vertical earth pipe cooling technology132
Table 5.8: Energy costs for residential customers. 133
Table 5.9: Energy cost savings using vertical earth pipe cooling system (costs in
Australian Dollars (AUD))
Table 5.10: Predicted average energy cost savings during autumn, winter, and spring
using the known savings of summer for VEPC
Table 5.11: Parameters used in the VEPC experiment and their mean value, probable
error, and the error in percentage136
Table 5.12: Air temperature and relative humidity in VEPC and HEPC room138
Table 6.1: Outlet temperature for different pipe lengths
Table 6.2: Different pipe sizes in terms of pipe diameter, area and thickness145
Table 6.3: Thermal conductivity of different pipe materials. 146
Table 6.4: Outlet temperature ranges for various materials. 147

List of Notations

Symbol	Definition (Unit)
ρ	Air density (kg m ⁻³)
q	Air flow rate $(m^3 s^{-1})$
\dot{m}_a	Air mass flow rate (kg s ⁻¹)
T_i	Air temperature at the pipe inlet (K)
T_o	Air temperature at the pipe outlet (K)
V	Air velocity (m s ⁻¹)
Α	Area of a region (m ²)
CO_2	Carbon Dioxide
$m{J}_{j}$	Component of diffusion flux (m ⁻² s ⁻¹)
X_i	Component of length (m)
$C = \tanh \left \frac{u_1}{u_1} \right $	Constant, U_1 and U_2 are the velocity components parallel and
$C_{3\varepsilon} = \tanh \left \frac{u_1}{u_2} \right $	perpendicular to the gravitational vector respectively
$C_{1arepsilon}$, $C_{2arepsilon}$	Constants
Y_{M}	Contribution of the fluctuating dilatation in compressible turbulence to
1 _M	the overall dissipation rate (kg m ⁻¹ s ⁻²)
D	Diameter of the pipe (m)
ΔT	Difference in temperature (K)
i, j, k (=1, 2, 3)	Direction vector index
Δx	Distance of heat transfer between two surfaces(m)
μ	Dynamic viscosity of air (kg m ⁻¹ s ⁻¹)
$k_{\scriptscriptstyle e\!f\!f}$	Effective conductivity (W m ⁻¹ K ⁻¹)
$P_{e\!f}$	Effective fan power (W)
\dot{W}_{in}	Energy input rate into the earth pipe cooling system (J)
h	Enthalpy (J kg ⁻¹)
η_o	Fan efficiency
u_i, u_j	Fluid velocity components (m s ⁻¹)
G_b, G_k	Generation of turbulence kinetic energy due to buoyancy and mean
U Ż K	velocity gradients respectively (kg m ⁻¹ s ⁻²)

R^2	Goodness of the fit of regression
Q	Heat flow rate (J/s)
$\nabla \cdot \left(k_{eff} \nabla T \right)$ $\nabla \cdot \left(\stackrel{=}{\tau_{eff}} \cdot \vec{v} \right)$	Heat transfer due to convection
$\nabla \left(\begin{bmatrix} = \\ \tau_{eff} . \vec{v} \end{bmatrix} \right)$	Heat transfer due to viscous diffusion
k	Kinetic energy for turbulent flow (m ² s ⁻²)
l	Length of the pipe (m)
m	Mass of a substance (kg)
$\frac{1}{x}$	Mean value of the measurements
$\upsilon = \mu / \rho$	Molecular kinetic viscosity of the fluid $(m^2 s^{-1})$
Ν	Number of observations (measurements)
р	Pressure (Pa)
ΔP_t	Pressure loss (Pa)
γ	Probable error
R_{e}	Reynolds number
$\nabla \cdot \left(\sum_{j} h_{j} \vec{J}_{j} \right)$	Species diffusion
$ abla . \left(\sum_{j} h_{j} \vec{J}_{j} \right)$ c_{p}	Species diffusion Specific heat capacity (J/kg-K)
	•
c _p	Specific heat capacity (J/kg-K)
$c_p \sigma$	Specific heat capacity (J/kg-K) Standard deviation
c_p σ T	Specific heat capacity (J/kg-K) Standard deviation Temperature (K)
c_p σ T T_2	Specific heat capacity (J/kg-K) Standard deviation Temperature (K) Temperature of a cold surface (K)
c_p σ T T_2 T_1	Specific heat capacity (J/kg-K) Standard deviation Temperature (K) Temperature of a cold surface (K) Temperature of a hot surface (K)
c_p σ T T_2 T_1 k	Specific heat capacity (J/kg-K) Standard deviation Temperature (K) Temperature of a cold surface (K) Temperature of a hot surface (K) Thermal conductivity (W/m-K)
c_p σ T T_2 T_1 k k_t	Specific heat capacity (J/kg-K) Standard deviation Temperature (K) Temperature of a cold surface (K) Temperature of a hot surface (K) Thermal conductivity (W/m-K) Thermal conductivity for turbulent flow
c_p σ T T_2 T_1 k k_t t	Specific heat capacity (J/kg-K) Standard deviation Temperature (K) Temperature of a cold surface (K) Temperature of a hot surface (K) Thermal conductivity (W/m-K) Thermal conductivity for turbulent flow Time (s)
c_p σ T T_2 T_1 k k_t t S_h	Specific heat capacity (J/kg-K) Standard deviation Temperature (K) Temperature of a cold surface (K) Temperature of a hot surface (K) Thermal conductivity (W/m-K) Thermal conductivity for turbulent flow Time (s) Total entropy (JK ⁻¹)
c_p σ T T_2 T_1 k k_t t S_h ε	Specific heat capacity (J/kg-K) Standard deviation Temperature (K) Temperature of a cold surface (K) Temperature of a hot surface (K) Thermal conductivity (W/m-K) Thermal conductivity for turbulent flow Time (s) Total entropy (JK ⁻¹) Turbulent energy dissipation rate (m ² s ⁻³)

List of Acronyms

ABSA	Association of Building Sustainability Assessors
AC	Air Conditioner
ACT	Australian Capital Territory
AG	Australian Government
AGO	Australian Greenhouse Office
ASHRAE	American Society of Heating, Refrigerating and Air-Conditioning Engineers
ATG	Australia Travel Guide
BAS	Body and Soul
BAU	Business-as-usual
BOM	Bureau of Meteorology
BP	British Petroleum
BPEO	British Petroleum Energy Outlook
BREE	Bureau of Resources and Energy Economics
BRESCU	Building Research Establishment, Sustainable Construction Unit
Btu	British thermal unit
CAD	Computer-aided Design
CBD	Commercial Building Disclosure
CCA	Climate Change Authority
CFD	Computational Fluid Dynamics
CIBSE	Chartered Institution of Building Services Engineers
CLEAR	Comfortable Low Energy Architecture
COAG	Council of Australian Governments
COP	Coefficient of Performance
COT	Climate and Temperature
COV	City of Vancouver
CPRS	Carbon Pollution Reduction Scheme
CSIRO	Commonwealth Scientific and Industrial Research Organization
СТ	Current Transformer
DEWHA	Department of the Environment, Water, Heritage and the Arts
DRET	Department of Resources, Energy and Tourism
DTI	Department of Trade and Industry
DU	Democratic Underground
EA	Energy in Australia
EAHE	Earth-to-Air Heat Exchanger

ECI	European Copper Institute
EER	Energy Efficiency Ratio
EIA	Energy Information Administration
EPA	Environmental Protection Agency
EPAHE	Earth-Pipe-Air Heat Exchanger
ETHE	Earth Tube Heat Exchanger
EU	European Union
GCHP	Ground-Coupled Heat Pump System
GHE	Ground Heat Exchanger
GOI	Government of Ireland
GWh	Giga Watt hour
HEPC	Horizontal Earth Pipe Cooling
HKGBTN	Hong Kong Green Building Technology Net
HVAC	Heating, Ventilating and Air Conditioning
IEA	International Energy Agency
IEO	International Energy Outlook
IMF	International Monetary Fund
kt	Kilo Tonnes
KWh	Kilowatt hour
LCD	Liquid-Crystal Display
LPG	Liquefied Petroleum Gas
MDH	Minnesota Department of Health
MFGSHP	Multi-function Ground Source Heat Pump
MW	Mineral Wool
NSW	New South Wales
NT	Northern Territory
NVP	Night Ventilation with PCM Packed Bed Storage
OECD	Organization for Economic Cooperation and Development
PAC	Passive Air Cooling
PCM	Phase Change Material
PDEC	Passive Downdraught Evaporative Cooling
PJ	Petajoules
PT	Potential Transformer
PVC	Polyvinyl Chloride
QLD	Queensland
REEA	Regional Energy and Environmental Agency

~ .	~
SA	South Australia
SE	Solar & Electrics
SEAV	Sustainable Energy Authority Victoria
SHESS	Soil Heat Exchanger-Storage System
SOx	Sulphur Oxide
SST	Shear Stress Transport
TAS	Tasmania
TECO	Taipei Economic and Cultural Office
TET	The Engineering Toolbox
TWh	Terawatt-hour
UK	United Kingdom
UNEP	United Nations Environment Programme
UOI	University of Iowa
US	United States
USA	United States of America
VD	Value of Dissent
VEPC	Vertical Earth Pipe Cooling
VIC	Victoria
WA	Western Australia
WEC	World Energy Consumption

Copyright Statement

This thesis may be distributed or copied for personal study and use; however, no part of this thesis or the information contained therein may be included in or referred to in any publication without the Author's prior permission and/or without any reference being fully acknowledged.

(Shams Forruque Ahmed) August 31, 2015

List of Publications with Author's Contribution

Journal Articles (Refereed)

- Ahmed, SF, Khan, MMK, Amanullah, MTO & Rasul, MG 2014, Selection of Suitable Passive Cooling Strategy for a Subtropical Climate, *International Journal of Mechanical and Materials Engineering*, 9(1): 1-11.
 - I prepared the draft manuscript after collecting and analysing a large set of data. Professor Masud Khan assisted me in the manuscript concept and write-up, provided technical feedback on data analysis, and reviewed the manuscript. A/Professor Amanullah Maung Than Oo and A/Professor Mohammad Rasul contributed to and/or helped in the manuscript concept, write up and revision.

The following manuscripts no. 2 to 10 were published from the work of my PhD project which were supervised by Professor Masud Khan as the principal supervisor and A/Professor Amanullah Maung Than Oo, A/Professor Mohammad Rasul and Dr. Nur Hassan as the associate supervisors. These articles were prepared at various stages of the project based on the results/outcomes obtained during those times. The supervisory team met regularly to provide academic advice and feedback to ensure successful completion of the project.

- Ahmed, SF, Khan, MMK, Rasul, MG, Amanullah, MTO & Hassan, NMS 2014, Comparison of Earth Pipe Cooling Systems with Two Different Piping Systems, *Energy Procedia*, 61:1897-1901.
 - I collected the experimental data and analysed those to develop the thermal model using the simulation program ANSYS Fluent15.0, and prepared the manuscript. Professor Masud Khan provided guidance, feedback, and reviewed the manuscript. A/Professor Mohammad Rasul reviewed the manuscript, and made valuable comments and recommendations. A/Professor Amanullah Maung Than Oo guided me to write the manuscript. Dr. Nur Hassan helped me in setting up the model and to set up the boundary conditions of the thermal model.

- Ahmed, SF, Khan, MMK, Amanullah, MTO, Rasul, MG & Hassan, NMS 2015, Performance assessment of earth pipe cooling system for low energy buildings in a subtropical climate, *Energy Conversion and Management*, 106: 815-825.
 - The entire manuscript was written by me after analysing the experimental and numerical results. Professor Masud Khan provided the idea and concept of this work, feedback and reviewed the manuscript. A/Professor Amanullah Maung Than Oo helped me by providing guidance and concepts. A/Professor Mohammad Rasul contributed to write the results and discussion section of the manuscript, and reviewed the manuscript. Dr. Nur Hassan provided valuable feedback and assisted me in getting the simulation results.
- Ahmed, SF, Khan, MMK, Amanullah, MTO, Rasul, MG & Hassan, NMS, Vertical earth pipe cooling performance in low energy buildings in summer, *Applied Energy*, Submitted on 20 June 2015, Under review.
 - I developed the numerical model, compared the experimental and numerical data, validated the model, and wrote the manuscript. Professor Masud Khan guided me to write the manuscript, provided feedback, and reviewed the manuscript. A/Professor Amanullah Maung Than Oo provided guidance in preparing the manuscript. A/Professor Mohammad Rasul helped me to analyse the experimental data, and reviewed the manuscript. Dr. Nur Hassan directed me to set up numerical modelling.

Book Chapters (Refereed)

- Ahmed, SF, Khan, MMK, Amanullah, MTO, Rasul, MG & Hassan, NMS 2015, Numerical Modelling of Vertical Earth Pipe Cooling System for Hot and Humid Subtropical Climate, In: *Progress in Clean Energy, Volume II: Novel Systems and Applications*, 1st ed. Cham: Springer International Publishing, pp. 277-299.
 - Professor Masud Khan provided me the concept to write the manuscript, technical feedbacks, and gave revision on the manuscript. A/Professor Amanullah Maung Than Oo provided feedback on the manuscript. A/Professor Mohammad Rasul contributed to data analysis, and reviewed the manuscript. Dr. Nur Hassan reviewed the numerical results. I was responsible for the remainder of the work including the manuscript write up.

- Ahmed, SF, Khan, MMK, Amanullah, MTO, Rasul, MG & Hassan, NMS 2015, Performance evaluation of hybrid earth pipe cooling with horizontal piping system, In: *Thermal Modelling for Energy Efficiency Applications*, San Diego: Elsevier Science Publishing Co Inc, pp. 1-30.
 - I developed the thermal model in ANSYS Fluent15.0 by analysing the experimental and numerical data, and prepared the manuscript. Professor Masud Khan provided feedback, made valuable comments, and reviewed the manuscript. A/Professor Amanullah Maung Than Oo contributed to the manuscript by providing feedback. A/Professor Mohammad Rasul assisted me to interpret and analyse data, and reviewed the manuscript. Dr. Nur Hassan guided me for the numerical modelling set up.

Conference papers (Referred)

- Ahmed, SF, Khan, MMK, Amanullah, MTO, Rasul, MG & Hassan, NMS 2013, Thermal Performance Analysis of Earth Pipe Cooling System for Subtropical Climate, Proceedings of the 12th International Conference on Sustainable Energy Technologies (SET2013), 26-29 August, Hong Kong, China, pp. 1795-1803.
 - I set the data logger for measuring the experimental data, developed the numerical model and prepared the manuscript. Professor Masud Khan contributed to the manuscript write up, provided guidance, and reviewed the manuscript. A/Professor Amanullah Maung Than Oo made valuable suggestions and provided feedback on the manuscript. A/Professor Mohammad Rasul reviewed the manuscript. Dr. Nur Hassan gave the concept for validating the numerical model.
- Ahmed, SF, Khan, MMK, Amanullah, MTO, Rasul, MG & Hassan, NMS 2014, Performance analysis of vertical earth pipe cooling system for subtropical climate, Proceedings of the International Conference on Clean Energy, 8-12 June, Istanbul, Turkey, pp. 691-700.
 - I analysed the experimental and numerical results, and wrote the manuscript by developing the thermal model. Professor Masud Khan made valuable comments and recommendations, reviewed the manuscript, and provided feedback. A/Professor Amanullah Maung Than Oo guided me to write the manuscript. A/Professor Mohammad Rasul reviewed the manuscript and

provided feedback. Dr. Nur Hassan contributed to select the appropriate turbulence model.

- Ahmed, SF, Khan, MMK, Amanullah, MTO, Rasul, MG & Hassan, NMS 2014, Numerical Modelling of Hybrid Vertical Earth Pipe Cooling System, Proceedings of the 19th Australasian Fluid Mechanics Conference, 8-11 December, Melbourne, Australia, pp. 336-338.
 - Professor Masud Khan guided me to write the manuscript, and reviewed the manuscript. A/Professor Amanullah Maung Than Oo made comments and recommendations on the manuscript. A/Professor Mohammad Rasul contributed to the manuscript review. Dr. Nur Hassan helped me to extract the simulation results, and I completed the remainder of the work.
- 10. Ahmed, SF, Khan, MMK, Amanullah, MTO, Rasul, MG & Hassan, NMS 2015, Integrated model of horizontal earth pipe cooling system for a hot humid climate, Proceedings of the 7th International Exergy, Energy and Environment Symposium, 27-30 April, Valenciennes, France.
 - I developed a numerical model by integrating two computational Fluid Dynamics (CFD) models, and prepared the manuscript. Professor Masud Khan assisted to write the manuscript, provided idea for the integrated model and feedback, made valuable comments, and reviewed the manuscript. A/Professor Amanullah Maung Than Oo provided guidance to improve the manuscript. A/Professor Mohammad Rasul reviewed the manuscript, and Dr. Nur Hassan reviewed the numerical parts of the work.

CHAPTER 1 : INTRODUCTION

1.1. Background of the Study

Energy issues have been the key elements for conceptual and strategic decisions on sustainable development worldwide. Energy consumption in different forms is steadily rising all over the world. The world energy use is projected to rise from 524 quadrillion Btu (552.85 exajoule) in 2010 to 630 quadrillion Btu (664.69 exajoule) in 2020 and 820 quadrillion Btu (865.15 exajoule) in 2040 as shown in Figure 1.1 (EIA, 2013). This projection indicates that energy usage will increase by around 56% over 30 years. During this period, more than 85% of this growing energy demand will occur within the developing nations outside the Organization for Economic Cooperation and Development (non-OECD nations), where demand is driven by strong long-term economic growth and increasing populations (EIA, 2013).

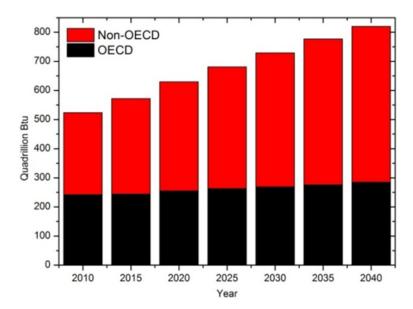


Figure 1.1: Global energy consumption (Data source: (EIA, 2013))

In the non-OECD nations, energy use will increase by 85%, a lot more than an 18% increase for the OECD economies (SE, 2013). Worldwide energy consumption by region over the period of 2010-2040 is summarised in Table 1.1.

Region	2010	2015	2020	2025	2030	2035	2040	Average
								annual change,
								2010-2040 (%)
OECD	242	244	255	263	269	276	285	0.5
Americas	120	121	126	130	133	137	144	0.6
Europe	82	82	85	89	91	93	95	0.6
Asia	40	41	43	44	45	46	46	0.5
Non-OECD	282	328	375	418	460	501	535	2.2
Europe and Eurasia	47	50	53	57	61	65	67	1.2
Asia	159	194	230	262	290	317	337	2.5
Middle East	28	33	37	39	43	46	49	1.9
Africa	19	20	22	24	27	31	35	2.1
Central and South America	29	31	33	35	39	42	47	1.6
World	524	572	630	680	729	777	820	1.5

Table 1.1: Global energy consumption (quadrillion Btu) (EIA, 2013).

India and China will keep on leading both the energy demand and world economic growth. Energy use in both the countries as part of the total energy consumption has increased substantially. They accounted together for around 10% of the total global energy consumption in 1990 and about 24% in 2010 (EIA, 2013). Their combined energy consumption is predicted to be 34% of the projected world energy use in 2040. Moreover, China which turned into the biggest energy consumer of the world recently is expected to consume more than twice the amount that the United States (previous largest energy consumer) will consume in 2040 as shown in Figure 1.2.

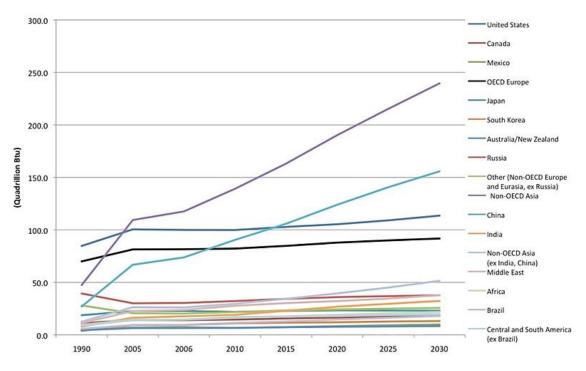


Figure 1.2: World primary energy consumption by region (WEC, 2009).

Higher income and population growth are the main reasons behind the significant energy demand. It is seen from Figure 1.2 that the countries with improved income and higher population will consume more energy. World population is estimated to be 8.3 billion by 2030, which indicates that more energy will be required for an additional 1.3 billion people. Moreover, the world income is expected to double by 2030 compared to the 2011 level (BPEO, 2012) and this will directly impact on more energy usage. Urban areas have expanded in size all around the globe throughout recent decades (Omer, 2008) and around half of the world's population (but just 7.6% in more developed nations) are urban residents (Givoni, 1998, Omer, 2012). The world population has expanded rapidly from 1900 to 2010, as shown in Figure 1.3.

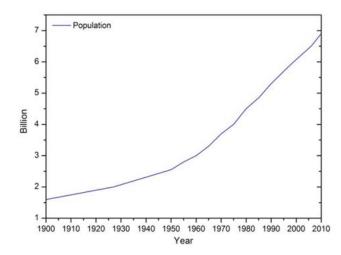


Figure 1.3: World population growth (Rosenberg, 2014).

It is evident from Figure 1.3 that from year 1950, population growth has been much faster than for previous years. Simultaneously, energy consumption started to rise rapidly because of the population growth. The average energy consumption per person increased by 10% from 1990 to 2008, whereas the world population increased by 27% (IEA, 2012). During this period, energy usage has increased by 170% in the Middle East, by 146% in China, by 91% in India, by 70% in Africa, by 66% in Latin America, by 20% in the USA, by 7% in the EU-27 block, and by 39% overall in the world (Wikipedia, 2015), as shown in Table 1.2.

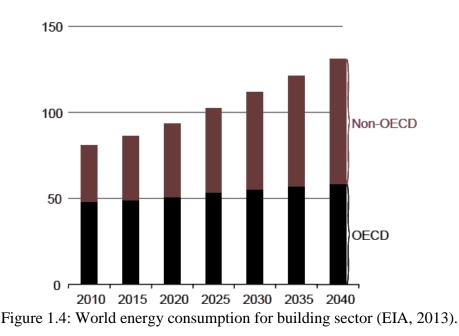
Region	kWh/capita			Рори	ulation (r	nillion)	Energy use (1000 TWh)		
	1990	2008	Growth	1990	2008	Growth	1990	2008	Growth
USA	89,021	87,216	-2%	250	305	22%	22.3	26.6	20%
EU-27	40,240	40,821	1%	473	499	5%	19.0	20.4	7%
Middle East	19,422	34,774	79%	132	199	51%	2.6	6.9	170%
China	8,839	18,608	111%	1,141	1,333	17%	10.1	24.8	146%
Latin America	11,281	14,421	28%	355	462	30%	4.0	6.7	66%
Africa	7,094	7,792	10%	634	984	55%	4.5	7.7	70%
India	4,419	6,280	42%	850	1,140	34%	3.8	7.2	91%
Others*	25,217	23,871	nd	1,430	1,766	23%	36.1	42.2	17%
The World	19,422	21,283	10%	5,265	6,688	27%	102.3	142.3	39%

Table 1.2: Regional energy use and growth 1990-2008 (Wikipedia, 2015).

Source: IEA/OECD, Population OECD/World Bank.

*Others: Countries in Asia and Australia

Almost all of the world population uses this energy at some point for their own needs. The building sector consumes more than 40% of global energy use (UNEP, 2009) and 40-50% of the total delivered energy in the UK and USA (DTI, 2003, EPA, 2007). Ventilating, heating and cooling together account for 70% of total energy consumption (BRESCU, 2000). Total world delivered energy demand for buildings shown in Figure 1.4 will increase from 81 quadrillion Btu (85.46 exajoule) in 2010 to about 131 quadrillion Btu (138.21 exajoule) in 2040 at an average yearly growth rate of 1.6% (EIA, 2013).



The energy consumption for the Australian residential sector has also increased, from around 299 petajoules (PJ) in 1990 to about 402 PJ in 2008, and is projected to increase to 467 PJ by 2020 (DEWHA, 2008). This signifies the increased energy consumption of 56% in this sector over this period from 1990 to 2020. The contribution of electricity to this residential energy consumption is predicted to increase from 46% of the total energy use in 1990 to 53% in 2020 as shown in Figure 1.5. Gas consumption is also predicted to increase from 30% in 1990 to 37% in 2020, whereas use of wood is expected to decrease from 21% to 8% over the same period (DEWHA, 2008). LPG (liquefied petroleum gas) use in the residential sector has remained constant and is estimated to contribute 2% in 2020.

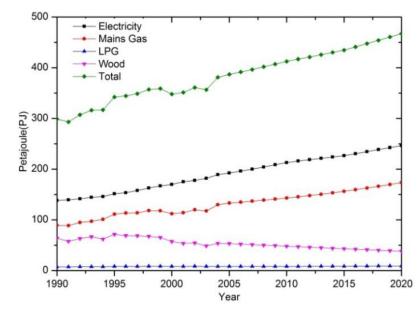


Figure 1.5: Total energy consumption of Australia by fuel (Data source: (DEWHA, 2008)).

Residential electricity consumption grew 1.5% per annum at a compound rate between 2008 and 2011 (CCA, 2013). Energy consumption in this sector has been less responsive to electricity price increases since 2008. Per capita residential energy consumption was nearly static between 2003 and 2012, suggesting that higher consumption was due to population growth rather than higher spending per capita. This residential energy consumption varies state to state in Australia. Victoria, New South Wales (NSW) and Queensland show steady growth of residential energy consumption over the period of 1990-2020, as shown in Figure 1.6. This energy consumption is primarily due to extensive use of gas for space heating and cooling.

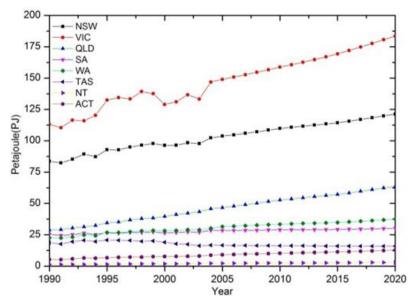


Figure 1.6: Total residential energy consumption by state (Data source: (DEWHA, 2008)).

1.2. Significance of the study

Australian buildings use 38% of their total energy consumption on cooling and heating purposes (Origin, 2013). This energy usage will be increased in upcoming years as the average temperature of Australia has increased by 0.9°C since 1950 (Shahiduzzaman, 2012). Projections from the Commonwealth Scientific and Industrial Research Organization (CSIRO) show an increase of average temperature by a further 0.6-1.5°C by 2030 and 1-5.0°C by 2070, depending on the levels of global emissions (CSIRO, 2009). According to this projection, more energy will be required for surviving and achieving thermal comfort.

Australia is the eighteenth leading energy consumer in the world and fourteenth on a per person basis (DRET, 2012). The energy demand in Australia is predicted to increase rapidly in future. Domestic energy consumption growth was at a slower rate than the energy generation over the past 20 years. Net energy consumption of Australia was increased by 1.8% average rate per annum over the 10 years from 1999-2000 to 2009-2010 (DRET, 2012). It is therefore essential to save energy in the Australian residential sector as most of the energy is used in this sector.

There has been an ongoing interest in improving building energy efficiency because of ecological concerns and the high cost of energy in recent years (Sadineni et al., 2011). Consumers are therefore looking for energy efficient and environmentallyfriendly building designs. Energy efficient buildings can be developed by employing either active or passive strategies. Passive air cooling (PAC) is one of the passive strategies which can assist in reducing energy consumption in buildings. It is energy efficient and less expensive than any other conventional cooling techniques.

Passive air cooling is an approach of cooling an interior space in a passive process without using any mechanical units such as fan, air conditioning unit, etc. Earth pipe cooling is one of these approaches that involve long buried pipes in which intake air comes through one end and passes through the buried pipes, and thus gets cooled by the soil. This cooled air is then blown out of the other end into a space. The buried piping layout may be in horizontal, vertical, slinky coil, etc.

The earth pipe cooling system utilises soil as a heat sink, where ambient air transfers heat to the earth through convection via the buried pipes. It is the least expensive means of cooling a room with the lowest environmental impact. The earth pipe cooling system offers numerous additional advantages such as protection from dust, noise, storms and radiation, partial air infiltration, etc. because of the usage of underground spaces. It also offers a great potential for energy saving for a hot and humid climate, like Northern Queensland, since it can supplement the air conditioning load of many homes with virtually no negative environmental impact.

The energy savings potential of the earth pipe cooling system has been proven by several researches. The cooling performance of the system is mainly affected by the parameters, namely pipe length, pipe radius and thickness, buried pipe depth and air flow rate. To assess the influence of these parameters, a study was carried out to investigate the earth pipe cooling performance under different conditions (Lee and Strand, 2008). The buried underground pipe depth and the pipe length turned out to influence the earth tube cooling rate, while air flow rate and pipe radius mainly affect the inlet air temperature entering the space.

In some cases, the earth pipe cooling system is assisted with a heat pump as a heat exchanger located within the buried pipe. This is also known as an earth-pipe-air heat exchanger, which can be utilised for reducing buildings cooling load during summer. The earth-pipe-air heat exchanger can also be used for heating interior spaces in buildings in winter. It is more effective in winter than summer (Ghosal et al., 2004).

The earth pipe cooling systems have been widely implemented in Germany, Denmark, Austria and India since the 1990s, and are gradually being adopted in North America (Bisoniya et al., 2013). The low energy cooling technique using earth became increasingly popular in Europe and America after the oil crisis in 1973 (Krarti and Kreider, 1996). There has been limited research on the earth pipe cooling techniques involving both numerical and experimental studies. However, no credible research is seen to have been undertaken for a hot and humid climate in Australia. Therefore, there is a need for the earth pipe cooling study to investigate energy saving potential in the Australian climate. This study is seen as timely and important for the Australian economy and environment as the outcome of this research is likely to provide an optimum earth pipe cooling guidelines. An optimum earth pipe cooling product guidelines is also required for the consumers to ensure the achieving of efficient performance of the system.

1.3. Research Questions

For the study of this project, four main research questions arise. They are as follows:

- How is the temperature field of Australian soil?
- How much reduction in temperature can be obtained within the buried pipe?
- What is the optimum configuration of buried pipes (length, diameter, and thickness) in the earth pipe cooling experiment?
- Would the air at the pipe outlet give adequate cooling?

1.4. Aims and Objectives

The main aim of this study is to investigate and analyse the thermal performance of the earth pipe cooling system in the subtropical climate in Australia. The performance of the system is evaluated through modelling and validation with experimental measurements. The earth pipe cooling experiments are to be conducted in summer (wet season). The specific objectives of this study are:

- To measure the thermal performance of the horizontal and vertical earth pipe cooling system using the experimental setup and model container in the sustainable precinct of Central Queensland University.
- To develop an integrated thermal model for both the horizontal and vertical earth pipe cooling system to evaluate their performance.
- To optimise the earth pipe cooling model for assessing the impacts of the parameters of pipe length, pipe diameter and thickness, pipe material, pipe depth and air velocity on room cooling performance.
- To recommend an optimum earth pipe cooling product guidelines and product unit(s) for consumers, and an energy efficient building design that incorporates appropriate passive design strategies for the occupants.

An exhaustive literature survey indicates that no earth pipe cooling study, either horizontal or vertical earth pipe cooling system, has been undertaken in Australia. This study is considered to be the first using this new approach for this climate. Furthermore, no integrated model for these earth pipe cooling systems has been developed for any hot humid climate like Queensland, Australia. This study thus is seen as a novel study.

1.5. Scopes and Limitations

The earth pipe cooling performance is investigated in this study, which has been undertaken in the sustainable precinct in the Rockhampton campus, Central Queensland University, Australia. From the literature it is seen that there is no record of the earth pipe cooling system being studied in hot and humid subtropical climates in Australia. The primary requirement for investigating the earth pipe cooling system is to measure the soil temperature and the heat transfer between the soil and air at different depths as no soil temperature data is available for this climate.

Studies undertaken in climatic conditions of other countries show that the soil temperature at the depth of 4.0 m is an optimum depth to bury the pipes underground since the temperatures below this depth remain nearly constant. In this study, the buried pipes were laid at a maximum of 1.1 m depth underground for minimising the earth pipe laying and installation cost. To lay and bury the pipes, an excavation using

an excavator was required which is an expensive operation in the Australian context. Furthermore, this study was carried out within a limited budget. Therefore, due to the budget constraints and experimental limitations, this research was investigated experimentally for a depth of 1.1 m and the optimum depth was considered using simulation through a parametric analysis.

A series of Polyvinyl Chloride (PVC) pipes were used in the earth pipe cooling system as it is commonly used for its light weight, non-corrosive properties, chemical resistance, availability, and ease of making connections. It is less expensive, affordable for most consumers and most importantly it has been used in almost all of the studies so far undertaken. Therefore, the experimental study was conducted with the PVC pipes only while a parametric analysis was undertaken for assessing performance with other pipe materials.

1.6. Thesis Structure

The thesis is comprised of seven chapters. Brief content of each chapter is given below. Chapter 1 describes the detailed background information, and discusses the significance of the earth pipe cooling technology in hot and humid subtropical climates. It also provides the aim and objectives of the study based on the research questions.

Chapter 2 presents a detailed review of the relevant literature. The literature review covers the hot and humid subtropical zone of Australia, thermal comfort analysis for hot humid climate, several existing passive cooling methods and their impacts, usefulness of bioclimatic chart for passive air cooling system, passive building design approach, and thermal modelling and simulation.

Chapter 3 describes the experimental design and measurement techniques and procedures used in this study. The experimental work is based on the field work conducted at the sustainable precinct, Central Queensland University, Rockhampton, Australia. The field work covers the earth pipe cooling technology installation, and data collection and measurement procedures. The chapter also explains the thermal model development and model validation technique for this study.

The performance of the horizontal earth pipe cooling system is analysed in Chapter 4. The chapter includes both experimental and numerical studies of the system. The numerical study involves thermal modelling and simulation in ANSYS Fluent 15.0. The numerical model is validated by the experimental results.

Chapter 5 presents the thermal performance of the vertical earth pipe cooling system. Development of a numerical model for the system is discussed and validated using ANSYS Fluent 15.0.

The earth pipe cooling model is optimised in Chapter 6 through a parametric analysis. The analysis was carried out through numerical modelling for the parameters, air velocity, pipe length, pipe diameter and thickness, pipe material, and pipe depth.

Finally, the overall research conclusions, recommendations and suggestions for further research are presented in Chapter 7. The diagram for the thesis structure is shown in Figure 1.7.

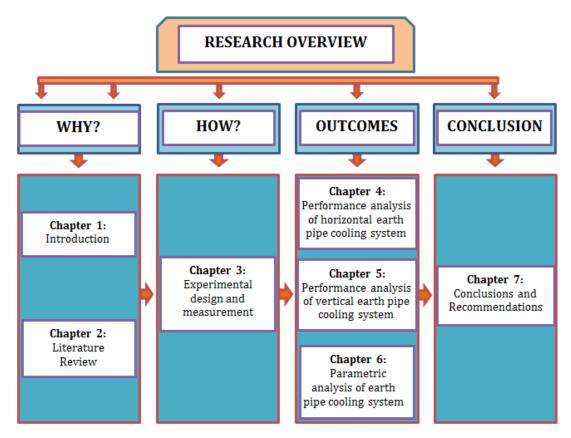


Figure 1.7: Organisation of the thesis.

CHAPTER 2 : LITERATURE REVIEW

2.1. Introduction

This chapter reviews the relevant literature of this research. Firstly, the hot humid climate in Australia, especially the subtropical climate where this research has been conducted is reviewed. Then thermal comfort for building occupants is analysed for a hot humid climate. A comprehensive survey on the common existing passive cooling strategies is carried out to assess their efficiency. The building design approach for the passive cooling techniques is also discussed. Numerical modelling methods and tools which are currently being used to measure the thermal performance of passive cooling are then reviewed. Finally, research gaps are identified for the study.

2.2. Hot Humid Climate in Australia

The Australian climate varies from tropical and sub-tropical to temperate because of its large geographical size. Queensland, Northern Territory and Western Australia lies in the northern part of Australia which are the tropical zone. The tropical climates have hot humid summers and warm winters as shown in Figure 2.1. Mild or warm summers and cold winters occur in south-eastern Australia, whereas warm humid summers and mild winters persist in the subtropical climatic zone. The subtropical climatic zone lies in the south-west and south of the warm humid subtropical zone as shown in Figure 2.2.

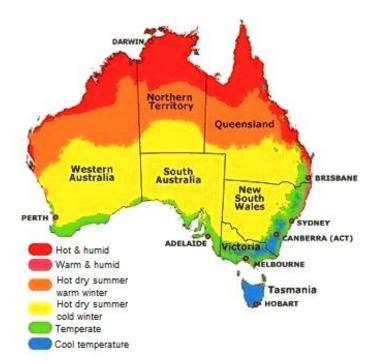


Figure 2.1: Different weather in different climate zones in Australia (ATG, 2013).

In the subtropical zone, the summer season is comprised of December, January and February; the autumn season includes March, April and May; the winter season contains June, July and August, and the spring season consists of September, October and November.

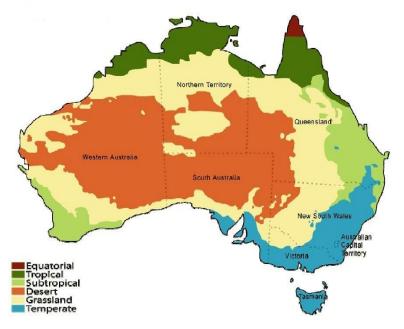


Figure 2.2: Different climate zones in Australia (AG, 2013).

The subtropical Rockhampton is situated 40 km inland from the Coral Sea and to the north of the Tropic of Capricorn in Central Queensland. It is located at the latitude of 23°22′40.49″S and longitude of 150°30′36.37″ as shown in Figure 2.3. Rockhampton has a warm and high humid climate as it is located close to the equator and within the tropical zone. It lies within the cyclone risk zone because of summer thunderstorms. The city experiences a subtropical climate with an average annual rainfall of 805 mm (BOM, 2014). Its average temperature varies from 22°C to 32°C in summer and from 9°C to 23°C in winter. However, the summer temperature can exceed 40°C and the winter temperature can get below 0°C (BOM, 2014).



Figure 2.3: Geographic position of Rockhampton on the Globe with longitude and latitude (Google Earth, assessed on 17 March 2015).

The average annual temperature and relative humidity in Rockhampton are observed as 22.9°C and 48.4% respectively (COT, 2014). The warmest average maximum temperature of 32°C occurs in January and December each year, while the coolest average minimum temperature of 11°C is recorded in July. Also, August is the driest and February the wettest month. The climatic conditions of Rockhampton in terms of temperature, relative humidity, rainfall and wind speed are shown in Figure 2.4.

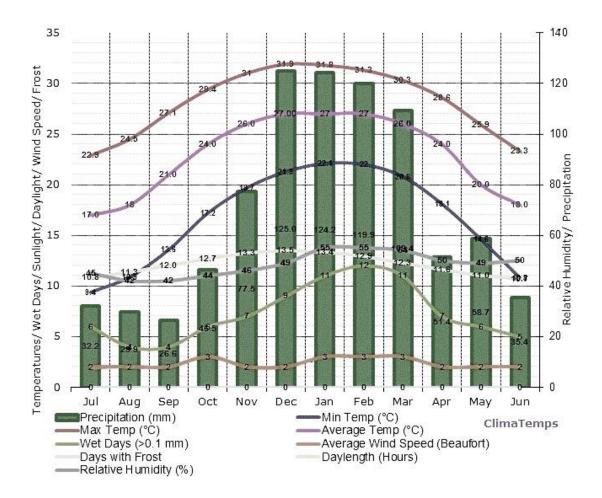


Figure 2.4: Climate of the subtropical zone Rockhampton, Queensland, Australia (COT, 2014).

For hot and humid subtropical climate like Rockhampton, the indoor room temperature in buildings can be reduced by adopting different passive strategies. The effective incorporation of passive features in designing buildings can significantly minimise the air conditioning load of the building while maintaining thermal comfort (Santamouris, 2007). The efficiency of the passive strategy relies on satisfying a range of thermal comfort parameters as discussed in the following section.

2.3. Thermal Comfort and Theory

An accurate understanding of the thermal comfort parameters is a crucial component of efficient building (COV, 2009). Mainly, it is important in effective passive design, where the buildings must keep up thermal comfort without using habitual mechanical units for however much of the year as could be expected. The thermal comfort is a condition of mind which expresses satisfaction with the thermal environment (Fanger, 1970). There are three major reasons behind the thermal comfort study: to achieve user satisfaction, to maintain efficient energy consumption and to set a standard with a range of thermal comfort temperature for a specific zone. A method to determine cooling or heating requirements for a building is to calculate the number of 'degree-days' using the local weather data. Thermal comfort temperature and outdoor temperature are required to determine this measure. For a cooling season, the 'degree-days' is the number of days multiplied by the temperature rise between the temperature for thermal comfort and the outside temperature (CIBSE, 2006).

2.3.1. Thermal Comfort Factors

The thermal comfort factors incorporate the factors related to the environment and person. Environmental and personal factors are major issues for achieving thermal comfort. The environmental factors consist of the climatic variables in the environment while the personal factors include the factors which affect the human thermal comfort. The thermal comfort assessment depends on different factors, as shown in Figure 2.5.

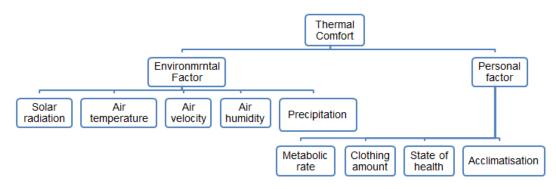


Figure 2.5: Thermal comfort factors.

2.3.1.1. Environmental Factors

The solar radiation reflected from ground, air velocity, air temperature, humidity and precipitation are the key variables in the environment, which are usually considered in environmental reactive building designs (Givoni, 1976). Solar radiation is the main environmental factor, which is projected from the sun onto the Earth's surface, when there is no obstruction. The amount of radiation that reaches the Earth's

surface can be decreased due to obstructions in the atmosphere such as absorption, reflection and diffusion. If there is a difference between the radiant temperatures of the Earth's surface and the ambient air temperature, radiation is emitted from the ground to the atmosphere (Sanusi, 2012). This occurs mainly at night when the Earth's surface is warmer than the air temperature. Solar radiation also causes evaporation if there is water on the surface.

Air temperature and air humidity, most commonly addressed in the conventional design process influences only 6% and 18% of our perception of thermal comfort respectively (COV, 2009). The temperature of neighbouring surfaces and the air velocity are also considered to take a more effective comfort-focused approach, which can account for 50% and 26% of thermal comfort impression respectively. Thus, air temperature is the main important environmental factor that can impact the heat discharged from a human body for achieving thermal comfort.

The amount of water vapour (moisture) held by the atmosphere is the relative humidity. The relative humidity has a noticeable effect on the thermal comfort as it is a measure of the ability of air to absorb moisture and thus affect the amount of heat a body can dissipate by evaporation (Cengel et al., 2002). Due to evaporation, the atmosphere collects water vapour from wet surfaces, vegetation or water features. Building occupants feel discomfort in the presence of high humidity and air temperature. An acceptable range of relative humidity level varies from 30% to 65% (Szokolay, 2008). Sufficient air flow is needed to reduce the humidity considering that human reactions would be different at various air speeds. Human reactions due to different air speed are shown in Table 2.1.

Reactions	Air Speed
Stuffy	<0.1 m/s
Unnoticed	to 0.2 m/s
Pleasant	to 0.5 m/s
Awareness	to 1.0 m/s
Draughty	to 1.5 m/s
Annoying	>1.5 m/s

Table 2.1: Human reactions at different air speeds (Szokolay, 2008).

Precipitation is another environmental factor that also affects thermal comfort, which is referred to as rain. It assists in reducing the solar radiation from the sun and hence in creating a comparatively cooler atmosphere than the norm. Cloud blocking solar radiation during rainfall is the main reason behind this. At the same time, the relative humidity is increased due to increasing water vapour in the atmosphere. All of these environmental factors play a role in changing the atmosphere and are affected by each other.

2.3.1.2. Personal Factors

Four personal factors: metabolic rate, clothing amount, the state of health and acclimatisation of the occupants can affect human thermal comfort (Fanger, 1970). Due to these personal factors people might not have the same thermal comfort perception at the same environmental condition. A high metabolic rate generates more heat compared to a low metabolic rate (UOI, 2014). Consequently, someone may feel warm with a high metabolic rate where a person may feel cold with a low metabolic rate. Metabolic processes are of two categories, muscular metabolism and basal metabolism. The muscular metabolism process happens when an individual is completing work, whereas basal metabolism is a continuous and automatic process. The amount of energy released by a human body depends on the activity of the person. The range of energy released from a human body would be 70 W to 700 W as shown in Table 2.2.

Activity	Energy released (Watts)
Sleeping	Minimum 70
Seating, moderate movement, e.g. typing	130-160
Standing, light work at machine or bench	160-190
Seating, heavy arm and leg movement	190-230
Standing, moderate work, some walking	220-290
Walking, moderate lifting or pushing	290-410
Intermittent heavy lifting, digging	440-580
Hardest sustained work	580-700
Maximum heavy work for 30 minutes duration	Maximum 1100

Table 2.2: Amount of energy released for different activities (Koenigsberger, 1975).

The personal factor of clothing is an item that protects the occupants from the environment. It is measured in a clo-value unit which is different for various types of clothing as shown in Appendix 2.1. To achieve the thermal comfort, the occupants normally wear low clo-valued clothing in warm weather and high clo-valued clothing in cold weather.

State of health is another personal factor that would also affect the thermal comfort of a human body. The human body would feel colder when the internal body temperature is greater than the air temperature. This may happen only when the body is not feeling well. Females feel colder than males although their bodies are quite better in rationing heat when the climate turns colder (BAS, 2014).

Another personal factor of acclimatisation for the occupants is the process by which the people get to be physically conformed to the temperature of their environment (UOI, 2014). It plays a vital role in how well the inhabitants endure cold and heat. The human body is warm blooded. It has thermal adjustment mechanisms, known as vasoconstriction in a cold environment and vasodilatation in a warm environment. In the case of vasoconstriction, the blood vessels contract, reducing blood circulation to the skin. Thus, the skin temperature is diminished and a decrease in heat dissipation arises. In the case of vasodilatation, the blood vessels expand, which increases the blood flow to the skin. As a result, heat transport increases and lifts the skin temperature which increases the heat dissipation (Szokolay, 2008).

2.3.2. Thermal comfort in Hot Humid Subtropical Climate

Several researches (Nicol, 2004, Han et al., 2007, Lin and Matzarakis, 2008, Cândido et al., 2010, Mallick, 1996) have been conducted to find the appropriate thermal comfort range for a hot and humid climate. The occupants living in naturally ventilated, air- conditioned or both air-conditioned and naturally ventilated buildings, were taken into consideration in these researches. The overall findings for naturally ventilated buildings show that the thermal comfort temperature ranges from 22.7°C to 33.0°C and the average maximum thermal comfort temperature is 30.0°C (Sanusi, 2012). For air-conditioned and both air-conditioned and naturally ventilated buildings, it was found that the thermal comfort temperature ranges from 20.8°C to 29.5°C and the average maximum thermal comfort temperature is 28.3°C.

The ASHRAE standard has a lower relative humidity that expands the thermal comfort temperature range. The suggested thermal comfort range is from 25°C to 28°C for this type of lower humidity at 10%, while the suggested thermal comfort range is from 24°C to 27°C for the humidity of 55% (ASHRAE, 2004).

The following section highlights the commonly used passive cooling strategies in operation on a worldwide scale for reducing the air-conditioning load in buildings and consequently constraining the consumption and cost of electricity.

2.4. Passive Air Cooling Strategies

As mentioned in the previous chapter, passive air cooling is a system of cooling an interior space in a passive process without using any mechanical units. It is a building configuration approach that concentrates on heat gain control and heat dispersal in a building to enhance the indoor comfort with minimal energy (Santamouris and Asimakopoulos, 1996, Samuel et al., 2013). Passive cooling minimises heat pick up from the outer environment and facilitates heat loss to natural cooling sources, for example, cooling breezes, evaporation, air movement and earth coupling.

Passive cooling involves designing buildings for cooling load avoidance (CLEAR, 2013). It could be used to decrease, and sometimes eliminate, mechanical unit requirements such as fans and compressors in regions where cooling is a dominant problem. Passive and low energy techniques use the cooling energy derived from four natural heat sinks, namely the sky or upper atmosphere, the outdoor air (ambient air), water and the earth (Cook, 1989, Givoni, 1994). There are several passive cooling strategies used in hot humid climatic zones. The relevance of each strategy relies upon the climatic conditions.

2.4.1. Natural Ventilation

Natural ventilation is a system for supplying and routing air through an indoor space without utilisation of any mechanical apparatus that consumes power. Ventilation gives cooling by empowering convective heat transfer from the interior of a warm building to a cool exterior (Chenvidyakarn, 2007). It is obviously a valuable design

tool for sustainable improvement as it depends only on natural air movement (Aynsley, 2007). There are two major techniques in natural ventilation systems: cross-ventilation and single-sided ventilation.

Cross-ventilation is comparatively effective where the windows on adjoining or opposite walls draw ventilation air over the occupied space. Several investigations (Tantasavasdi et al., 2007, Tantasavasdi, 2002, Tantasavasdi et al., 2001) were made to accomplish effective ventilation in hot climates. The investigations concurred that no less than two large operable windows ought to be provided on different walls, ideally one opposite the other, with one of them intercepting the predominate wind. Therefore, cross-ventilation is attained when rooms have no less than two walls interface externally in opposite directions as shown in Figure 2.6(a) and single-sided ventilation is achieved when rooms have only one external facade as shown in Figure 2.6(b).

In the cross-ventilation system, the activity of any wind creates pressure differences between the openings, and so pushes a strong airflow through an inward space (Bhatia, 2012). But in the single-sided ventilation system, the wind driven ventilation flow is commanded by the turbulence of the wind, as brought on by transient changes in wind speed and direction as shown in Figure 2.6(b). Therefore, cross-ventilation is the choice of design.

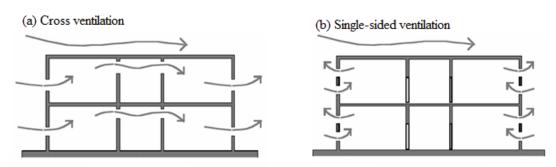


Figure 2.6: Natural ventilation strategy (Bhatia, 2012). (a) Cross-ventilation. (b) Single-sided ventilation.

The utilisation of natural ventilation is a great benefit with the increasing concerns in regards to the expense and ecological effects of energy use. The benefits of using natural ventilation are 40% lower energy cost than the air-conditioned equivalents,

savings in capital costs in the area of 10-15%, and increased fresh air supply to a space (Bhatia, 2012).

The major disadvantage of using natural ventilation is control of the airflow direction in buildings. This difficulty may occur because of the absence of negative pressure. Contamination of corridors and connecting rooms is likewise a risk (Escombe et al., 2007). Moreover, the buildings with natural ventilation require more land space including surrounded free space to take advantage of warm weather winds. In the case of industrial and commercial buildings, natural ventilation requires HVAC systems that are extremely energy intensive with habitual mechanical units.

2.4.2. Evaporative Cooling

A strategy for converting overly hot air into a cool wind using the technique of evaporating water is evaporative cooling. Evaporative cooling is a procedure in which the sensible heat in an air stream is exchanged for the latent heat of water droplets or wetted surfaces (Cook, 1989). By evaporating water, energy is lost from the air and the temperature is reduced. Fresh outside air is drawn through humidified filters that cool the air through water evaporation (Bhatia, 2012). The cool air is then circulated throughout a room by a blower wheel.

The four key factors that influence the evaporation rate are relative humidity, air temperature, air movement and surface area. Evaporative cooling can be categorised in two ways: direct and indirect. Direct evaporative cooling, as shown in Figure 2.7(a), involves air movement past a water spray or other moisturised medium. In this system, water evaporates directly in the air stream, creating an adiabatic process of heat exchange in which the air dry bulb temperature diminishes with the rise of humidity (Gómez et al., 2010). The direct evaporative cooling system builds indoor humidity levels, and is therefore generally not appropriate for hot and humid climates.

Indirect evaporative cooling systems tackle the issue of high humidity levels generated by direct evaporative cooling with the assistance of a heat exchanger as shown in Figure 2.7(b). The external wall of the heat exchanger contacts air that needs to be conditioned before it is provided to the occupied space. The internal wall

is in contact with air that originates from the surrounding environment or building fumes.

The main benefits of using evaporative cooling are lower energy consumption, indoor air quality being enhanced and lower CO_2 emission because of higher air turnover. In very dry environments, evaporative cooling of air provides the additional benefit of conditioning air with more moisture for achieving thermal comfort. Indirect evaporative cooling could be accomplished in several ways, for example, a spray of water over a roof surface, a roof garden and a roof pond.

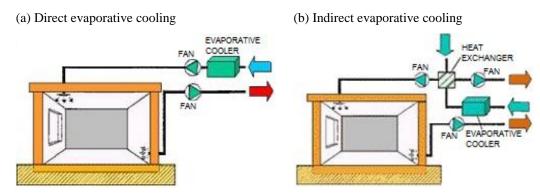


Figure 2.7: Evaporative cooling system (REEA, 2012). (a) Direct evaporative cooling. (b) Indirect evaporative cooling.

The main difficulty of this system is that bacteria can enter in the air stream supplied to the room such as Legionnaires, when water evaporates at the temperature of the environment (Gómez et al., 2010). Another weakness is water consumption related to operating these systems as water is a limited resource in hot and dry climates.

2.4.3. High Thermal Mass

Thermal mass is a property to be considered in designing a building that measures the building's capacity to store and regulate internal heat. The structure of a thermal mass can absorb and store heat during a day as shown in Figure 2.8(a) and release it during the night as shown in Figure 2.8(b). At the point when thermal mass is present inside the building, it retains heat from interior sources and reduces the amplitude of the inside temperature swing.

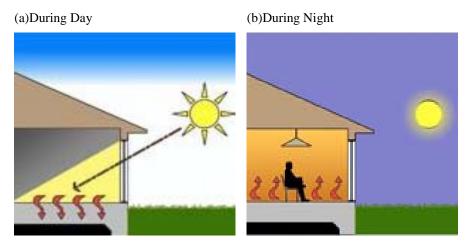


Figure 2.8: Strategy of High thermal mass (ABSA, 2010). (a) During Day. (b) During night.

The thermal mass exists in all materials; and common building materials are capable of absorbing, retaining and steadily discharging heat. Heavy and compact building materials like brick, concrete and masonry have high thermal mass. Buildings with high thermal mass are mainly designed to cool the houses during the day in summer.

The main advantages of using high thermal mass are yearly energy use reduction, a steadier internal environment, expanded assemblies' acoustic insulation and fire ratings improvement of assemblies. Noticeable indoor temperature reduction can be attained in buildings with the high thermal mass (Givoni, 1994). Existing studies showed that the cooling load reduction can vary between 18-50% by using thermal mass (Ruud et al., 1990, Brown, 1990, Kusuda and Bean, 1981, Burch et al., 1984).

The performance of high thermal mass is significantly affected by the surface area of thermal storages (Sodha et al., 1992, Shaviv et al., 2001) and the effective layer thickness of exterior walls (Antonopoulos and Koronaki, 2000). Materials with very high thermal mass retain heat and release it slowly when there is a difference in temperature between the surrounding space and the mass. Buildings having high thermal mass can take more time to heat and cool the interior space. By contrast, buildings having low thermal mass heat up and cool down very quickly as they are very receptive to changes of inside temperature (Yellowhouse, 2013).

2.4.4. High Thermal Mass with Night Ventilation

Buildings with high thermal mass can decrease peak cooling demand, and consequently induce low energy consumption of the building, especially when it is incorporated with night ventilation (Yang and Li, 2008). Cold night air is used in night ventilation to cool the building so that it can absorb heat in the daytime to reduce the daytime temperature.

Constructing buildings having high thermal mass with the provision of night ventilation is an overheating prevention technique which uses slight or zero fossil energy. The success of this strategy is however highly dependent on large diurnal temperature differences. Heat is typically absorbed and stored by the elements of the building structure during the day and released back into the spaces in the evening. To optimise the daytime thermal mass cooling facility, the mass ought to be ventilated during the night to permit comparatively cool air to evacuate heat ingested in the daytime mass as shown in Figure 2.9.

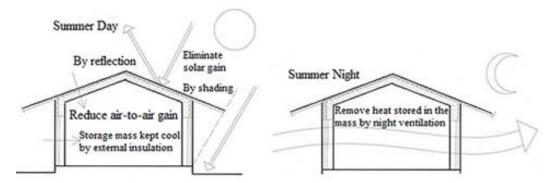


Figure 2.9: High thermal mass with night ventilation system (CLEAR, 2013).

Buildings can be cooled and heat can be removed through the windows during the night and early morning. Night ventilation is utilised during the hotter times of a year from 00:00 to 9:00 am. An indoor temperature reduction of around 3-6°C below the outer surface air may be attained depending on the local climate, mass volume, mass distribution and ventilation. Night ventilation for this situation can utilise the air temperature fluctuation to cool the envelope of the building and bring outside fresh air into the building.

2.4.5. Radiant Cooling

Radiant cooling is a method by which a body sheds heat by thermal radiation. In this cooling system, the unwanted heat is transferred to a cooler heat sink. In one of the radiant cooling techniques, a building's roof is used as a radiator to scatter heat to the night sky. The sky provides a definitive continuous heat sink to keep up the earth's thermal equilibrium (La Roche, 2011). The roof is cooled by this process, which thus serves as a heat sink for the enclosed space underneath.

Radiation is important in keeping the thermal balance of the Earth. Outgoing radiation discharges energy to an outer space from the atmosphere and the earth, and cosmic space is the ultimate absorber, adjusting the energy inputs from the sun and different sources (La Roche, 2011). At the point where two surfaces of distinctive temperatures confront each other, radiative heat exchange will arise between them.

Radiant cooling depends on this concept to dissipate heat from a building or an inhabitant's body. The efficacy of such a scheme depends mostly on the local climate and subtle elements of the roof construction. It will work effectively in hot and humid climates only when the skies are largely clear; in such conditions, night air passing close to the roof can be cooled by around 2°C - 3°C, which can then be directed to the interior of the building to give additional cooling as shown in Figure 2.10 (Givoni, 1994).

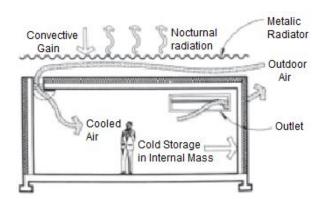


Figure 2.10: Radiant cooling technology (Chenvidyakarn, 2007).

Radiant cooling has minimum thermal effect on the immediate outer environment, which is one of the major advantages of this system. The following heat transfer

procedures influence the performance of this cooling system (Givoni, 1994, La Roche, 2011):

- Long wave radiation released by the radiator; this is enlarged by clear skies and diminished when overcast.
- Radiation discharged by the deep sky and absorbed by the transmitting surface.
- Convective heat exchange between the ambient air and the radiator.
- Cold energy exchange from the radiator to the building, either by conduction or by constrained wind stream as shown in Figure 2.10.
- Convective heat transfer between the medium and radiator.

2.4.6. Wind Tower

In a wind tower system, air enters into the tower through the openings of the tower, gets cooled, and subsequently becomes heavier and sinks down (Majumdar, 2001). The wind tower is a massive structure made of high specific heat materials with the purpose of minimising heat transfer into the building interior environment (Reyes et al., 2013). It has some windows which are opened and appropriately oriented in order to capture wind. Air is cooled more effectively in the presence of wind and streams quickly down the tower and into the room. Therefore, a wind tower makes the indoor environment comfortable without any electric or mechanical air-conditioned device (Bahadori, 1985).

The wind tower shown in Figure 2.11 becomes warm by evening after a whole day of air exchanges. Cooler ambient air interacts with the base of the tower through the rooms during the night (Gamboc, 2012). The heat is absorbed by the tower walls during daytime and it discharges during the night, heating the cool air at night in the tower. Creating an upward draft, warm air moves up and draws cool night air through the windows and doors into the building.

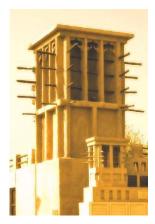


Figure 2.11: Wind tower in a residence (DU, 2011).

In hot and dry climates, the system works effectively where temperature fluctuations are high. It works efficiently for individual units, but not for multi-storied apartments, which is one of the disadvantages of using this system. The system has been practised mainly in the Middle and Near Eastern countries. In dense urban regions, the wind tower must be long enough to have the capacity to capture enough air (Gamboc, 2012). The main disadvantage of this technique is the difficulty of protecting the room from heavy rain.

2.4.7. Earth Pipe Cooling

As defined in chapter one, the earth pipe cooling technology involves long buried pipes in which intake air comes through one end and passes through underground pipes, then the air is cooled by the cold soil and finally the cold air is released into the room through the outlet end. The pipe is covered underground at an optimum depth that provides the most effective results with the two pipe ends above the ground as shown in Figure 2.12. There needs to be enough air flow into the pipe inlet to generate cool air at the outlet end. A blower is likely to be needed to suck the fresh air from the pipe intake and to generate the air flow into the room.

The earth pipe cooling technique is a reasonable and economical option to ordinary cooling as no customary mechanical units are needed. It utilises the earth's near constant underground temperature for cooling air in industrial, residential and agricultural buildings. The infinite thermal capacity of earth has made it a very useful heat sink for building cooling. This fact has been studied and proven by several researchers (Mihalakakou et al., 1995). The rationale behind this is that the

daily and regular temperature variation is significantly diminished in the ground below a certain depth where the soil temperature remains constant (Krarti and Kreider, 1996).

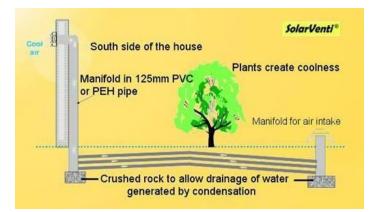


Figure 2.12: Earth pipe cooling system (Ahmed et al., 2014).

The constant soil temperature is approximately equivalent to the mean yearly air temperature (Krarti and Kreider, 1996). The soil temperature increases in winter with increasing depth to a certain point, hence the use of earth as a heat source. Meanwhile, the soil temperature decreases in summer with increasing depth, which allows the utilisation of earth as a heat sink. The earth pipe cooling systems can be categorised in two ways: open loop and closed loop as shown in Figure 2.13. In the open loop system, air comes through the buried pipes into the room and passes it through a ventilation system. It provides ventilation while also cooling the interior of a house (Zaki et al., 2007).

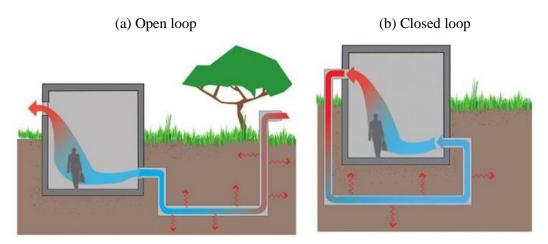


Figure 2.13: Earth pipe cooling strategies.

In a closed loop system, air is constantly re-circulated from the buried pipes underground to the room. The system is more operative than the open loop system. This system does not exchange air with the outside of the house. The latter pipe arrangement can also reduce the tunnel length since the conditioned air is re-circulated within the buried pipe (Goswami and Biseli, 1993). The buried pipes may be installed in horizontal trenches or borings, vertical borings, slinky coil, or even in a surface water body as shown in Figure 2.14.

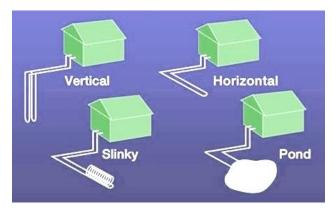


Figure 2.14: Different types of closed loop system (MDH, 2010).

There are some advantages and disadvantages using these systems that are summarised in Table 2.3.

System	Advantages	Disadvantages
Closed	Can be installed almost anywhere	• Earth is not as good a conductor
loop	 Fewer maintenance issues 	Less energy per foot of loop
	 Less temperamental 	
Open	 More energy per foot of loop 	 More maintenance issues
loop	• Water is a better conductor of energy	 Could have local environment risks
	than earth	 Requires lake or well nearby
		 More complex

Table 2.3: Comparison between closed and open loop systems (Johnston, 2011).

There are two main strategies for earth pipe cooling: direct and indirect earth contact (Jacovides et al., 1996). Direct earth contact involves a total or partial building envelope being placed in contact with the ground surface directly, and the indirect earth contact involves an earth-to-air heat exchanger (EAHE) system through which

air is circulated between the interior and exterior of the building and is subsequently brought into the building (Mihalakakou et al., 1997).

The direct earth-to-building contact ground cooling is a low maintenance passive cooling strategy with minimal heat gains and solar exposure. To use this advantage, underground houses were built in southern Tunisia and eastern Spain to protect occupants from the hot and arid climates and large houses were excavated in northern China to cope with the severe winter climate (Krarti and Kreider, 1996). Despite the advantages of the direct-to-building contact ground cooling, it also creates environmental problems such as indoor condensation and poor indoor air quality (Jacovides et al., 1996). Moreover, in some places such as desert and semi-desert countries, large excavation is not suitable due to geological conditions.

The subtropical climates of Australia, like Queensland, have a high level of humidity and temperature. This climate has inadequate average air velocity throughout a year, and the direct earth-to-building contact ground cooling system would reduce the number of openings, which causes the minimising of the natural ventilation rate and therefore produces a lower velocity into the buildings. Considering the potentiality of the direct earth-to-building contact ground cooling and that the indirect earth-tobuilding contact, ground cooling was anticipated to be less unsafe - this study analyses the performance on the later ground cooling system.

2.4.7.1. Applications of Earth Pipe Cooling System

The earth pipe cooling technology is mainly used in hot humid climates, where cooling is a dominant problem. It was studied in several countries all over the world although it was substantially practised in the greater portion of Europe and America. The applications of this technique and the outcome found in several investigations are displayed in the following tables.

Author (s)	Location	Experimental Design	Ambient Temp	Output Temp
Sodha et al. (1985)	Mathura, India	Total length of the tunnels = 80 m; Air velocity = 4.89 m/s; 2 exhaust fans 500W each.	(°C) 24°C-43°C; RH = 40 -53%; Inlet temp = 29.1°C-36.1°C	(°C) Outlet temp= 23.1°C-28.2°C; RH = 75-89%;
Goswami and Biseli (1993)	Florida, USA	30.5 m long pipe with dia 0.305m; pipe depth = 2.7 m; Fan power = 0.184kW; Heat pump =2 $\frac{1}{2}$ ton	23.9°C-33.1°C	26.7°C-28.3°C
Mihalakakou et al. (1994)	Greece	4 plastic pipes with radius 0.125 m; Pipe length =30 m; Pipe depth = 1.5 m; Gap between 2 pipes = 1.5 m; air velocity = 1 m/s	July: 23.2°C- 40°C; August: 25.3°C-39.3°C	July: 24.1°C- 28.2°C; August: 25.4°C- 29.7°C
Pfafferott (2003)	DB Netz AG (Hamm)	26 Polyethylene ducts; Pipe length = $67-107$ m; Pipe diameter = 200 mm and 300 mm; Air velocity = 2.2 m/s	22°C-34°C	10°C-19°C
Tiwari et al. (2006)	Lamparter (Weilhem)	2 Polyethylene ducts each of length 90 m; Diameter = 350 mm; Air velocity =1.6 m/s	22°C-34°C	10°C-22°C
Bansal et al. (2010)	Ajmer, India	PVC and steel pipe each of length 23.42 m; Pipe depth = 2.7 m; Air Velocity = 2-5 m/s; Pipe diameter = 0.15 m; Air flow rate = $0.033 \text{ m}^3/\text{s}$	43.1°C	Drop in temperature: 8.0°C-12.7°C
Ahmed et al. (2014)	Australia	20 PVC buried pipes with diameter 0.125 m; Each Pipe length = 8 m; Maximum pipe depth = 1.1 m; Gap between two pipes = 0.02 m; air velocity (inlet to the room) = 3.4 m/s	22.4°C-30.1°C	Drop in temperature: 1.0°C-2.7°C

Table 2.4: List of earth pipe cooling studies applied to different climatic zones.

Author (s)	Location	Experimental Design	Ambient Temp	Optimal Design
			(°C)	
Goswami	Florida,	30.5 m long pipe with dia	23.9°C-33.1°C	Diameter of
and Biseli	USA	0.305m; pipe depth = 2.7		single pipe =
(1993)		m; Fan power =		0.305 m;
		0.184kW; Heat pump = 2		Multiple pipe
		¹ /2 ton		diameter =
				0.203m to
				0.254m

Mihalakakou et al. (1994)	Athens, Greece	Pipe radius = 0.125m, 0.180m, 0.250m; Pipe length = 30m, 50m, 70m; Pipe depth = 1.2m, 2.0m, 3.0m. Average velocity = 5 m/s, 10 m/s, 20 m/s	21°C-38°C	Short grass cover to the soil; Pipe radius = 0.125m; Pipe length = 70m; Pipe depth = 3.0 m; Average velocity = 5 m/s
Krarti and Kreider (1996)	USA	Pipe radius = $0.1m$, $0.2m$, 0.4m, $0.8m$; Average velocity = $3.5m/s$, $14m/s$, 31.5m/s, $56m/s$; Pipe depth = $1.5m$; Pipe length = $80m$	Average: 19°C Amplitude = 9°C	Pipe radius = 0.1m; Average velocity = 3.5m/s

Author (s)	Location	Experimental Design	Ambient Temp (°C)	Energy Saving
Sodha et al. (1985)	Mathura, India	Total length of the tunnels = 80 m; Air velocity = 4.89 m/s; 2 exhaust fans 500W each.	24°C-43°C; RH = 40-53%; Inlet temp = 29.1°C-36.1°C	No. of cooling rooms having each $16m^2$ floor area = 7
Goswami and Biseli (1993)	Florida, USA	30.5 m long pipe with dia 0.305m; pipe depth = 2.7 m; Fan power = 0.184kW; Heat pump = 2 $\frac{1}{2}$ ton	23.9°C-33.1°C	COP for open loop system = 12; COP (air- condition) = 1 to 4; COP of heat pump = 13
Pfafferott (2003)	DB Netz AG (Hamm)	26 Polyethylene ducts; Pipe length = $67-107$ m; Pipe diameter = 200 mm and 300 mm; Air velocity = 2.2 m/s	22°C-34°C	COP = 88
	Fraunhofer ISE (Freiburg)	No. of Polyethylene ducts = 7; Pipe length = 95m of diameter 0.25m; Air velocity = 5.6 m/s	22°C-35°C	COP = 29
	Lamparter (Weilhem)	No. of Polyethylene ducts = 2; Pipe length = 90m of diameter 0.35m; Air velocity = 1.6 m/s	22°C-34°C	COP = 380
Bansal et al. (2010)	Ajmer, India	PVC and steel pipe each of length 23.42 m; Pipe depth = 2.7 m; Air Velocity = 2-5 m/s; Pipe diameter = 0.15 m; Air flow rate = $0.033 \text{ m}^3/\text{s}$	43.1°C	COP = 1.9 to 2.9

The published literature illustrates that the earth pipe cooling performance is usually affected by the parameters, namely pipe diameter, pipe length, pipe material, air velocity, and pipe depth, which are discussed in the following section.

2.4.7.2. Factors Affecting Earth Pipe Cooling Performance

In earth pipe cooling studies, it is found that the resulting outlet temperature at the buried pipe decreases with the decreasing mass flow rate in the pipe, decreasing pipe radius, increasing pipe length and increasing depths up to 4m (Santamouris et al., 1995, Ghosal and Tiwari, 2006).

A. Impact of pipe radius or diameter

An earth pipe cooling system with various pipe diameters provides different cooling rates. Three different buried pipes of radius 0.125 m, 0.180 m and 0.250 m were used to assess their performance by Mihalakakou et al. (1994b). It was found that the temperature at the outlet of the buried pipe gets higher with increased pipe radius. A bigger pipe radius reduces the convective heat transfer coefficient. A pipe of small radius allows transfer of excess heat quickly from air inside the pipe to the soil, since the centre point of the buried pipe gets closer to the outside soil (Santamouris et al., 1995, Krarti and Kreider, 1996). Ghosal and Tiwari (2006) agreed with these statements and reported that the temperature at the pipe outlet can be decreased with reducing the pipe radius. An equation was explained by Krarti and Kreider (1996) to show the relationship between the pipe radius and the heat transfer coefficient:

$$U_s = \frac{k_s}{r_o} \tag{2.1}$$

where, U_s is the heat transfer coefficient (W/m²K), k_s is the ground conductivity, and r_o is the radius of the buried pipe. This equation shows that the heat transfer coefficient is increased when the buried pipe radius is small, which agrees with the statement of Santamouris et al. (1995).

Krarti and Kreider (1996) conducted a study to investigate the effect of the buried pipe diameter using a developed numerical model and validated it against a set of experimental data. The diameters of 0.1 m, 0.2 m, 0.4 m and 0.8 m were considered for this investigation. The study shows that smallest diameter gives the lowest temperature range at the outlet of the buried pipe. In the case of small diameter, air pressure increases inside the buried pipe and hence delivers faster air flow. However, the residence time can be influenced by increased length. For quicker air flow in the buried pipe, the air does not get enough time to dissipate additional heat onto the earth, unless the length of the pipe is long enough.

B. Impact of pipe length

Another major parameter which affects the performance of the earth pipe cooling system is the length of the buried pipe. A longer pipe provides lower air temperature at the outlet of the buried pipe, which has been proven by several researches. An investigation was made by Mihalakakou et al. (1994) on the earth pipe cooling performance using different pipe lengths of 30 m, 50 m and 70 m. The results demonstrated that the outlet temperature decreases with increasing length of the pipe.

A similar result was found in the study carried out by Santamouris et al. (Santamouris et al., 1995). Two different pipe lengths of 10 m and 50 m were used in this study, and it was found that the outlet temperature using the 50 m long pipe gets 2°C lower than for the 10 m length. Ghosal and Tiwari (2006) got the same result through another study, which was conducted at a greenhouse in Delhi, India. The better performance is found for the longer pipe as it allows a longer time for air to circulate underground and hence can transfer more heat into the earth.

Sometimes the length of the buried pipes is limited by economic constraints. The pipes do not need to be expensive for an efficient cooling system. Cost efficiency of the earth pipe cooling system was evaluated in a hot, arid climate in Kuwait (Hanby et al., 2005). The cost efficiency was measured by calculating the payback time of the system. The payback time for the optimum configuration was found as 7.24 years, where the pipe length was 56.97 m, pipe diameter 0.35 m and buried underground at 5.47 m depth.

C. Impact of air velocity

Air velocity is a key factor that influences the earth pipe cooling performance. The effect of the air velocity on the earth pipe cooling performance was assessed by a few studies. To find the efficient velocity speed, three different velocities of 5 m/s, 10 m/s and 20 m/s were considered in an analysis conducted by Mihalakakou (1994b). The results showed that the higher velocity produces high temperature at the buried pipe outlet. A similar study was carried out by Krarti and Kreider (1996) to compare the cooling performance at four different velocities, namely 3.5 m/s, 14 m/s, 31.5 m/s and 56 m/s. The study also provided a similar result. The higher velocity gets less time for heat exchange, so it can't produce a cooler temperature at the pipe outlet.

The impact of two air velocities of 2 m/s and 5 m/s on the earth pipe cooling performance was investigated in summer by Bansal et al. (2010). The pipe outlet temperature was increased by increasing the air velocity at the pipe inlet, which agrees well with the previous researches. This leads to the difference in temperature reduction between the inlet and outlet of the pipe.

D. Impact of pipe material

The material of the pipe is another factor which can affect the earth pipe cooling performance. Each material has different thermal conductivity. Material with higher thermal conductivity is expected to have higher heat transfer rate, and hence transfer more heat from the air inside the pipe to the soil. Therefore, the materials having the higher thermal conductivity can reduce the buried pipe outlet temperature. However, Goswami et al. (1981) analysed the effect of different pipe materials through a number of studies. The studies have shown that the pipe material has little impact on the cooling performance.

E. Impact of pipe depth

The depth of the pipe buried into the soil also affects the cooling performance. The amplitude of diurnal soil temperature decreases with increasing soil depths because of the distance of soil from the ambient air and soil surface. This soil temperature stops decreasing when the buried pipe is beyond 4 m deep as the ground temperature

becomes stable under this depth (Mihalakakou et al., 1994). The cooler soil temperature influences the air temperature circulating inside the pipe.

A study was carried out by Mihalakakou et al. (1994) to assess the impact of different pipe depths. The depth of 1.2 m, 2 m and 3 m were taken into account for this study, where 3 m depth provided the lowest temperature range at the pipe outlet. Mihalakakou et al. (1994) conducted a similar study on the earth pipe cooling performance with different pipe depths of 2.5 m, 4m and lower than 4 m. The findings of this study give a similar result as obtained from the previous researches.

F. Impact with Different Surface Conditions

Despite the above five parameters, the surface condition of soil could affect the earth pipe cooling performance. An uncovered (bare) ground surface would permit exposure to solar radiation, especially in hot and humid climates like Queensland, Australia. Two different soil surface conditions with bare soil and short grass covered soil were observed by Jacovides et al. (1996) over the period of 1917-1990. In summer, a significant temperature reduction of 7°C was found for short grass covered soil in comparison with the bare soil. Generally, the average bare soil temperature is higher in summer than the average air temperature. The soil temperatures were also compared under two different soil covering conditions; one was shaded by tall trees and the other by a raised building (Givoni, 2007). The lower temperature was achieved under the raised building rather than from under the tall trees.

The effect of these parameters on the earth pipe cooling performance depends on the heat transfer rate in the earth pipe cooling system, which is discussed in the following section.

2.4.7.3. Heat Transfer Process in Earth Pipe Cooling System

The laws of physics allow the amount of driving heat energy in a system to flow until an equilibrium state is obtained. Heat transfer is considered to be a nonequilibrium process as a temperature gradient has to be present for it to occur (Bergman et al., 2011). The heat is transferred from one fluid to another fluid, or from one body to another, which can be determined by the following:

- There must be difference in temperature between the bodies.
- Heat will be transferred from a hot body to a cold body.
- The amount of heat lost by the hot body will be equal to the amount of heat gained by the cold body, except for the case of heat loss to its surroundings.

Heat transfer rate can be measured in three modes, namely conduction, convection and radiation, which are discussed below:

A. Heat Conduction

Due to heat conduction, the energy is transferred between stationary fluids or solids by the movement of molecules or atoms. Air particles' conduction occurs through the solid materials in the earth pipe cooling system. For a hot climate, the outside hot air on the outside of the earth pipe cooling room wall, or glass windows with steel frames transfers energy onto the cooler inside of the room. Thus the inside room wall temperature is raised in this heat transfer process. The more excited molecules in the hot surface transfer energy to the colder surface. Higher temperatures are associated with higher molecular energies (Bergman et al., 2011). At the point when neighbouring molecules collide with each other, the energy is transferred from the more energetic to the less energetic molecules. The conduction energy transfer must then occur toward the decreasing temperature. Thus, the outdoor air having higher temperature transferring heat to the indoor air having lower temperature, is an example of the conductive heat transfer in the earth pipe cooling system as shown in Figure 2.15.

The heat conduction process is shown in Figure 2.15 through a large plane. In this process, the heat exchange rate can be calculated using the equation of Fourier's law, which is given by (Bergman et al., 2011):

$$\dot{q}_{Conduction} = k \frac{T1 - T2}{L} = k \frac{\Delta T}{L}$$
(2.2)

where k is the heat transfer coefficient by conduction (W/m K), ΔT is the temperature differences between the air and soil, and L is the length of the buried

pipes (m). The heat transfer coefficient by conduction is a parameter that is unique to each material and its properties. The rate of heat gain or loss of an Area in Watts is given by

$$q_{Conduction} = \dot{q}_{Conduction} \Box A \tag{2.3}$$

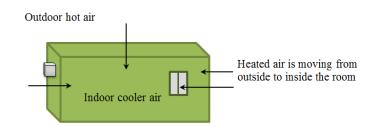


Figure 2.15: Heat conduction process through the earth pipe cooling room.

B. Heat Convection

Heat energy is transferred in the mode of convection between a fluid and the adjacent solid surface. The convection process involves both the effects of fluid motion and conduction (Cengel et al., 2002). Heat convection may occur in two ways: natural convection and forced convection. In the natural convection, the movement of a medium relies entirely on temperature and density differences whereas the movement of the medium depends totally or partially on the results of the outside influence in the forced convection. Movement of a fluid caused by a pump is one of the examples of the forced convection.

The forced convection is used in the earth pipe cooling system as the system uses a fan at the pipe outlet, which sucks the air from the pipe inlet and passes through the pipes buried underground. In summer, the hot atmospheric air comes through the pipe inlet via buried pipes underground, and finally the air cooled by the soil moves to the room through the pipe outlet. When the hot air passes through the buried pipes, it transfers heat to the soil by convection and gets cooler. The convective heat transfer process between the buried pipe and soil is shown in Figure 2.16. The total amount of heat transfer depends on the thermal conductivity of the material used in the system. For example, a material having high thermal conductivity can transfer more heat than the material of low conductivity.

The governing equation for the convection heat transfer process is described by Newton's law of cooling:

$$\dot{q}_{convection} = h(T_s - T_{\infty}) \tag{2.4}$$

where \dot{q} is the convection heat flux (W/m²), T_s and T_{∞} are the surface and fluid temperatures, and h is the convective heat transfer coefficient (W/m²). The value of the heat transfer coefficient represents the ability of the material to resist convective energy flow. The convective heat loss can be expressed by the following equation:

$$q_{Convection} = \dot{q}_{Convection} \Box A \tag{2.5}$$

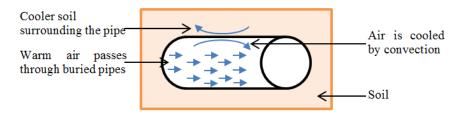


Figure 2.16: Convection through buried pipe in hot climate

C. Heat Radiation

Energy emitted by matter in the form of electromagnetic waves (or photons) is the radiation (Cengel et al., 1998). The energy transfer by radiation is different from conduction and convection heat transfer process as it does not need the presence of an intervening medium. Heat transfer radiation is how the sun's energy reaches the earth.

Radiation is emitted by the sun that incidents the surface at a rate of $\dot{q}_{incident}$, where some of the radiation energies are absorbed by the surface. The amount of solar radiation absorbed by the surface is calculated by the following formula:

$$\dot{q}_{Absorbed} = \alpha \dot{q}_{Incident}$$
 (2.6)

where $\dot{q}_{Incident}$ is the radiation rate which is incident on the surface and α is the surface absorptivity.

The difference in the radiation rate between the surface emission and absorption is the net heat transfer by radiation. If this absorption rate is higher than the emission rate, the surface will gain energy by radiation, otherwise the surface will lose energy by radiation. For example, the earth surface gains heat which is absorbed from the sun, and thus the earth surface temperature is raised. A partial solar radiation is emitted from the surface as shown in Figure 2.17. The net rate of solar radiation from the earth surface can be described by the following equation:

$$\dot{q}_{Radiation} = \dot{q}_{Emitted} - \dot{q}_{Absorbed} = \frac{q}{A} = \varepsilon \sigma \left(T_{Surface}^4 - T_{Air}^4 \right)$$
(2.7)

where $\dot{q}_{Emitted}$ and $\dot{q}_{Absorbed}$ are the emission and absorption rate of the surface respectively, A is the surface area, ε is the surface emissivity, σ is the Stefan-Boltzmann constant which is equal to $5.67 \times 10^{-8} \text{ W/m}^2$.K⁴, $T_{Surface}$ and T_{Air} are the temperature of the earth surface and the atmospheric air.

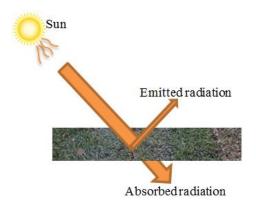


Figure 2.17: Solar radiation to the ground surface

Queensland weather is hot and humid, and so solar radiation occurs on most days apart from rainy seasons. The earth surface can store heat easily due to its large heat capacity. As a result, after a certain point within the shallow depth of the earth, there must be equilibrium between the heat gain from the sun through the earth surface and the heat flow from the core.

2.4.7.4. Heat Flow within the Earth

According to Fourier's law, the heat flow amount through the earth structure depends on the thermal conductivity of the earth's structure. The heat flow of the earth underground is affected by a number of factors such as altitude, latitude, weather conditions, landscaping, shading, soil properties, time of the year and rainfall (Krarti et al., 1993).

The basic concept of heat flow within the earth and its structure is essential as this research concerns the Earth's heat capacity to store heat. The Earth structure consists of four layers as shown in Figure 2.18. The first is the solid inner core that is a metallic iron-nickel with radius 1370 km, the second is the molten outer core that also contains iron-nickel of thickness 2100 km, the third layer is the mantle composed by ultrabasic iron (Fe) and a rich amount of magnesium (Mg). The thickness of this layer is 2900 km, and the last one is the very thin crust (Banks, 2012). The thickness of the last (fourth) layer varies from 15 to 50 km below the continents, and from 5 to 8 km below the oceans.

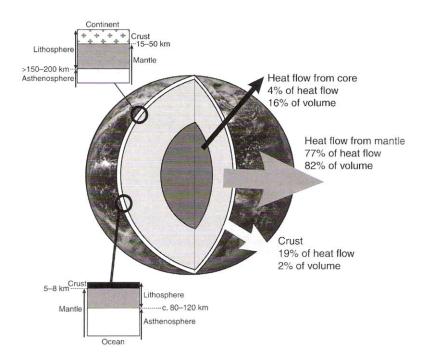


Figure 2.18: Earth structure showing Earth surface layers with thickness (Banks, 2012).

Section 2.4 focused on researches into the technical challenges and potentiality of different passive cooling techniques. Major technical challenges observed are air velocity (speed and direction), moisture content, ventilation, soil temperature, air temperature, relative humidity, pipe material, pipe diameter, length and depth. It was also found from the literature survey that proper orientation of the buildings, sufficient ventilation and optimum design tools for passive cooling techniques all play important roles in minimising the cooling load of the buildings and increasing the energy savings.

All the passive cooling techniques discussed in this section rely on the local climatic conditions. To adopt most suitable passive cooling strategies in a particular climatic zone, it is important to produce a bioclimatic chart for that location. The bioclimatic chart making procedure is described in the following section to select an appropriate passive cooling strategy for a hot humid subtropical climate.

2.5. Bioclimatic Chart for Passive Air Cooling Systems

The Bioclimatic Chart is a preliminary analysis tool used during the early planning stages of a building project. It is capable of identifying desirable adaptations of structure to meet human comfort needs under specific climatological conditions. The bioclimatic chart can identify a comfort zone where no cooling or heating system is required to maintain thermal comfort. Using the chart, simple building techniques and methods such as incorporating natural cooling systems and techniques, passive solar heating systems as well as natural lighting systems and techniques can be applied to the buildings to reduce energy consumption.

The chart making procedure is also essential for the analysis and design of HVAC systems. Monthly statistical data are required to create a bioclimatic chart for a particular location. The bioclimatic chart shows the boundaries of different passive design strategies. It is created by plotting two points for every month. The first plotting point is used to indicate the minimum temperature and maximum relative humidity, and the second plotting point is used to indicate maximum temperature and minimum relative humidity.

A generic bioclimatic chart was developed by Givoni to identify the appropriate passive cooling strategies for a climate (Givoni, 1992, Givoni, 1994) as shown in Figure 2.19. The chart is focused around the linear relationship between the vapour pressure and temperature amplitude of the outside air. It was developed by first recognising the average monthly climatic condition. The average daily maximum temperature was calculated for each month and coordinated with the average minimum daily humidity to create a point. Another chart was also developed based on temperature and relative humidity to select suitable passive cooling strategies as shown in Figure 2.20 (Brown, 1985).

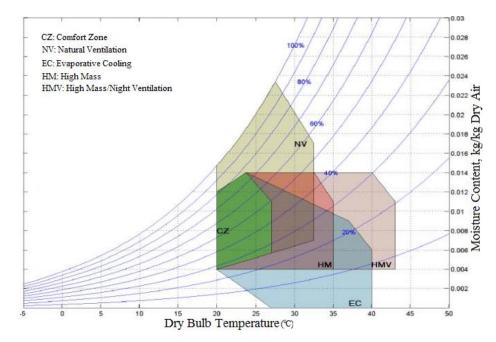


Figure 2.19: Givoni's Bioclimatic chart for passive cooling strategies (Givoni, 1994).

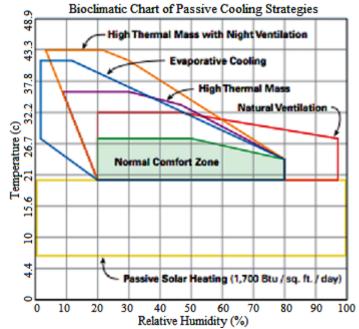
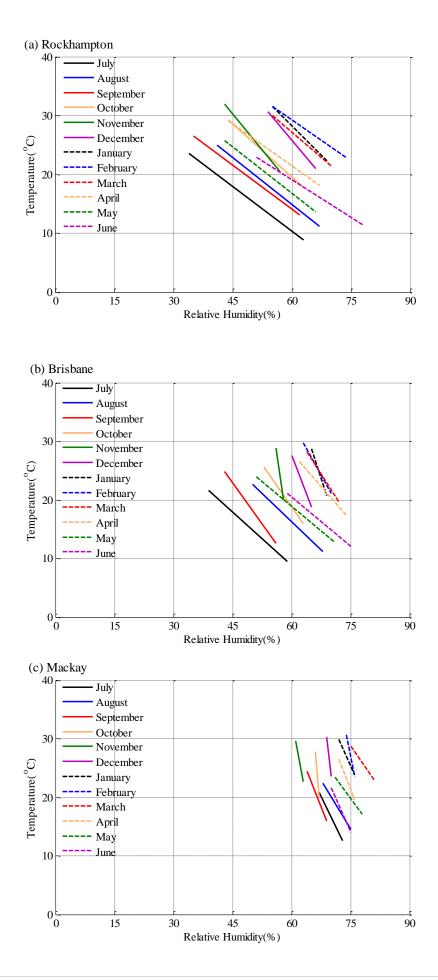


Figure 2.20: Brown's Bioclimatic chart for passive cooling strategies (Brown, 1985).

All the passive cooling strategies used in the charts depend on daily changes in relative humidity and temperature. Both charts are suitable for all buildings with high internal heat loads. The charts identify the appropriate passive cooling strategy for a particular climatic zone using the plotted lines for each month in a year.

A suitable passive cooling strategy can be selected using the bioclimatic chart developed by Brown or Givoni. For these charts, two or more passive cooling strategies have to be installed for different months throughout a year to design a building. To minimise the cost, it is necessary to develop a chart that would select only one passive cooling strategy for a specific location.

Based on two climatic factors of air temperature and relative humidity, a chart was produced for selecting an appropriate passive cooling strategy for the entire life of the buildings of a hot and humid subtropical climate, Rockhampton, Australia (Ahmed et al., 2014). Average maximum and minimum temperature and average maximum and minimum relative humidity in percentages were taken to analyse the climatic conditions of six cities, namely Rockhampton, Brisbane, Mackay, Townsville, Charleville and Mount Isa in the subtropical zone of Queensland, Australia. Figure 2.21 shows the change in temperature and relative humidity in the cities.



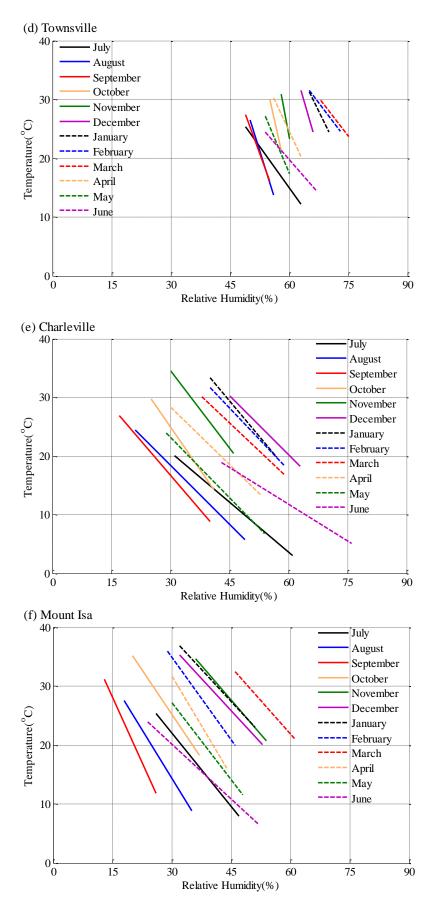


Figure 2.21: Change in temperature and relative humidity in Queensland, Australia.

As seen from Figure 2.21 (a-f), each city has high temperatures which occur mainly from three major sources: direct solar effects on the building and through skylights and windows; heat infiltration and heat transfer of outside high temperatures through the building materials and components; and the interior heat generated by the equipment, appliances and inhabitants.

To find the maximum temperature-humidity zone of the cities, six curves were drawn for six cities by taking the most exterior points of the plotted lines for the change in temperature and relative humidity as shown in Figure 2.22. The zones plotted in the chart were compared with the Brown's chart to identify the appropriate cooling strategy for the buildings of each city.

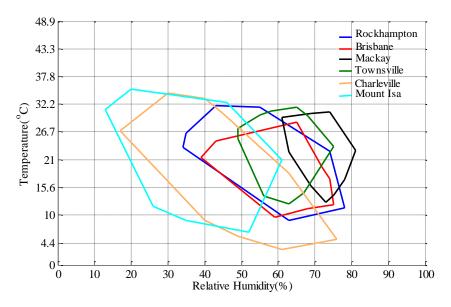


Figure 2.22: Temperature-humidity zone for Queensland, Australia (Ahmed et al., 2014).

The plotted zones for Rockhampton, Brisbane, Mackay and Townsville are close to the natural ventilation zone as shown in Figure 2.23(a) indicating that natural ventilation would be applied to these locations as the appropriate passive cooling strategy. The Charleville and Mount Isa zones shown in Figure 2.23(b) are close to the zone of high thermal mass so the high thermal mass would be the appropriate passive cooling strategy for those regions.

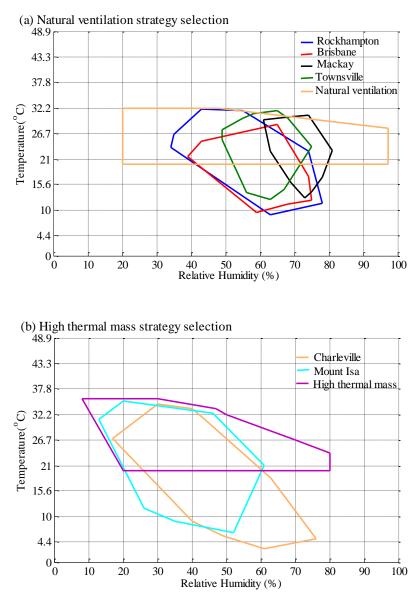


Figure 2.23: Passive cooling strategy selection.

If a zone was close to two or more zones in Brown's chart (Figure 2.20), one or two strategies would be chosen from the strategies to reduce the cost so that they are compatible with each other and the building design. This selection procedure for a suitable passive cooling strategy will assist homeowners to install the most suitable passive cooling strategy for the entire life of their building in any hot and humid subtropical climatic location.

This bioclimatic chart was derived from Brown's chart, which was developed in 1985. Therefore, natural ventilation may not be suitable for the current climatic condition of Rockhampton, Queensland due to its increasing temperatures in recent years. It is therefore important to investigate an alternative energy efficient technology for the hot, humid, subtropical climatic zone.

As discussed in the previous section, passive air cooling through the use of ground cooling technology offers a great potential for energy saving for the Australian climate as it can supplement the air-conditioning load of the buildings with virtually no negative environmental impact. Moreover, it is the least expensive means of cooling a room and is seen as appropriate for all Australian climates. Due to its great advantages and suitability for the Australian climate, the earth pipe cooling system has been adopted in this study.

The earth pipe cooling technique can be further improved by employing proper building orientation, choosing appropriate building construction materials, accurate colour and texture selection, and shading buildings. These are discussed in the following section.

2.6. Building Design Approach

The orientation and shape of a building plays a significant role in achieving overall energy efficiency within the building. An oddly shaped wall that is not properly angled has the potential to trap and divert sound, actually making a howling noise which might be problematic. Properly oriented walls and windows help a building to benefit as much as possible from the winter sun, exclude the summer heat and capture and harness the summer breezes.

2.6.1. Orientation of the Building

Orientation is a parameter characterised for every one of the outside walls of a building (Ford et al., 2007). The orientation can be measured using the angle between the north direction and the normal to the wall. North orientation of buildings provides the best result for the energy demand in cooling, but the worst results for the energy demand in heating (GOI, 2010). Therefore, south orientation is the best orientation for the middle European climate to reduce the energy demand for cooling, while west and east orientation lead to noticeably bad results. As a rule, the orientation in a qualitative manner that could be described by utilising the four

cardinal points: East, West, North and South. The quantitative description permits us to allocate a range of angles with an orientation. If the angle between the normal to one facade and the north (α_0) is 75°, the facade might be viewed as East oriented (Ford et al., 2007). Table 2.7 represents the effective orientation of a building.

Position	Angle
North	$\alpha_{0} < 60; \alpha_{0} \ge 300;$
East	60≤α₀<111
Southeast	$111 \le \alpha_0 < 162$
South	$162 \le \alpha_0 < 198$
Southwest	$198 \le \alpha_0 < 249$
West	$249 \le \alpha_0 < 300$

Table 2.7: Effective orientation of a building facade (Ovacen, 2014).

Size and orientation of transparent building components (windows) have a significant impact on the demand for cooling (Heimo Staller, 2010). A building with a proper orientation ought to have a high heat loss area oriented to the south. This measure needs a well-planned arrangement of solar control in summer, otherwise the building or at least the adjoining zone will be overheated due to solar radiation. An adequate overhang is needed to control solar radiation for the south oriented walls. East and west building orientations are avoided due to the low amount of radiation in winter (ECI, 2008). Moreover, solar control in these orientations is substantially complicated in comparison to south orientation in summer. Various orientations with their corresponding range of angles are shown in Figure 2.24 using a compass card.

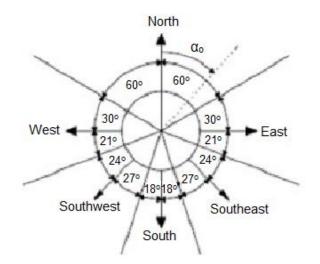


Figure 2.24: Compass card with different orientations (ECI, 2008).

Properly designed orientation is a goal for buildings in all climates. This objective cannot always be achieved because of external restrictions like urban layout. Therefore, some additional treatments may be needed in order to neutralise the external constraints as much as possible. Besides the appropriate orientation of the building, an energy efficient building also involves some key strategies such as proper use of materials, colour and textures, shading, vegetation, etc.

2.6.2. Materials, Colour and Texture

The materials used to develop a building have a significant impact on the environment from extraction, transportation, transforming, utilisation and transfer. Proper selection of sustainable materials can diminish these effects. Some traditional buildings utilise lightweight materials along with comparatively porous constructions, for example, woven bamboo strip flooring and wooden walls with ventilation gaps (Leaurungreong et al., 2005). These permit the building interior to cool quickly at night emulating the outdoor air temperature and thus attaining a generally agreeable environment during sleeping hours. These materials give poor insulation, and hence may not be suitable today, especially in urban areas because of expanded pollution levels and population densities. To minimise the thermal effect of solar radiation, several layers of materials may be needed to construct an appropriate building envelope. Moreover, a layer of protection, for example, glass fibre or foam, is often needed to efficiently reduce conductive heat exchange through opaque surfaces that absorb solar radiation.

Various new materials have been produced in addition to the utilisation of imported and conventional materials for hot, humid climates. Examples of new materials include particleboards from a blend of rice husks and rice straw (Pasilo et al., 2007) and vetiver grass (Leaurungreong, 2004); sandwich walls from rice husks and rice straw (Thongkamsamut, 2003); insulation board from corncobs and cassava (Pakunworakij et al., 2006); bricks from a mixture of coconut coir and soil (Khedari et al., 2005); a composite solid from a mixture of coconut coir, coconut fibre and durian peel (Khedari et al., 2001); concrete blocks from oil palm fibres and baggage (Boonma et al., 2005); and a concrete board from coconut coir (Asasutjarit et al., 2007). The concrete board from coconut coir is more appropriate for construction as it has lower thermal conductivity than conventional materials such as concrete and bricks.

Colour and texture selection for the building envelopes and surrounding surfaces are also important to minimise heat gains. In general, lighter coloured floor coverings reflect more light around the surroundings, while darker colours absorb heat. Smooth surfaces also reflect light whereas rough or diffuse surfaces such as carpet absorb light. Therefore, lighter colours and smoother surfaces are desirable for achieving thermal comfort. A white building top can have a normal diurnal temperature which is a couple of degrees less than that of outdoor air (Givoni and Hoffman, 1968). Moreover, utilising floor surfaces to benefit as much as possible from natural light will go towards bringing down the dependence on artificial lighting. Indeed, around evening time, light coloured or reflective floors assist in minimising lighting that illuminates the same area.

2.6.3. Shading and Vegetation

Solar gain through windows is the major element for a building's heat gain. Window shading attachments used to control solar heat are gaining more consideration and renewed efforts are being made to develop models for devices such as venetian blinds, roller blinds, drapes and insect screens (Van Dijk and Goulding, 1996, Rosenfeld et al., 2001, Pfrommer et al., 1996, Yahoda and Wright, 2004, Yahoda and Wright, 2005, Kotey et al., 2009a, Kotey et al., 2009c, Kotey et al., 2009b, Kotey et al., 2009d). Intelligent shading components which are different as required by the orientation are additional measures to reduce solar heat (Heimo Staller, 2010). Several investigations (Liping and Hien, 2005, Garde et al., 2001) were made which highlight the significance of effective shading as a component of an overall strategy for pre-ventilating overheating in hot and humid climates. Some of these researches recommend that shading hazy areas, for example, walls and roofs is most likely of no less significance than shading glass areas.

Vegetation can be used to reduce a building's cooling requirement, which is achieved by providing effective shading to the walls and windows of the building. Vegetation applications may be trees, high shrubs, climbers and pergolas. It also assists in reducing the amount of solar energy absorbed by the soil surface. In addition, climbers over the walls can decrease the air speed near the wall surfaces and give warm protection when the outdoor air temperature is more significant than that of the walls.

A green roof and green walls in a building is an important tool to mitigate environmental degradation and improve liveability. An investigation (Anwar et al., 2013) was made to measure thermal performance in summer of a rooftop greenery system in a subtropical climate of Australia, which showed a temperature reduction of 4°C in room temperature. The average wall temperature of the building shaded by plants can be reduced by 5-15°C depending on the planting details and local climate (Laopanitchakul et al., 2007, Parker, 1983, Parker, 1987, Parker, 1989). A roof garden can also reduce the temperature by 10-30°C depending on planting details, surrounding conditions and roof construction (Nyuk Hien et al., 2007, Wong et al., 2003).

Several external and internal treatments of the buildings have been discussed in this section to improve the overall performance of the earth pipe cooling techniques. The thermal performance of the earth pipe cooling technique can be measured through both the experimental investigation and numerical simulation. The following section describes the numerical modelling and simulation used for the earth air cooling system.

2.7. Thermal Modelling

Thermal modelling can define a thermal comfort standard that responds to the local climatic condition. It could reduce the differences between outdoor and indoor temperature by keeping indoor conditions comfortable. Thermal modelling is the most useful method to utilise for decision making during design, and assists in analysing thermal performance of a system. Thermal performance has been assessed by several researchers, Ahmed et al. (2009), Sawhney et al. (1998) and Sodha et al. (1991), through earth-air-pipe studies. The cooling potential of the earth-air-pipe system was achieved in these researches.

Since this study deals with the thermal performance of the earth pipe cooling systems, a thermal model is required to analyse the cooling performance of the earth pipe cooling system; discussed in later chapters. The thermal model deals with the temperature and airflow distribution, size and number of fans, and impact of the changes in configuration.

A computer-based tool becomes necessary when the complexity of an analysis increases. As the earth pipe cooling analysis is more complex, simulation software is needed to develop the thermal model. Software packages such as Energy Plus, Design Builder, TRNSYS, PHOENICS, ANSYS Fluent, etc. are used for the thermal modelling and numerical simulation. From this software, the ANSYS Fluent has vast applications in modelling technology. It was used to develop a thermal model and predict the thermal performance of the earth-pipe-air heat exchanger (Bansal et al., 2010).

ANSYS Fluent runs efficiently and robustly for all the flow type physical models such as steady-state or transient, turbulent or laminar flows. However, specific focus is given to turbulence models, as it provides substantial advantages for heat transfer problems. The Realisable $k - \varepsilon$ turbulence model has been selected for the thermal modelling of this study as it is reliable and more accurate. The flow passed through the outlet (inlet to the room) of the horizontal and vertical earth pipe cooling system was found as turbulent. The flow was calculated at the pipe outlet as the outlet (inlet to the room) flow mainly affects the room cooling performance. This flow is characterised by the Reynolds number, which was found as 8,214.77 and 5,774.74 for the horizontal and vertical earth pipe cooling system respectively. The Reynolds number (Re) is calculated by the following formula:

$$R_e = \frac{\rho v D}{\mu} \tag{2.8}$$

Where, R_e is the Reynolds number, ρ is the air density = 1.204 kg/m³, ν is the air velocity = 1.01m/s and 0.71 m/s in the HEPC and VEPC system respectively, D is the diameter of the pipe = 0.125m, and μ is the dynamic viscosity of the air = 1.850387e-05 kg/m-s.

2.8. Numerical Simulation in ANSYS Fluent

Numerical simulation helps in understanding the fluid flow distributions. Simulations can be set up easily for fluid-structure interaction using the unified ANSYS Workbench platform. Fluid flows are governed by mass, momentum, and energy balanced principles which are described by the incompressible Navier-Stokes equations.

ANSYS fluent used a discretisation method which approximates the differential equations by a system of algebraic equations. The finite element method, finite difference method and finite volume method are the most important discretisation methods. The CFD code 'Fluent' uses the finite volume method for discretisation of the computational domain that was used in this study to solve the heat transfer problem of the earth pipe cooling system.

The finite volume method (FVM) is a numerical method that solves partial differential equations and calculates the values of the conserved variables averaged across the volume. It satisfies the conservation of quantities such as mass, momentum, energy, and species for any control volume as well as for the whole computational domain. In this method, the governing equations are integrated over a volume assuming piecewise linear variation of dependent variables. Using these integrations, the fluxes can be balanced across the boundaries of individual volumes.

ANSYS Fluent is adopted in this study for developing the thermal model and numerical simulation due to the availability of the software in the university. Moreover, it has the capabilities for modelling, simulation and optimisation of the earth pipe cooling system.

The Realisable k- ε turbulence model in ANSYS Fluent has been employed to study the earth pipe cooling system in Chapter 4 and Chapter 5. A detailed description of the governing equations, simulation procedure, boundary conditions and simulation results and validation are discussed and presented in those chapters.

2.9. Conclusion

A detailed review has been undertaken of the literature relevant to the passive air cooling system in buildings considering the efficient building orientation and design with different internal and external treatments. The most popular and common existing passive cooling techniques, especially the earth pipe cooling technique were broadly discussed for hot and humid climates. The hot and humid tropical climates in Australia, as well as the subtropical climate were also discussed.

The researches carried out in past decade that are relevant to this study were presented. Through the literature survey, it has been found that many attempts have been made to reduce the energy consumption using passive air cooling systems; mostly investigated in Europe and America, but there are virtually none for the Australian climate. Moreover, no integrated model was developed for the earth pipe cooling system. The earth pipe cooling studies investigated the thermal performance of the earth pipe cooling system using both horizontal buried piping layout and vertical buried piping layout. It is seen from these researches that the earth pipe cooling has the potential to save energy.

The research gaps for the earth pipe cooling system were identified on the basis of the research questions that no earth pipe cooling study has been practised in Australia and no integrated model has been developed for the earth pipe cooling system in any hot humid climate like Queensland, Australia. The novelty of this study is to develop an integrated model for both the horizontal and vertical earth pipe cooling system; a thermal performance assessment of hybrid earth pipe cooling system using air conditioner; and a recommendation of optimum earth pipe cooling product guidelines for the consumers. To fill these gaps the earth pipe cooling system has been adopted in a hot humid subtropical climate in Australia.

CHAPTER 3 : EXPERIMENTAL DESIGN AND MEASUREMENT

3.1. Introduction

This chapter presents the experimental design and measurement procedures used in this study. Two shipping containers were converted into an office space and were used for the earth pipe cooling experimental measurements. The installation and conversion of the shipping containers into the office space, and installation of the horizontal and vertical earth pipe cooling technology in the sustainable precinct of the Rockhampton Campus of Central Queensland University, Australia is presented in detail.

A set of data measuring instruments were used to measure the performance of the earth pipe cooling system. Average soil temperature, air temperature, air velocity, and relative humidity were recorded through the measuring instruments. Moreover, the energy consumed by the earth pipe cooling system was also measured to assess the energy efficiency of the system, discussed in a later chapter. As the study assesses the cooling effect, all the data were collected during the summers from 2013 to 2015. The general approach followed in this study is summarised in the flowchart as shown in Figure 3.1.

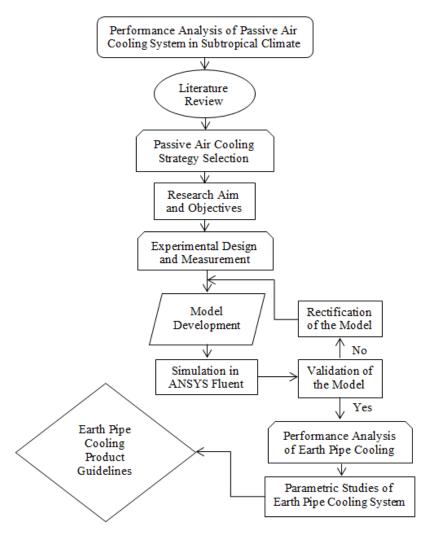


Figure 3.1: Flowchart of the general methodology applied in the study.

3.2. Experimental Set Up

Two shipping containers, each with dimensions 5.63 m x 2.14 m x 2.26 m, were converted into office rooms and were installed with suitable fittings to investigate the cooling capacity and its effect. One of them was connected to a vertical earth pipe cooling (VEPC) system and the other to a horizontal earth pipe cooling (HEPC) system. For excess rainwater overflow, both the containers were installed with a 3° pitch from North to South. Figure 3.2 shows the experimental shed of the earth pipe cooling system.



Figure 3.2: Experimental shed of the earth pipe cooling system.

3.2.1. Earth Pipe Cooling Room Fitting

Both the shipping containers were fitted with an entrance door and a window to be used as an office room. A single sliding dark grey glass door of thickness 5 mm was used for the entrance sliding door. The shipping containers were built with steel frames, completely vertical-corrugated steel front wall and sides, and die-stamped steel corner fittings and roof. The inside configuration of the shipping container is shown in Figure 3.3.



Figure 3.3: Inside the shipping container before making an office room.

Each room wall in the form trapezium was fitted with a number of layers of plywood filling the gap with mineral glass wool rolls. The wall was welded together with these layers into a single panel as shown in Figure 3.4. There was a 25mm air gap between the glass rolls and plywood sheet of thickness 13 mm. The air gap ensures less thermal conductivity and better insulation. Moreover, the air gap assists in reducing the solar energy absorption by the outside wall material. Typically,

plywood is used rather than plain wood in view of plywood's resistance to cracking, splitting, shrinkage and twisting or warping and its high strength (Bulian and Graystone, 2009). Most importantly it is inexpensive, flexible and workable.

Mineral wool (MW) glass rolls of thickness 6 mm were used as insulation. It was made by premium quality virgin stable glass fibres and bonded with thermosetting resins by the TEL process. Generally, glass wool is non-toxic, non-combustible and resistant to corrosion. It has low weight by volume, stable chemical properties, low thermal conductivity and a low moisture absorption rate due to its excellent hydrophobicity.



Figure 3.4: Number of layers of room walls.

The roof of the containers was constructed by several die-stamped, corrugated steel sheets. These sheets were joined together to form one panel by automatic welding. The container floors were constructed by 19 hard plywood boards of thickness 28 mm. The plywood boards were placed on the base frames using zinc plated self-tapping screws. Figure 3.5 shows the inside pattern of the container after conversion into an office room.



Figure 3.5: Inside the shipping container after making an office room.

Both containers were set on flat ground which had a minimum shading effect. Electricity, internet and water supplies were available at this location. TECO (model LA2314CS) window type air conditioner of cooling capacity 5.7 kWh was installed in the containers as shown in Figure 3.6. The system was designed to be a fully automated unattended system with comfort condition. The air conditioner temperature was set at 24°C based on thermostats as thermostats to ensure optimal comfort and energy savings. Moreover, the air conditioners were installed to cool both the rooms, using lower energy in combination with the earth pipe cooling system.



Figure 3.6: Air conditioning unit used in both the containers.

3.2.2. Earth Pipe Cooling Pipe Installation

Buried pipes were aligned vertically underground in a VEPC system while the pipes were aligned horizontally underground in a HEPC system. Both the vertical and horizontal piping systems consisted of two simple Polyvinyl Chloride (PVC) pipes of diameter 125 mm with thickness 4 mm, which are also known as manifolds. Intake air comes through one of the manifolds and passes through a series of buried pipes and moves into the room through another manifold. A blower was fitted inside one of the manifolds and was closed to the wall as shown in Figure 3.2. The blower sucks air from the pipe inlet and pushes it through a series of buried pipes and finally into the room.

3.2.2.1. Blower (Fan) Selection

To drive air through the buried pipes and finally into the rooms, a suitable blower is necessary. Air pressure losses may occur within the pipe, which could reduce the air flow through the pipe. A careful selection of a blower is thus important to ensure the fan power could overcome the pressure loss through the long pipe. A centrifugal inline fan of dimension 125 mm shown in Figure 3.7 was selected to suck the air from pipe inlet. The in-line centrifugal fan of type Vent-Axia of model MAN1503 was used in this study as it is suitable for a variety of domestic, commercial and industrial applications. The dimensions of the data logger can be found at Appendix 3.1.



Figure 3.7: Centrifugal in-line fan.

3.2.2.2. Horizontal Earth Pipe Cooling Pipe Installation

An excavation of dimension 8.1m x 2m was made using an excavator for installing the horizontal earth pipe cooling system as shown in Figure 3.8. Two manifolds as shown in Figure 3.9 were installed at both ends of the excavation.



Figure 3.8: Excavated hole made for horizontal earth pipe cooling system.

Each manifold contains 20 holes of 21 mm diameter each to accept 20 PVC tubes of 20 mm each. The tubes, each of 7.5 m in length with diameter 20 mm, were connected with the manifold. These PVC tubes with a wall thickness of 2 mm were pressed (friction fitting) into the manifold horizontally, i.e. all the PVC tubes were aligned in a single row. Each tube in the row was separated from its neighbour by approximately 20mm. The horizontal earth pipe cooling diagram is shown in Figure 3.9.

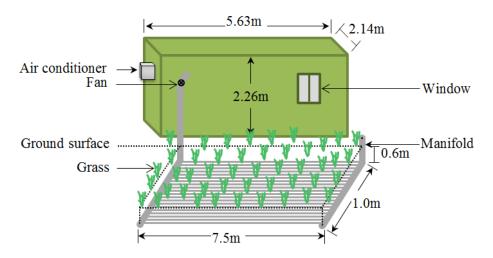


Figure 3.9: Horizontal earth pipe cooling diagram

3.2.2.3. Vertical Earth Pipe Cooling Pipe Installation

An excavation of dimension 8.1m x 1m was made for installing the vertical earth pipe cooling system as shown in Figure 3.10.



Figure 3.10: Excavated hole made for vertical earth pipe cooling system.

Each manifold contains 20 holes of 21 mm diameter each to accept 20 PVC tubes of 20 mm each as shown in Figure 3.11. The tubes of 6 m each in length with diameter 20 mm were connected with the manifold. These PVC tubes with a wall thickness of 2 mm were pressed (friction fitting) into the manifold vertically in 5 rows (Figure 3.11), i.e. each row contained 4 tubes as shown in Figure 3.12.



Figure 3.11: Manifold for vertical installation system.



Figure 3.12: Four PVC tubes connected in a row of the manifold.

Each row of the manifold was separated from one another by 100 mm and each tube in each row was separated from its neighbour by approximately 20mm. Figure 3.13 shows the diagram of the horizontal earth pipe cooling system.

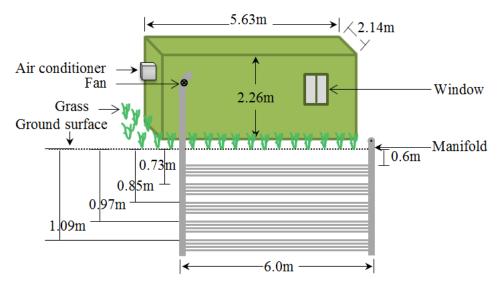


Figure 3.13: Vertical earth pipe cooling diagram

3.2.2.4. Shading for Soil Covering

To increase the cooling effect of the system, small trees were planted (Figure 3.14) to provide shade to the soil which covered the underground pipes. This was intended to reduce the amount of solar energy absorbed by the soil surface. An auto-irrigation system shown in Figure 3.15 was installed to maintain the plants.



Figure 3.14: Plants covered the soil and buried pipes.



Figure 3.15: Auto irrigation system installed to maintain the plants.

The following figures (Figure 3.16 to Figure 3.21) show the construction works at different stages from commencing to finishing the work.



Figure 3.16: Two containers installed at same site in the sustainable precinct.

Figure 3.17: Excavated hole made for installing the buried pipes.



Figure 3.18: Manifold fitted into the ground.



Figure 3.20: Soil distributed to cover the PVC buried tubes.



Figure 3.19: PVC tubes set buried underground for connecting with the manifolds.



Figure 3.21: Small tress and grasses planted into the soil, which covered the PVC buried tubes.

3.3. Instrumentation and Data Collection

The cooling performance of the earth pipe cooling systems was assessed through a suite of experimental design and tests, and field investigation. The field investigation involves soil temperature, air temperature, air velocity, relative humidity and active energy consumed by the air conditioner and fan.

Soil temperature was recorded at 5 different depths (0.60 m, 0.73 m, 0.85 m, 0.97 m and 1.10 m) and 2 different ground surface conditions with bare soil and short grass covered soil. Average air temperature, air velocity and relative humidity data were collected at the pipe inlet, and pipe outlet (Figure 3.22), inside and outside the HEPC and VEPC rooms. All average data were collected at 20 minutes intervals.

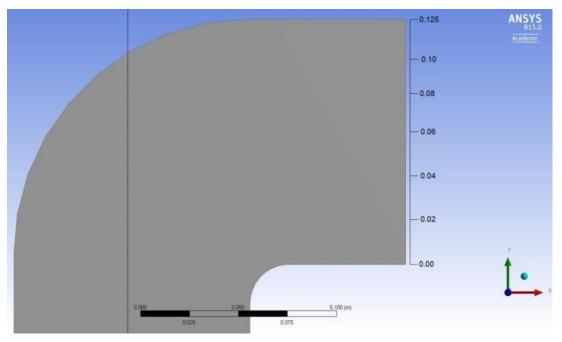


Figure 3.22: Pipe outlet (inlet to the room).

The air conditioner and fan were operated 24 hours daily from 1 December 2013 to 31 March 2014 for measuring the HEPC performance and from 1 December 2014 to 18 February 2015 for measuring the VEPC performance. The operation of the VEPC room was turned off to turn this room into a standard room so that comparison can be made with the HEPC measurement and performance. Likewise, the HEPC room was turned off for assessing the VEPC performance.

To compare the performance between the HEPC and VEPC systems, both the systems was running together during April 2014. The air conditioner and fan was also running 24 hours a day during this period. Types of data and data collecting locations for the HEPC and VEPC system are summarised in Table 3.1. These data will be used in Chapter 4 and Chapter 5 for experimental and numerical analysis of the HEPC and VEPC system.

Data	Location
Outdoor air temperature	Outside the room
Indoor air temperature	At different points inside the room closed to the wall (along the centre and close to the room wall)
Outlet air temperature	At the pipe outlet (inlet to the room)
Inlet air temperature	Inlet to the pipe
Soil temperature	At ground surface with grass covered soil and bare soil, and at different depths underground (0.60 m, 0.73 m, 0.85 m, 0.97 m, and 1.10 m)
Outdoor Relative Humidity	Outside the room
Indoor Relative Humidity	At different points inside the room closed to the wall (along the centre and close to the room wall)
Inlet air velocity	Inlet to the pipe
Outlet air velocity	At the pipe outlet (inlet to the room)
Active energy	From air conditioner

Table 3.1: List of measured data and data logger locations.

All the data were collected through data logging instruments. Table 3.2 presents various measuring instruments that have been used for reading and collecting specific data used in the experimental investigation.

Table 3.2: Measuring instruments used to log data in the experiment.

Data to be Acquired	Measuring Instruments
Outdoor air temperature	HOBO U23-001 Pro v2 Temperature/Relative Humidity Data
	Logger
Indoor air temperature	HOBO U10-003 Temperature Relative Humidity Data
	Logger
Outlet air temperature	HOBO U10-003 Temperature Relative Humidity Data
	Logger
Inlet air temperature	HOBO U23-001 Pro v2 Temperature/Relative Humidity Data
	Logger
Soil temperature	BTM-4208SD 12 CH temperature recorder
Outdoor Relative	HOBO U23-001 Pro v2 Temperature/Relative Humidity Data
Humidity	Logger
Indoor Relative Humidity	HOBO U10-003 Temperature Relative Humidity Data
	Logger
Inlet air velocity	Reed Vane Anemometer
Outlet air velocity	Reed Vane Anemometer
Active energy	G4400 BLACKBOX fixed power quality analyser

Brief descriptions of these measuring instruments are given below:

3.3.1. HOBO U23-001 Pro v2 Temperature/Relative Humidity Data Logger

The HOBO U23-001 Pro v2 is a waterproof data logger, which has built-in relative humidity and temperature sensors. The sensor of relative humidity offers superior stability in any humid environments. It can be utilised for a long period as it is user replaceable. Two data loggers were set outside the container and at the pipe inlet to measure outdoor air temperature and relative humidity, and inlet air temperature. The specification of HOBO U23-001 Pro v2 Temperature/Relative Humidity Data Logger is given in Appendix 3.2.

An optical USB communication interface was used in this logger for reading out and launching the logger. This interface permits the logger to be offloaded without compromising the electronics (Onset, 2010). The compatibility of the USB allows for fast downloads and easy setup. A HOBO waterproof shuttle or an USB-optic base station with a coupler is required for the data logger to connect with the computer as shown in Figure 3.23.

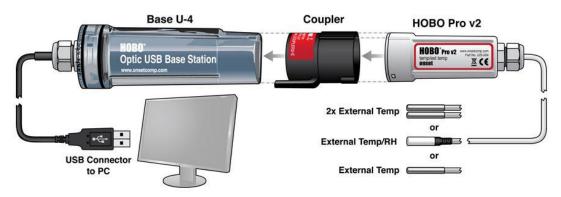


Figure 3.23: HOBO Pro v2 connected with optic base station (Onset, 2015b).

3.3.2. HOBO U10-003 Temperature Relative Humidity Data Logger

The HOBO U10-003 data logger shown in Figure 3.24 was used to measure indoor air temperature, indoor relative humidity and outlet air temperature. It is an economic data logger for monitoring relative humidity and air temperature. The data loggers were set inside the room, one was at the middle of the room and the others were much closer and at different heights along the centre to the wall. Another data logger was set at the pipe outlet (inlet to the room) to record the outlet air temperature, and relative humidity. The main advantage of using this data logger is that it is small in size and has a large memory capacity. The specification of the data logger can be found at Appendix 3.3.



Figure 3.24: HOBO U10-003 data logger (Onset, 2015a).

Soil temperature measurement was one of the key field investigations of this study. The rationale behind measuring the soil temperature at various depths is to determine the optimum depth that could give the most effective result where the pipes were to be buried. Therefore, a multi-channel data logger was required to record the soil temperature at 7 different locations. A Lutron 12 channels temperature recorder of model BTM-4208SD was used to measure soil temperatures.

3.3.3. Lutron 12 Channels Temperature Recorder

T-type Teflon thermocouple wires were used with the Lutron 12 channels data logger to collect the soil temperature data. One end of each thermocouple wire was joined with a custom sized stainless steel tip probe of dimension 100 mm x 4.7 mm, which is shown in Appendix 3.4. The other end was connected with a mini plug (miniature male connector) for fixing with the data logger. The mini plug can be viewed in Appendix 3.5. The steel probes were placed at 5 different depths, namely 0.60 m, 0.73 m, 0.85 m, 0.97 m, and 1.10 m and also on the ground surfaces with grass and without grass.

The Lutron 12 channels temperature recorder is shown in Figure 3.25, which has universal thermocouple input and no cable or special software is required for data logging. Data are saved directly on an SD card and are transferrable to a computer. Data can be analysed off the SD card using a standard spreadsheet program (ECEFast, 2015). The large illuminated display can demonstrate 8 values at a time and the remaining 4 on the other screen. The units come with a hard case and a 2 GB SD card.



Figure 3.25: Lutron 12 channels temperature recorder (Lutron, 2011).

The T-type thermocouple wire used in the data logging process measures the temperature ranges from -50 to 400°C with accuracy \pm (0.4%+0.5). Each of the 7 thermocouple wires was connected to the data logger by a Type T. The data logger was connected to a 9 Volts AC/DC Power Adapter to operate it for a long period as it only has one hour back up. The specifications of the adapter and the temperature recorder data logger are presented in Appendix 3.6 and Appendix 3.7 respectively.

3.3.4. Reed Vane Anemometer

Air velocity was measured at the inlet and outlet of the pipe, since it has a significant influence on the earth pipe cooling performance. A Vane Anemometer data logger, as shown in Figure 3.26, was used to record the air velocity. A 9 Volts AC/DC Power Adapter was connected with this data logger to power it for the required period. The specifications of the instrument are given in Appendix 3.8.



Figure 3.26: Vane Anemometer data logger (MicroDAQ, 2015).

3.3.5. G4400 BLACKBOX Fixed Power Quality Analyser

Energy consumption of the air conditioner installed in the rooms for the earth pipe cooling system analysis was measured using the G4400 Blackbox as shown in Figure 3.27. This device was used for monitoring active energy consumed by the air conditioner as it can provide accurate detection and isolation of power quality monitoring (SUPREME, 2014). It can store all the data on board in the waveforms of each network cycle for up to one year and at up to 1024/cycle resolution.



Figure 3.27: Power quality analyser Blackbox

The power quality analyser requires power quality management software to analyse, configure, compare and control time synchronised data. PQSCADA is such a software and was used for data logging. It can be linked by TCP, RTU, GPRS, or IP wireless. The data were logged remotely using the University network. The specification of the logger is provided in Appendix 3.9.

3.4. Conclusion

A complete experimental design and approach has been presented for achieving the objectives of this study. Experimental and data measuring procedures are described and explained. For the experimental measurement, two containers were converted into office rooms and were connected with horizontal and vertical earth pipe cooling systems. The appropriate and suitable data measuring tools and instruments were fitted in the proper places. Air velocity, air temperature, soil temperature, relative humidity, and the energy consumption were recorded using the data measuring instruments for measuring the earth pipe cooling performance.

CHAPTER 4 : PERFORMANCE ANALYSIS OF HORIZONTAL EARTH PIPE COOLING SYSTEM

4.1. Introduction

This chapter presents the results and analysis of the horizontal earth pipe cooling (HEPC) system. The chapter also reports the development of an integrated model for the horizontal earth pipe cooling system. The cooling performance of the horizontal earth pipe cooling system was measured in summer (wet season). An investigation was carried out for soil temperature to observe the cooling potential of the soil in Rockhampton, Australia. The impact of air temperature, air velocity and relative humidity on room cooling performance was assessed to measure the horizontal earth pipe cooling performance. The energy consumption consumed by the system was also assessed to evaluate the energy efficiency of the system.

The experiment was carried out in December 2013, and January and February 2014 during the summer. In Rockhampton, the summer is from December to February, whereas the winter is from June to September (AG, 2013). The winter was not considered for this investigation as this research deals with the cooling potential of the horizontal earth pipe cooling system. Moreover in winter, the soil temperature is normally greater than the outdoor air temperature, so this season is more suitable for assessing heating performance of a space.

An integrated model for the horizontal earth pipe cooling system was developed using ANSYS Fluent 15.0. The numerical results obtained through the simulation of this model were compared with the experimental results. The horizontal earth pipe cooling model was found to be validated as the numerical data showed a good agreement with the experimental data. Both the experimental and numerical results showed a temperature reduction in the room which will assist in saving energy costs in buildings.

4.2. Soil Temperature Investigation in Summer 2013-2014

The soil temperature investigation was conducted in summer to seek potential cooling using the earth pipe cooling system buried in the soil of Rockhampton, Australia. The temperature sensors of the data logger, Lutron 12 channels temperature recorder discussed in chapter 3, was buried into the ground at different depths of 0.60 m, 0.73 m, 0.85 m, 0.97 m, and 1.10 m, where the ground surface was covered by grass. The soil temperatures were recorded at these points to compare them with the outdoor temperature. Data were collected at 20 minutes interval during the summer of 2013-2014. Figure 4.1 shows a typical soil temperature profile over a 24 hour period at different depths.

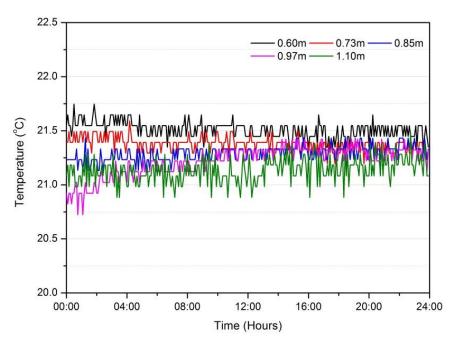


Figure 4.1: Hourly average soil temperature distribution during summer 2013-2014.

Figure 4.1 illustrates the hourly average soil temperature over the period of December 2013-February 2014. As seen, the soil temperature at the various depths varies from 20.72°C to 21.75°C. The lowest average soil temperature distribution was observed at the depth of 1.10 m underground. The maximum average temperature reduction of 0.70°C was found between the soil temperatures at 0.60m and 1.10m depth. This reduction occurred at the middle of the day (12:20 pm) on 12 January 2014. Usually, soil temperature gets cooler during the hot peak hours than during the off peak hours in summer. However, the soil temperature at 0.60 m depth

(where the pipes were buried) was compared with the outdoor air temperature to find the maximum temperature difference as shown in Figure 4.2.

It is seen that the underground soil temperatures were lower than the ground surface temperature and that the soil temperature decreases with increasing depth. However, from various literature, it is seen that this temperature reduction continues up to a depth of 4m underground as the soil temperature is fairly constant and stable at that depth (Santamouris et al., 1995).

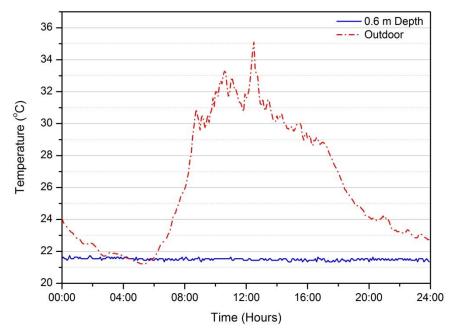


Figure 4.2: Temperature distribution of soil at 0.6 m depth and outdoor air.

Figure 4.2 shows the hourly average temperature on a typical day at 0.6 m depth and at the outdoor, where the outdoor temperature varies from 21.22°C to 35.10°C. The maximum diurnal temperature during this period was 14.9°C, which occurred on 7 December 2013. Meanwhile, the minimum diurnal temperature was 3.6°C, which occurred on 19 December 2013. Figure 4.2 illustrates that the outdoor air temperature is lower after midnight from 4:20 am to 5:40 am. The outdoor air temperature normally falls during the late night and increases during the day.

The average temperature reduction between the outdoor and soil temperature at 0.6 m depth was observed as 5.25°C, while the temperature reduction varies from 0.1°C to 13.35°C. The maximum temperature reduction occurred at middle of the day

(12:40 pm), whereas the minimum reduction was observed at late night (4:20 am). The reduction in temperature during the day contributed to the cooling of the room with the horizontal earth pipe cooling technology. As the soil temperature was below the outdoor minimum temperature during the peak warming hours of the day, it worked as an effective heat sink to cool the room.

The surface condition of the ground is an important factor that affects the earth pipe cooling performance. A bare ground surface allows exposure to solar radiation especially in a hot, humid climate like Rockhampton, Australia. The ground surface with bare soil is comparatively warmer than the ground surface with covered grass soil as the heat generated due to the solar radiation dissipated into the soil. Figure 4.3 shows the temperature distribution of the ground surfaces between grass covered soil and bare soil.

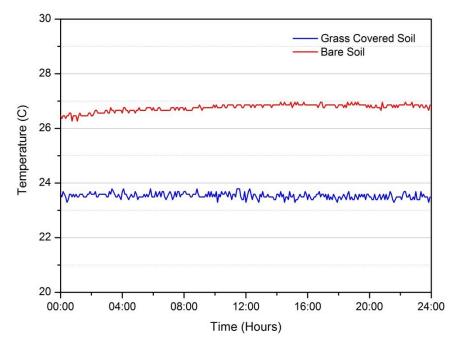


Figure 4.3: Ground surface temperatures of grass covered soil and bare soil.

Short grass covered soil offers more cooling potential than the bare soil (Mihalakakou et al., 1994). An average temperature reduction of 3.12°C was found between the two ground surfaces of bare soil and grass covered soil, where the grass covered soil temperature was found to be lower. This result also agrees with the other studies (Mihalakakou et al., 1994, Jacovides et al., 1996). This difference occurred due to the effect of high solar radiation on unshaded or uncovered soil.

4.3. Experimental Investigation for Horizontal Earth Pipe Cooling System

The horizontal earth pipe cooling investigation was carried out during the summer from December 2013 to February 2014. Data were collected from both the HEPC and VEPC room by turning off the VEPC system. In this case, the VEPC system was turned off and the room was considered as a standard room (not connected to any earth pipe cooling system). All the data collected included the amount of radiation, and were recorded at 20 minutes interval. Impact of the climatic variables which affects the earth pipe cooling performance was assessed through this investigation. Average soil temperature at different depths; average air temperature and relative humidity at pipe inlet, pipe outlet, inside and outside the room; average air velocity at the pipe inlet and outlet; and average energy consumed by the air conditioner were taken into consideration for this investigation.

As indicated earlier, the earth pipe cooling performance impacts on the climatic variables of air temperature, relative humidity and air velocity. The HOBO U10-003 data logger, discussed in chapter 3, was set at different points inside both the HEPC and the standard room to measure indoor air temperature and relative humidity. Another data logger, namely HOBO U23-001 Pro v2, was placed just outside the room to record the outdoor temperature and relative humidity. The temperature profile of horizontal earth pipe cooling, standard room and outside the room is shown in Figure 4.4.

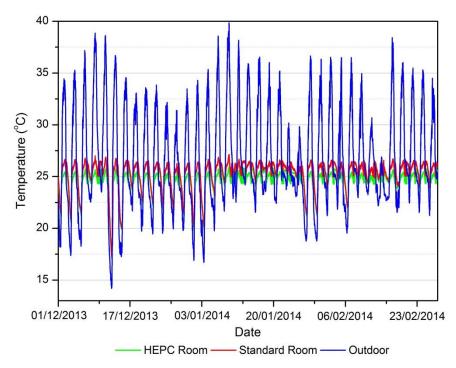


Figure 4.4: Temperature fields in the horizontal earth pipe cooling and standard room close to the wall, and outdoor.

The Figure 4.4 illustrates the daily indoor room temperature, which varies from 17.03°C to 27.18°C in the horizontal earth pipe cooling room, and 17.13°C to 27.33°C in the standard room, while the outdoor temperature ranges from 14.19°C to 39.86°C. A maximum temperature reduction of 2.18°C was observed between the horizontal earth pipe cooling and the standard room, whereas the average room temperature reduction was 1.13°C between those two rooms. It is noted that the outdoor temperature gets lower than the room temperature during the night due to cooler weather.

The relative humidity of the air has also a noticeable impact in the context of thermal comfort. It is an essential variable to measure, especially in hot climates. The relative humidity of the rooms as shown in Figure 4.5 was measured to assess its impact inside the rooms. The air temperature and relative humidity inside and outside the rooms are summarised in Table 4.1.

	Indoor Temperature			Outdoor Temperature			Relative Humidity		
Modelled rooms	Min (°C)	Max (°C)	Avg (°C)	Min (°C)	Max (°C)	Avg (°C)	Min (%)	Max (%)	Avg (%)
HEPC	17.03	27.18	24.64	14.19	39.86	26.76	40.68	84.5	64.89
Standard Room	17.13	27.33	25.77				41.08	82	63.67

Table 4.1: Air temperature and relative humidity in the HEPC and standard room.

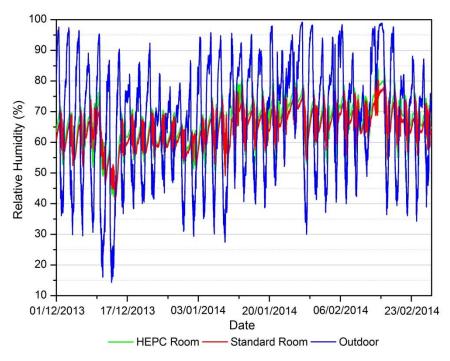


Figure 4.5: Relative humidity measured in the HEPC room, standard room and outdoor.

As seen from Table 4.1, the relative humidity ranges from 40.68% to 84.50% in the HEPC room, from 41.08% to 82% in the standard room, and from 14.35% to 99.2% outside the rooms as shown in Figure 4.5. The average relative humidity of HEPC was 64.89%, which is acceptable in the context of thermal comfort for the average measured temperature of 24.64°C as indicated by Szokolay (2008). It was also observed that the horizontal earth pipe cooling room humidity is 1.22% higher than the standard room. The incoming air through buried pipes into the room creates this additional humidity in the earth pipe cooling system.

The measurement carried for HEPC system was compared with the ASHRAE standard 55-2010 using the centre for the built environment (CBE) thermal comfort tool. The measured average temperature and relative humidity of the horizontal earth pipe cooling system displayed in Table 4.1 complies with the ASHRAE standard 55-2010 (ASHRAE, 2004), Brown's bioclimatic chart (Brown, 1985) and Givoni's chart (Givoni, 1992).

The air temperature and velocity were also measured at the pipe inlet and outlet (inlet to the room) to evaluate their impact on HEPC performance. For measuring the inlet air temperature, the waterproof data logger of HOBO U23-001 Pro v2 was set at the pipe inlet to protect it from heavy rain. Meanwhile, HOBO U10-003 data logger was placed at the pipe outlet (inlet to the room) to observe the outlet air temperature. The inlet and outlet temperature data were recorded over 24 hour duration as shown in Figure 4.6.

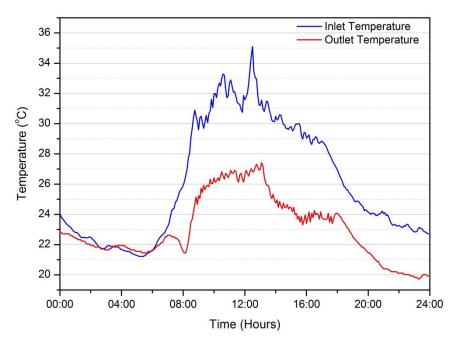


Figure 4.6: Temperature field at pipe inlet and outlet.

Figure 4.6 shows the inlet and outlet air temperature profile, where both the profiles present a similar trend. The inlet temperature varies from a minimum of 21.22°C at 3:40 am to a maximum of 35.10°C at 12:20 pm, while the outlet temperature varies from 19.74°C at 4:40 am to 27.42°C at 12:40 pm. The inlet air temperatures get lower during the night and started to rise during the day. The rising temperatures

reach to peak from around 10 am to 5 pm. The inlet temperature was found as quite lower during the late night and early morning from 2:35 am to 2:50 am and 3:35 am to 6:00 am respectively. Usually, the outdoor temperature in Rockhampton falls at the late night and early morning. When the cooler outdoor temperature comes to the inlet and goes through the buried pipes, it gains heat from the soil as the soil works as a heat source in cool weather. Then the heated air moves to the pipe outlet and hence the higher temperature arises during this period.

The inlet and outlet data were recorded over the summer 2013-2014 (92 days). The average of these data showed 3.08°C temperature reduction at the pipe outlet. This reduction increases to 5.45 °C during the hot peak hours of the day from around 10:00 am to 5 pm. The temperature profiles at the pipe inlet and outlet is shown in Figure 4.7. As the outside temperature warmed up due to the sun light, the soil temperature remained cooler. The higher temperature differential between the inlet air temperature and the soil temperature improves the cooling process and thus produces more temperature reduction during this period.

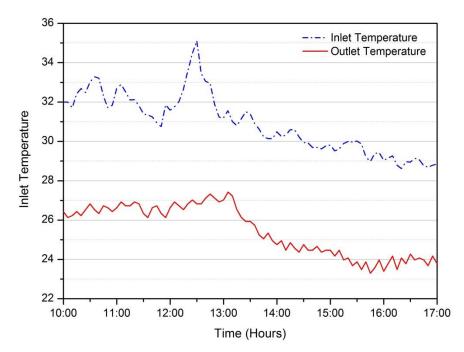


Figure 4.7: Temperature profile at pipe inlet and outlet during hot pick hours.

Although the pipe outlet temperature dropped more during the warming hours, a 24 hour data collection and measurement were taken for evaluating the overall

performance of the earth pipe cooling system during the whole summer. This approach is consistent with other studies undertaken elsewhere. It is noted that the higher temperature reduction at the pipe outlet indicates that the earth pipe cooling system has the potential to reduce more temperature in the room, and hence save more energy during the warming hours from 10:00 am to 5:00 pm. To reduce the air temperature at the pipe outlet, the air velocity plays an important role. The trend of air velocity at the pipe inlet and outlet is shown in Figure 4.8.

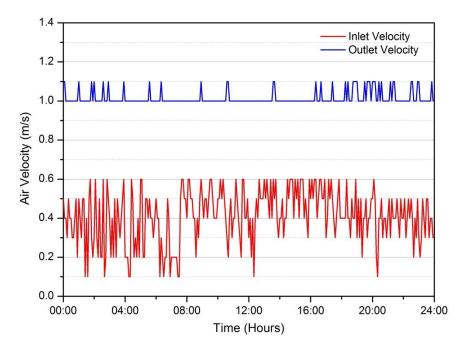


Figure 4.8: Trend of air velocity at pipe inlet and outlet.

As seen from Figure 4.8, the air velocity at the pipe inlet ranges from 0.1 m/s to 0.6 m/s and the mean value of these velocities of 0.41 m/s was taken for the simulation of pipe model in section 4.4.2.1. Meanwhile, the outlet velocity (inlet to the room) varies from 1 m/s to 1.1 m/s, while the average velocity is 1.01 m/s. As discussed in chapter 3, a blower was set at the pipe outlet to suck the air from the pipe inlet. This increases the air velocity at the pipe outlet which is cooled by the soil under the ground. This cooler outlet velocity produces cooler temperature, which assists the earth pipe cooling technology to cool the room. The amount of the cooling rate of the air at the pipe, temperature difference between soil temperature and ambient air temperature, and the thermal conductivity of the buried pipe.

4.4. Model Development for Horizontal Earth Pipe Cooling System

An integrated model was developed for the horizontal earth pipe cooling system. But for the simplicity of the model, the integrated model was divided into two parts, one includes all the pipes considered as the earth pipe model and the other consists of the room only; considered as the room model. The procedures for the development of the integrated model are described below.

4.4.1. Modelling Approaches

The modelling approaches used for both the horizontal and vertical earth pipe cooling system in this research are presented in this section. A thermal model was developed for the horizontal earth pipe cooling system. The model involves heat transfer process, where the air when passing through the buried pipes underground, transfers excess heat to the earth and thus gets cooled.

The Realisable $k - \varepsilon$ turbulence model was used to analyse the heat transfer problem of the system. This is a reliable and more accurate model which is applicable for an extensive class of turbulent flows in heat transfer and industrial flow simulations. The turbulence model was selected for the modelling as the flow passing through the buried pipe outlet (inlet to the room) was turbulent. It was calculated from the Reynolds number equation discussed in section 2.7. The problem was solved numerically by using the CFD code "Fluent in ANSYS 15.0", which employs the finite volume method for discretisation of the computational domain that was discussed in section 2.8.

4.4.1.1. Modelling Equations

The Realisable $k - \varepsilon$ model is derived from the Navier-Stokes equations. The Navier-Stokes equation of motion and the transport equations for the Realisable $k - \varepsilon$ model are given by (ANSYS, 2010):

$$\frac{\partial u_i}{\partial t} + u_j \frac{\partial u_i}{\partial x_j} = -\frac{1}{\rho} \frac{\partial p}{\partial x_i} + \upsilon \frac{\partial^2 u_i}{\partial x_j \partial x_j}$$
(4.1)

and

$$\frac{\partial(\rho k)}{\partial t} + \frac{\partial(\rho k u_j)}{\partial x_j} = \frac{\partial}{\partial x_j} \left[\left(\mu + \frac{\mu_t}{\sigma_k} \right) \frac{\partial k}{\partial x_j} \right] + G_k + G_b - \rho \varepsilon - Y_M + S_K$$
(4.2)

$$\frac{\partial(\rho\varepsilon)}{\partial t} + \frac{\partial(\rho\varepsilon u_j)}{\partial x_j} = \frac{\partial}{\partial x_j} \left[\left(\mu + \frac{\mu_t}{\sigma_\varepsilon} \right) \frac{\partial\varepsilon}{\partial x_j} \right] + \rho C_1 S \varepsilon - \rho C_2 \frac{\varepsilon^2}{k + \sqrt{\upsilon\varepsilon}} + C_{1\varepsilon} \frac{\varepsilon}{k} C_{3\varepsilon} G_b + S_{\varepsilon} \quad (4.3)$$

where u_i , u_j are the fluid velocity components (m s⁻¹), x_i is the component of length (m), p is the pressure (Pa), $v = \mu / \rho$ is the molecular kinetic viscosity of the fluid (m² s⁻¹), μ is the fluid viscosity (kg m⁻¹s⁻¹), ρ is the fluid density (kg m³), t is the time (s), k is the kinetic energy (m² s⁻²), ℓ is the dissipation rate (m² s⁻³), G_k is the generation of turbulence kinetic energy due to the mean velocity gradients (kg m⁻¹s⁻²), G_b is the generation of turbulence kinetic energy due to buoyancy (kg m⁻¹s⁻²), Y_M represents the contribution of the fluctuating dilatation in compressible turbulence to the overall dissipation rate (kg m⁻¹s⁻²), $C_{1\epsilon}$ and $C_{2\epsilon}$ are constants, $C_{3\epsilon} = \tanh \left| \frac{u_1}{u_2} \right|$ where u_1 and u_2 are the velocity components parallel and perpendicular to the gravitational vector respectively, σ_k and σ_{ϵ} are the turbulent Prandtl numbers for kand ℓ respectively, S_k and S_ϵ are user-defined source terms, and i, j, k (=1, 2, 3) are the direction vector index.

The energy equation for this heat transfer problem is solved throughout the entire domain and is given by:

$$\frac{\partial(\rho E)}{\partial t} + \nabla . \left(\vec{v} \left(\rho E + P\right)\right) = \nabla . \left(k_{eff} \nabla T - \sum_{j} h_{j} \vec{J}_{j} + \left(\vec{\tau}_{eff} . \vec{v}\right)\right) + S_{h}$$

$$(4.4)$$

where k_{eff} is the effective conductivity (W m⁻¹ K⁻¹), k_t is the thermal conductivity for turbulent flow, J_j is the component of diffusion flux (m⁻² s⁻¹), T is the temperature (K), $\nabla \cdot (k_{eff} \nabla T)$ is the heat transfer due to convection, h is the enthalpy (J kg⁻¹), $\nabla \cdot (\sum_j h_j \vec{J}_j)$ is the species diffusion, $\nabla \cdot (\stackrel{=}{\tau_{eff}} \cdot \vec{v})$ is the heat transfer due to viscous diffusion and S_h is the total entropy (JK⁻¹). The term S_h represents the radiation source terms when radiation model was used.

4.4.1.2. Geometry of the Model

Two 2D geometries were created in DesignModeller; one is for the pipe model and the other is for the room model. The geometry of the pipe model consists of 20 PVC pipes, each of length 7.5 m, diameter 20 mm and thickness 2 mm. These 20 PVC pipes were connected with two manifolds of thickness 4 mm, which have also been included in this model. The room model geometry comprises the earth pipe cooling room only of dimension 5.63 m x 2.26 m. The geometries can be found in Appendix 4.1.

4.4.1.3. Mesh Generation

A typical mesh was generated for both the pipe and room model using DesignModeller in ANSYS 15.0 as shown in Figure 4.9 and Figure 4.10 respectively. To generate the mesh, a 0.01m element size was used for both the models. This element size produced 46,245 and 127,367 elements in the meshing of pipe and room model respectively. However, a study was carried out to check the impact of grid variation and to establish optimum mesh size to ensure consistent results for every mesh size as discussed in section 4.4.1.5.

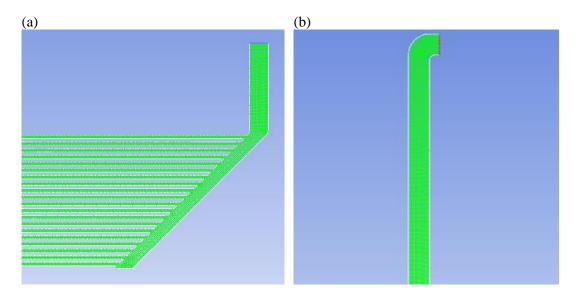


Figure 4.9: Mesh for HEPC pipe model. (a) Showing inlet. (b) Showing outlet (inlet to the room)

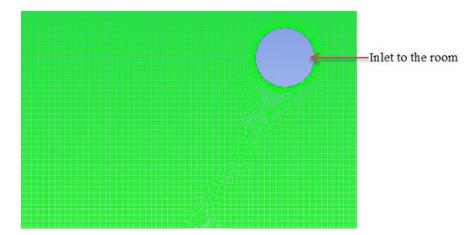


Figure 4.10: Mesh pattern for HEPC room model.

4.4.1.4. Solver Approaches

A two dimensional pressure-based-coupled solver was used for the numerical calculations of the model. It solves a coupled system of equations along with the pressure-based continuity and momentum equations (Tan et al., 2012). With the coupled algorithm, each iteration consists of the following steps as shown in the Figure 4.11.

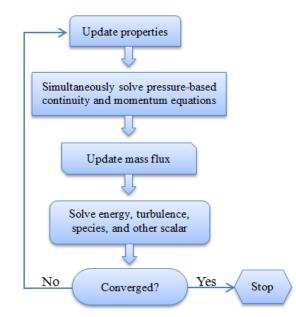


Figure 4.11: Pressure-based coupled algorithm.

The pressure-based-coupled solver offers some additional advantages over a segregated or non-coupled approach, although it has some limitations. The coupled scheme allows a robust and efficient single phase execution for steady-state flows

with high performance compared to the other solution schemes (ANSYS, 2006). It is necessary to use the coupled algorithm for transient flows, when the mesh quality is poor or the time step used in the solver is large. To account for the radiation effect, Rosseland radiation model was used in the simulation which is also available in the pressure based solver. This radiation model is faster than the other models, and it requires less memory (ANSYS, 2006).

Pressure was discretised with a PRESTO scheme in view of its strong convergence ability. The scheme is available for all meshes such as tetrahedral, triangular, hexahedral, quadrilateral and hybrid meshes. Spatial discretisation with second-order upwind schemes was used for the turbulent dissipation rate, turbulent kinetic energy and momentum as the second-order discretisation of the viscous terms is always accurate in Fluent. Moreover, the differencing scheme of second-order upwind was utilised to overcome numerical dispersion. At the end of the solver iteration, the moment coefficient, lift and drag are calculated and stored to create a convergence history. The standard initialisation in the entire domain used in this study allows setting the initial values of the flow variables and initialising the solution with these values.

4.4.1.5. Grid Independence Study

Three grids were generated for both the pipe and room model of the HEPC system using different element sizes as summarised in Table 4.2. The pipe model involves the element sizes of 0.01m, 0.005m and 0.003m, where 0.01m element size was used for generating the mesh of the pipe model for this study. Grid 2 and Grid 3 in Table 4.2 represent different mesh size, which was obtained by changing 0.01 m element size to 0.005m and 0.003m respectively. Likewise, the room model comprises the element sizes of 0.01m, 0.008m and 0.005m, where 0.01m element size was used for generating the mesh of the room model of this study. The Grid 2 and Grid 3 shows different mesh size, which was produced by changing 0.01m element size to 0.008m and 0.005m respectively.

Grid size	Element size (m)		No	des	Elements		
	Pipe	Room	Pipe	Room	Pipe	Room	
Grid 1	0.01	0.01	59066	128202	46245	127367	
Grid 2	0.005	0.008	179759	200504	153903	199464	
Grid 3	0.003	0.005	447920	510956	403149	509296	

Table 4.2: Different grid sizes for HEPC model.

The temperature fields at the outlet of the pipe model are shown for different mesh sizes in Figure 4.12. The simulated pipe outlet temperature using Grid 1 shows consistent results with the outlet temperature using Grid 2 and Grid 3. The figure illustrated that the simulated outlet temperature using Grid 2 and Grid 3 lie within 1-2% of values attained with Grid 1. A similar result was found for the room model as shown in Figure 4.13. Consequently, this study was progressed using Grid 1 for simulating the HEPC pipe and room model as this grid size takes less time for numerical computations.

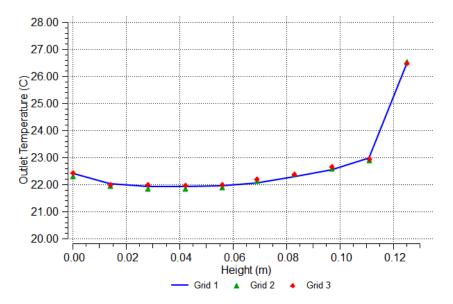


Figure 4.12: Temperature fields at the outlet of pipe model for different mesh size.

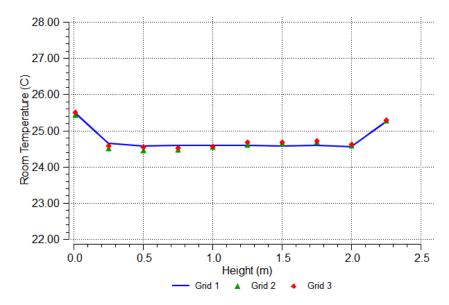


Figure 4.13: Temperature fields at different heights of HEPC room for 3 mesh sizes.

4.4.2. Simulation Results and Discussion

Performance of the earth pipe cooling system was calculated numerically. The flow and thermal variables for the boundary and cell zone conditions were set on the boundaries of the models. No slip boundary conditions were applied on the pipe walls and room walls. The cell zone condition for the surface body was defined as fluid in both the pipe and room models. The following section shows the simulation results for both the models.

All the simulations were run on an Intel Xeon CPU E3-1225 V3 @ 3.20 GHz processor computer of RAM 16.0GB (15.8 GB usable). Two simulations were allowed to run simultaneously on the computer, one is for the pipe model and other is for the room model. The solutions were convergent at 139 and 174 iterations, which required the total CPU time of 44.20 seconds and 55.32 seconds for the pipe and the room model respectively. The total CPU time does not include any waiting time for communications or load imbalances.

To check the convergence of the solutions, the residuals were used for the equations of continuity, momentum, energy, k and ε . 1e-06 was used as the absolute convergence criterion since 1e-06 provides better result for the convergence of the solutions to the turbulent flows (ANSYS, 2006). The lower convergent residuals

have not been considered here since residuals less than 1e-06 are used for the laminar flows.

4.4.2.1. Simulation for HEPC Pipe Model

The simulation results of the pipe model were obtained using the boundary conditions which are shown in Table 4.3. The measured average air velocity of 0.41 m/s and the average air temperature of 26.76°C at the pipe inlet were set as the inlet velocity and inlet temperature respectively in the boundary conditions of the model. The exhaust fan operated in the horizontal earth pipe cooling technique was set as the outlet of the pipe model. A soil temperature of 21.51°C at 0.6 m depth (where the 20 PVC pipes were laid and aligned) was also used in the boundary conditions. The soil temperature was found to be 5.25°C lower than the outdoor temperature. As mentioned earlier, soil temperature decreases in summer with increasing depth, which allows the utilisation of earth as a heat sink.

Parameters	Value
Inlet velocity	0.41 m/s
Inlet temperature	26.76°C
Soil temperature at 0.6 m depth	21.51°C
Thermal conductivity of PVC pipe	0.16 W/m-K
Density of PVC pipe	1390 kg/m ³
Specific heat of PVC pipe	1000 J/kg-K
Air thermal conductivity	0.024 W/m-K
Air density	1.204 kg/m ³
Specific heat of air	1006.43 J/kg-K
Air viscosity	1.850387e-05 kg/m-s

Table 4.3: Parameters used in boundary conditions of the HEPC pipe model.

Figures 4.14, 4.15 and 4.16 show the temperature distribution throughout the pipes, at the pipe inlet and pipe outlet respectively, while Figures 4.17, 4.18 and 4.19 show the velocity distribution through the entire pipes, at the pipe inlet and pipe outlet respectively.

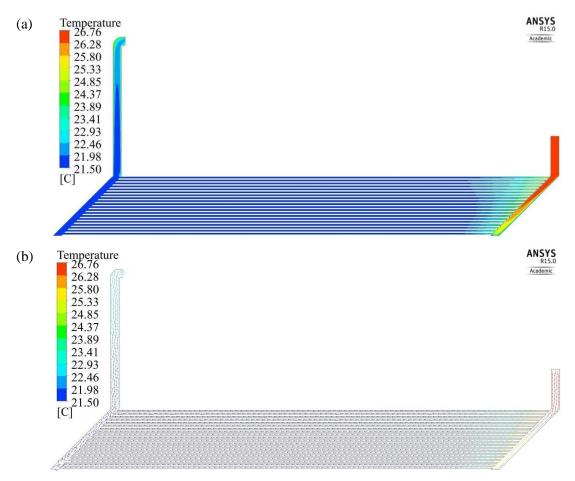


Figure 4.14: Temperature fields throughout the pipes in HEPC system. (a) Temperature magnitude. (b) Temperature vector.

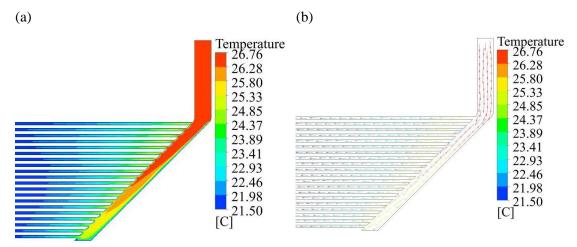


Figure 4.15: Temperature fields at the pipe inlet in HEPC system. (a) Temperature magnitude. (b) Temperature vector.

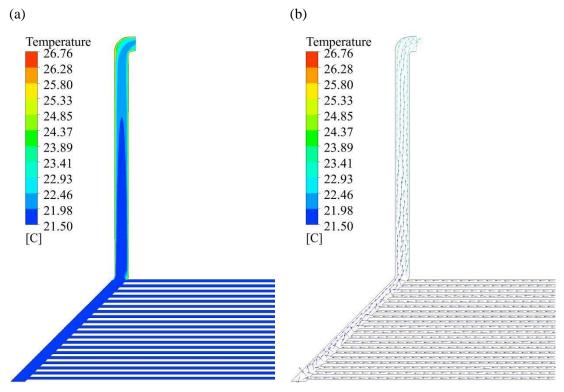


Figure 4.16: Temperature fields at the pipe outlet in HEPC system. (a) Temperature magnitude. (b) Temperature vector.

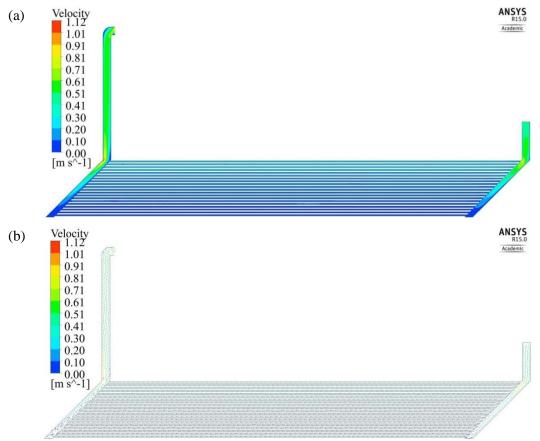


Figure 4.17: Velocity fields throughout the pipes in HEPC system. (a) Velocity magnitude. (b) Velocity vector.

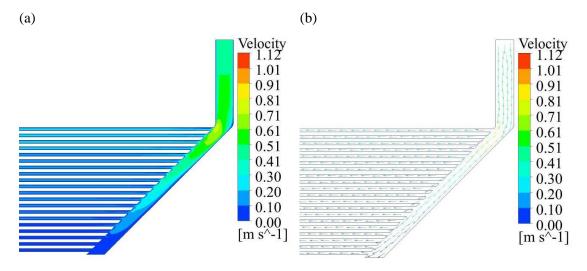


Figure 4.18: Velocity fields at the pipe inlet in HEPC system. (a) Velocity magnitude. (b) Velocity vector.

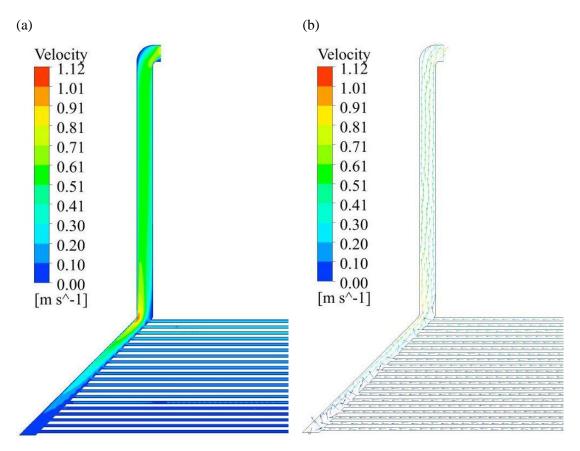


Figure 4.19: Velocity fields at the pipe outlet in HEPC system. (a) Velocity magnitude. (b) Velocity vector.

Referring to the Figure 4.14, the air temperature varies from 21.50°C and 26.76°C throughout the pipes, where the maximum occurs at pipe inlet and the minimum occurs in the buried pipe underground. The reason is that the outside hot air moves to

the pipe inlet, goes down to the buried pipes and gets cooler by transferring heat to the soil, and finally moves the cooler air to the pipe outlet. When the air passes through the 7.5 m long buried pipes, it gets adequate time to transfer heat to the soil by convection, and thus the air is cooled.

The outlet air temperature was found to be higher than the buried pipes end as shown in Figure 4.16. This higher outlet temperature occurs because of the heat generated by the motor of the fan set at the pipe outlet. When the cooler air comes through the buried pipes to the pipe outlet, the air absorbs heat from the atmosphere due to conduction. Air velocity may be another reason for this higher air temperature at the pipe outlet.

An average outlet temperature of 22.65°C and air velocity of 0.89 m/s were found in the simulation results, which shows a good agreement with the measured average outlet temperature of 23.08°C and velocity of 1.01 m/s. These results show a 1.90% difference with the average outlet temperature, while an 11.88% difference with the average outlet velocity. Differences between the numerical and experimental results at different heights of the pipe outlet are shown in Table 4.4.

Height (m)	Experimental (°C)	Numerical (°C)	Differences (%)
0.13	26.95	26.45	2.21
0.11	24.18	22.98	5.30
0.10	22.85	22.55	1.32
0.08	22.75	22.27	2.12
0.07	22.35	22.05	1.32
0.06	21.85	21.95	0.41
0.04	22.15	21.92	1.05
0.03	22.18	21.94	1.06
0.01	22.21	22.02	0.85
0.00	23.33	22.40	4.11

Table 4.4: Comparison of temperature between experimental and numerical (simulation)results at pipe outlet.

Figure 4.20 shows the temperature profile plotted by experimental and numerical results along the centre of the pipe outlet, where the maximum temperatures occur at

both end of the outlet. This maximum temperature is due to the solar impact on the outlet ends. The temperature at top end of the outlet (0.12 m) is higher than that of the bottom end of the outlet as there is a direct solar impact on the top end, while the bottom end is slightly shaded by the pipe. The minimum temperature occurs close to the middle of the pipe outlet.

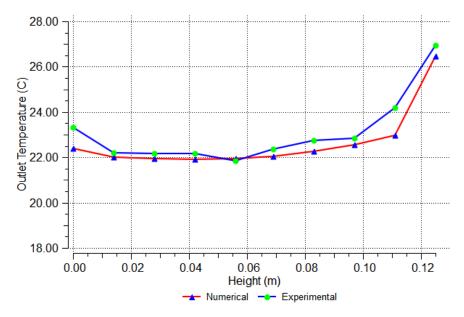


Figure 4.20: Numerical data plotted against experimental data at the pipe outlet.

The overall simulated results are in very good agreement with the corresponding experiments as shown in Figure 4.20, though there are some slight variations (Table 4.4) between these results. The probable reason for these variations is the measurement uncertainties in the experiments due to the instrument accuracy, reading, test planning, environment, condition, calibration etc. Other reason is the uncertainties and errors in CFD simulations because of the auxiliary physical models (Oberkampf et al., 2001) of turbulence model used in this study. Additionally, this may also occur due to the initial and boundary conditions, discretisation and solution.

4.4.2.2. Simulation for HEPC Room Model

The outlet of the pipe model was used as the inlet of the horizontal earth pipe cooling room model. The average outlet air temperature (Table 4.4) and velocity calculated at the pipe outlet (inlet to the room) of the pipe model were set as the inlet air temperature and velocity in the room model respectively. The average maximum room temperature recorded from the standard room was set as the room temperature

of the model. The simulation results of the room model were obtained using the boundary conditions which are shown in Table 4.5. Figure 4.21 and Figure 4.22 show the temperature and velocity profile in the horizontal earth pipe cooling room respectively.

Parameters	Value
Inlet velocity	0.89 m/s
Inlet temperature	22.65°C
Standard room temperature	25.77°C
Air thermal conductivity	0.024 W/m-K
Air density	1.204 kg/m ³
Specific heat of air	1006.43 J/kg-K
Air viscosity	1.850387e-05 kg/m-s

Table 4.5: Parameters used in boundary conditions of the room model.

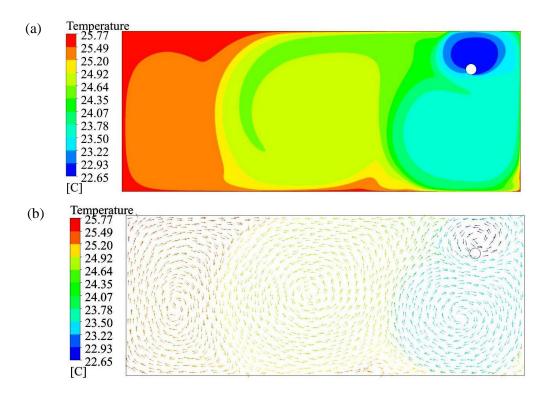


Figure 4.21: Temperature profiles in horizontal earth pipe cooling room (a) Temperature magnitude. (b) Temperature vector.

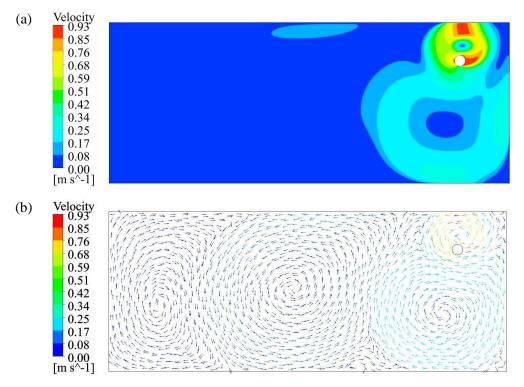


Figure 4.22: Velocity profiles in horizontal earth pipe cooling room. (a) Velocity magnitude. (b) Velocity vector.

The simulation result presented in Figure 4.21 shows the room temperature of the horizontal earth pipe cooling system, which ranges from 22.65°C to 25.77°C. The room temperature gets cooler at the inlet and its surroundings, while the temperature gets warmer at the points closed to the room walls. The air velocities at the inlet are comparatively stronger than the other points of the room as shown in Figure 4.22. Moreover, no noticeable airflow is seen at other points except the inlet and its surroundings.

The average temperature of 24.74°C was found in the HEPC room, which is 1.03°C lower than the standard room temperature. This temperature reduction was achieved because of the incoming cooled air through the pipe outlet (inlet to the room). As mentioned earlier, the air is cooled by transferring heat to the soil when it passes via buried pipes.

The room temperatures obtained using simulation was compared with the corresponding experimental results at different heights along the centre of the room wall. Table 4.6 shows the comparison in room temperature between the simulation

and experimental results. The overall simulated results are in very good agreement with the corresponding experiments as shown in Figure 4.23, and lie within 0.37%-4.11% variation in the earth pipe cooling room.

Height (m)	Experimental (°C)	Numerical (°C)	Differences (%)
0.01	24.72	25.49	3.03
0.25	23.88	24.65	3.13
0.50	24.05	24.57	2.12
0.75	24.32	24.58	1.07
1.00	24.33	24.58	1.03
1.25	24.69	24.58	0.44
1.50	24.82	24.57	1.01
1.75	24.49	24.58	0.37
2.00	24.82	24.54	1.13
2.25	26.28	25.24	4.11

 Table 4.6: Comparison in room temperature between experimental and simulation (numerical) results of room model.

An average temperature reduction of 1.13°C was observed through the field work investigation, while 1.03°C was found through the simulation works. The simulation results showed some deviations from the experimental results which are believed to be due to the measurement errors (section 4.7), and the uncertainties and errors in CFD simulations as discussed in section 4.4 .2 .1.

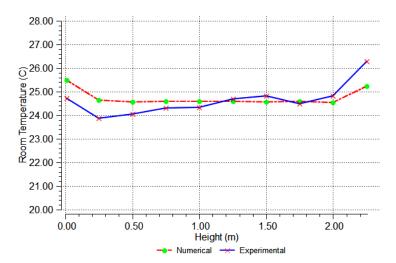


Figure 4.23: Numerical data plotted against experimental data along middle of the HEPC room.

4.5. Energy Savings Using Horizontal Earth Pipe Cooling System

The energy efficiency of the horizontal earth pipe cooling technology is evaluated in this section. The technology involves an 8 watt fan and an air conditioner as discussed earlier. The energy used by the fan and the air conditioning unit in both the horizontal earth pipe cooling and standard room are displayed in Figure 4.24. For measuring the energy efficiency, hourly energy data were recorded during the summer from December 2013 to February 2014. The maximum energy was consumed at the hot peak hours of the day, whereas the minimum was consumed at the off peak hours at night as shown in Figure 4.24.

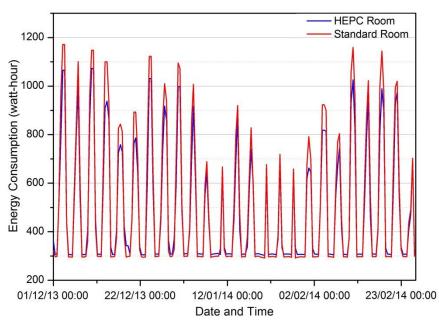


Figure 4.24: Energy consumption of HEPC and standard room.

Air conditioning energy consumption varies depending on the outdoor air temperature. The Figure 4.24 shows the energy usage in the HEPC and standard room and room. As seen, the HEPC room consumes less energy than the standard room during day time, and higher energy during midnight and early morning. During midnight and early morning, the outdoor temperature gets cooler and the soil acts as a heat source in the cooler weather. When air passes through the buried pipes in the HEPC system, it absorbs heat from the soil. Therefore heat can be obtained in the HEPC system and an additional 13.16 Wh (sum of the differences in energy consumption between HEPC and standard room) is consumed compared to the

standard room during this period. The overall energy consumption of the HEPC and standard room is summarised in Table 4.7.

			-			-		
Modelled rooms	Hourly e	energy cons	umption	Hourly energy savings				
		(watt-hour))	(watt-hour)				
	Min	Max	Avg	Min	Max	Avg	Avg (%)	
HEPC	301.61	1073.39	493.18	9.20	190.44	27.43	5.27	
Standard Room	291.55	1171.29	520.61					

Table 4.7: Hourly energy savings using horizontal earth pipe cooling technology.

Table 4.7 shows an average hourly energy savings of 27.43 Wh that has been achieved using the HEPC system. It also shows that the HEPC system has the potential to save energy a maximum of 190.44 watts per hour, while the minimum is 9.20 watts per hour. This maximum saving was achieved on 12 December 2013 at hot peak hours of the day at 12:40 pm and the minimum was obtained on 10 January 2014 at 1:20 pm as shown in Figure 4.24. The energy savings were calculated from the differences between the HEPC and standard room energy consumption. However, total average energy savings achieved is 60.57 kW (calculated from Table 4.7) and maximum is 420.49 kW by operating the HEPC system during summer from December 2013 to February 2014 (92 days).

A noticeable amount of energy costs can be saved using the HEPC system due to the reduction of energy consumption shown in Table 4.7. There are several energy usage charging categories used in Australian buildings. The most common category, namely tariff 11, is used for residential customers in Australia (EE, 2014). The energy cost for tariff 11 is summarised in Table 4.8. It includes the cost of energy usage at a flat rate throughout the day and night, plus a daily supply charge as a service fee.

Tariff 11 Residential	GST inclusive from 1 July 2015
All consumption (cents per kWh)	24.462
Daily supply charge (cents per day)	117.401

Table 4.8: Energy costs for residential customers (EE, 2014).

The daily supply charge used in tariff 11 is a fixed cost, whereas all energy consumption is a variable cost as the energy consumption rate is varied with the energy consumers. The daily energy cost savings for a building can be calculated by multiplying the daily energy savings in kWh (can be calculated from Table 4.7) by` the energy cost for kWh and, finally adding this cost to the daily supply charge as shown in Table 4.8. The total average energy cost savings during the summer 2013-2014 are calculated and tabulated in Table 4.9.

 Table 4.9: Average energy cost savings using horizontal earth pipe cooling system (costs in Australian Dollars (AUD)).

Weekly			Monthly -			Summer 2013-2014			
Min	Max	Avg	Min	Max	Avg	Min	Max	Avg	Avg (%)
8.60	16.04	9.35	36.84	68.76	40.05	112.98	210.87	122.82	4.02

Table 4.9 shows an average energy savings of \$122.82 (4.02%) in the HEPC system during summer. It is also found that the maximum savings of \$210.87 (7.23%) can be made using the system for the period. The savings gained is for a single room of dimensions 5.63 m x 2.14 m x 2.26 m only. There is an opportunity of a substantial energy savings using the horizontal earth pipe cooling technology for a complete building in summer. Cost effectiveness of this technology can be measured by its payback period which is calculated by incorporating the total cost (initial investment) and the energy cost savings (cash inflow) per year using this technology.

4.6. Payback Period

To calculate the payback period of the HEPC system, it is required to measure the total cost savings over the whole year. But the savings was calculated for 3 months of summer only as the HEPC system works effectively in summer in hot humid climates like Queensland, Australia. However, it was required to find the savings in other seasons (autumn, winter, and spring) to get the payback period. This can be found by interpolation method using the monthly known average cost savings for corresponding temperatures in summer. Such approach was found in other studies, for example in the study by Azad et al. (2015). The monthly average savings of the corresponding temperatures are predicted using the polynomial interpolation (4.5) as shown in Table 4.10, and presented graphically in Fig. 4.25.

$$y = -0.0831x^2 + 7.55x - 117.47 \tag{4.5}$$

Where, x is the monthly average temperature and y is the average savings cost. The predicted savings for corresponding temperatures are the best fit with the polynomial interpolation as shown in Fig. 4.25. The goodness of the fit of regression is measured by the unit less number R^2 , which was found as 0.995 that is nearly close to the best value 1.

The polynomial interpolation was used to predict the energy cost savings for autumn, winter, and spring as the summer energy cost savings data are not linear. Moreover, it can overcome most of the problems of linear interpolation.

Seasons	Months over	Average	Average energy
	2013-2014	Temperature (°C)	cost savings (AUD)
Autumn	March	28.9	31.35
	April	27.7	27.93
	May	24.8	18.68
Winter	June	23.6	14.44
	July	24.2	16.59
	August	27.1	26.13
Spring	September	31.1	37.00
	October	31.6	38.18
	November	32.2	39.53
Summer	December	33.5	40.61
	January	33.9	44.37
	February	30.9	36.84
Yearly			371.64

 Table 4.10: Predicted average energy cost savings during autumn, winter, and spring using the known savings of summer for HEPC.

Since the HEPC system performs better in summer, the maximum savings is found in this period. As seen in Table 4.10, the minimum amount of savings is obtained in winter due to the lower difference in temperature between the outdoor and the soil underground than in any other seasons. However, a noticeable saving of \$371.64 would be expected using the HEPC system per year as obtained in Table 4.10.

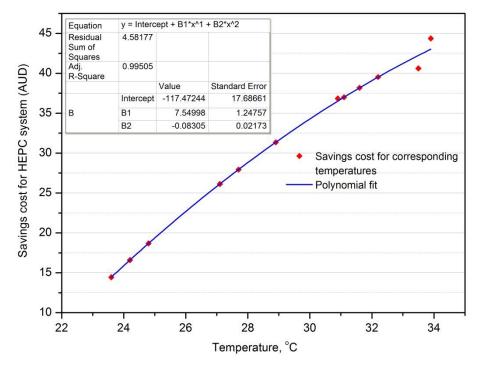


Figure 4.25: Average savings cost in each month throughout the year using VEPC system.

The initial cost was also calculated for the HEPC system. The initial cost of \$1704.95 involves pipe cost (\$364.27), excavator hiring (\$300), labour cost for installing the pipes underground (\$450), gardening (\$320.68), and the fan (\$270). Therefore the payback period of the HEPC system is given by

Payback period =initial investment/cash inflow per year
$$(4.6)$$

=\$1704.95/\$371.64 = 4.59 year

Where cash inflow is the maximum rate of return per year comes from the energy cost savings. The cash inflow was considered as even (same in each year) due to unavailable data for the whole payback period. Thus 4.59 years period would be required to get the rate of return for the horizontal earth pipe cooling system.

4.7. Error Analysis

Instrument selection, reading, test planning, observation, environment, condition and calibration can produce errors and uncertainties. An error analysis is needed to measure the experimental accuracy. The probable error of various parameters such as soil temperature, air velocity, air temperature, relative humidity and energy consumption were calculated for the HEPC system using the following formula (Zwillinger and Kokoska, 1999), and is shown in Table 4.11.

Probable Error,
$$\gamma = 0.6745 \times \sigma$$
 (4.7)

Where $\sigma = \sqrt{\frac{1}{N-1}\sum_{i=1}^{N} (x_i - \overline{x})^2}$ is the standard deviation, N is the number of

observation, x_i are the experimental measurements, and \bar{x} is the mean value of the measurements.

Table 4.11: Parameters used in the HEPC experiment and their mean value, probable error,and the error in percentage.

Parameters		Mean	Standard Deviation	Probable	Percentage	
		Value	$1 \sqrt{1 - 1}^{2}$	Error	Error (%)	
		$\frac{-}{x}$	$\sigma = \sqrt{\frac{1}{N-1} \sum_{i=1}^{N} \left(x_i - \overline{x}\right)^2}$	$\gamma = 0.6745 \times \sigma$		
Indoor air	HEPC	24.64	1.236	0.834	3.383	
temperature	room	21101	1.200	01051	2.202	
(°C)	Standard	25.77	1.529	1.031	4.002	
	room	23.11	1.527	1.051	1.002	
Relative	HEPC	64.89	6.152	4.150	6.395	
Humidity (%)	room	01.09	0.152		0.575	
	Standard	63.67	4.931	3.326	5.224	
	room	05.07		5.520		
	Outdoor	66.84	8.364	5.642	8.440	
Active	HEPC	493.18	30.294	20.433	4.143	
energy	room	475.10	50.274	20.433	4.145	
(watt-hr)	Standard	520.61	39.837	26.870	5.161	
	room	520.01	57.057	20.070	5.101	
Outdoor air ter	Outdoor air temperature		2.869	1.935	7.231	
(°C)		26.76	2.007	1.755	1.201	
Inlet air velocity (m/s)		0.41	0.053	0.036	8.719	
Outlet air velocity (m/s)		1.01	0.104	0.070	6.945	
Soil temperature at		21.31	0.813	0.548	2.573	
0.6m depth (°C	C)	21.31	0.015	0.540	2.313	

The probable error of each measurement carried out for the HEPC system was estimated in the Table 4.11, which lie within 2.58% to 8.72%.

4.8. Conclusion

This chapter presented the thermal performance of the horizontal earth pipe cooling system in the summer from December 2013 to February 2014. The performance was measured in terms of temperature reduction in the horizontal earth pipe cooling room and its energy efficiency. All the measurements were carried out in the sustainable precinct of Central Queensland University, Rockhampton campus, Australia. Soil temperature, air temperature, air velocity, relative humidity, and energy consumption were taken into consideration for these measurements to assess the impact on the room cooling performance. The experimental measurements were analysed and investigated. A thermal integrated model was developed for the horizontal earth pipe cooling system using ANSYS Fluent 15.0. It was validated by comparing the numerical results and the experimental results obtained from the field work experiment.

The horizontal earth pipe cooling study demonstrated that there is a potential to reduce temperatures by 1.13°C using the horizontal earth pipe cooling technology, although this is not a huge temperature reduction. This reduction saved an average amount of energy of 60.57 kW and a maximum of 420.49 kW in the summer of 2013-2014. This translates to an average energy savings of \$101.32 (5.28%) during the period, while the maximum savings is \$201.78 (16.26%). The maximum rate of return (payback period) for the HEPC system was calculated as 4.59 years. The findings of this study develop a guideline for the regulators, manufacturers and inhabitants for the deployment of horizontal earth pipe cooling techniques in hot humid climates.

CHAPTER 5 : PERFORMANCE ANALYSIS OF VERTICAL EARTH PIPE COOLING SYSTEM

5.1. Introduction

This chapter presents the thermal performance of the vertical earth pipe cooling (VEPC) system, where the pipes are buried vertically into the ground. The impact of soil temperature, air temperature, air velocity and relative humidity on room cooling performance was assessed in this investigation. The energy consumed by the vertical earth pipe cooling system was also observed under this investigation to measure the efficiency of the system.

The experimental investigation was carried out in summer (wet season) from December 2014 to 18 February 2015 as the average maximum temperature occurs during this season in Rockhampton, Australia. The data from 19 February to 28 February 2015 were not considered in this investigation due to insufficient data. Rockhampton was affected by the cyclone Marcia on 20 February 2015. As a result, some of the experimental equipment including the data measuring tool was damaged and power was lost.

A thermal integrated model was developed using ANSYS Fluent 15.0 to measure the thermal performance of the vertical earth pipe cooling system. The experimental results measured from the actual field investigation were compared with the numerical results obtained through the simulation. The numerical results show a good agreement with the experimental results. Both the experimental and numerical results show a temperature reduction in the vertical earth pipe cooling room which will assist the building occupants in saving energy costs.

Thermal performance of the vertical earth pipe cooling system was compared with the horizontal earth pipe cooling system. The vertical earth pipe cooling system shows better performance when compared to the horizontal earth pipe cooling performance.

5.2. Soil Temperature Investigation in Summer 2014-2015

Soil temperature investigation is a crucial part for assessing the vertical earth pipe cooling performance. The soil temperature investigation was conducted in this study to observe its potential for applying the vertical earth pipe cooling technology in Rockhampton, Australia. All the temperatures were recorded at 20 minutes interval during summer 2014-2015, when the ground surface was covered by grass.

In this present study, the soil temperatures were measured at different depths, namely 0.60 m, 0.73 m, 0.85 m, 0.97 m, and 1.10 m where the pipes were buried underground for the vertical earth pipe cooling system. The soil temperatures at these depths are shown in Figure 5.1. It is seen from the figures that the temperature decreases with increasing depth, and the lowest average temperature occurs at 1.10 m depth. In summer, soil temperature normally decreases with increasing depths as mentioned in the previous chapter. As stated before and as per the literature, this reduction can be increased up to at 4m depth underground as the soil temperature beyond this depth is fairly constant and stable (Santamouris et al., 1995). The buried pipes were fitted at the maximum depth of 1.10 m in this study to keep the installation cost of the vertical earth pipe cooling system within the budget.

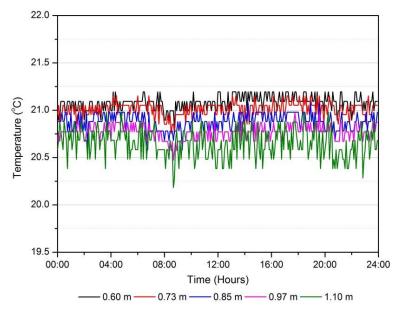


Figure 5.1: Soil temperature distribution during summer 2014-2015.

Figure 5.1 illustrates the hourly average soil temperature distribution during the summer from December 2014 to 18 February 2015. All the underground soil temperatures were found to be lower than the ground temperature in the VEPC system, like for the HEPC system. The temperature range is from 20.18°C to 21.19°C over the various depths. In the VEPC system, the maximum average temperature reduction of 0.81°C was found between the soil temperatures at 0.60m and 1.10m, whereas 0.70°C was observed in the HEPC system. This maximum reduction occurred at the middle of the day (12:40 pm) on 9 December 2014. As mentioned earlier, the soil temperature gets cooler than the outdoor temperature during the hot peak hours than during the off peak hours in summer.

The performance of the vertical earth pipe cooling system depends on the temperature difference between the outdoor air temperature and soil temperature at the depth where the pipe is buried underground. The soil temperature at 1.10 m depth (maximum depth) was compared with the outdoor air temperature to find the temperature difference between the soil and outdoor air temperature as shown in Figure 5.2.

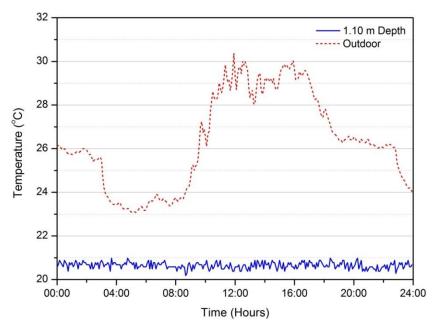


Figure 5.2: Temperature distribution of soil at 1.10 m depth and outdoor air.

Figure 5.2 shows the hourly average outdoor temperature that ranges from 23.07°C to 30.36°C. The maximum diurnal temperature of 11.18°C occurs on 27 December

2014 whereas the minimum diurnal temperature of 4.23°C occurs on 23 January 2015. The outdoor temperatures were quite a deal lower between 4:40 am to 6:20 am compared to other periods. The air temperature normally increases during the day and falls during the late night and early morning.

The average temperature reduction between the outdoor and soil temperature at 1.10 m depth was seen as 5.72°C, where the reduction ranges from 2.27°C to 9.98°C. The maximum temperature reduction was observed at midday (12:00 pm), whereas the minimum reduction occurs at the late night (4:40 am). The reduction in temperature during the day contributed to cool the room using the vertical earth pipe cooling system.

As mentioned in the previous chapter, the surface condition of the ground is an important factor that affects the performance of the earth pipe cooling system. A grass covered ground surface protects the ground from solar radiation in a hot humid climate like Rockhampton, Australia. The grass covered surface is comparatively cooler than the bare ground surface during daytime as grass can absorb solar radiation through their biological functions.

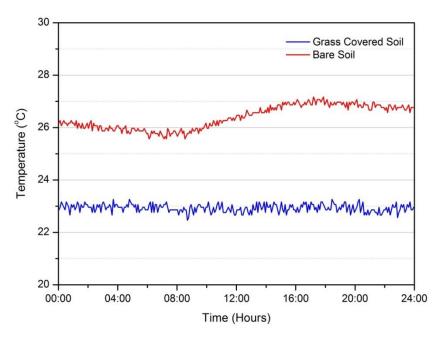


Figure 5.3: Temperature fields of the ground surface with grass covered and bare soil during summer 2014-2015.

Figure 5.3 illustrates the hourly average soil temperature of the ground surface with grass covered soil and bare soil. An average temperature reduction of 3.46°C was found between the ground surfaces with these surface conditions, where the reduction varies from 2.4 °C to 4.3°C. As seen in the figure, the short covered grass provides the lower temperature. This agrees with the studies of Mihalakakou et al. (1994b) and Jacovides et al. (1996).

5.3. Experimental Investigation for Vertical Earth Pipe Cooling System

The vertical earth pipe cooling investigation was conducted in summer from December 2014 to 18 February 2015. Data were collected from both the VEPC and HEPC room by turning off the HEPC system. The amount of radiation was considered in the experimental measurements. Since no technology was running with the HEPC room, the HEPC room was considered as a standard room. The impact of soil temperature, air temperature, air velocity and relative humidity on room cooling performance was assessed throughout the investigation.

To measure indoor air temperature and relative humidity, the HOBO U10-003 data logger was set at different points inside both the VEPC and standard room. HOBO U23-001 Pro v2, the waterproof data logger, was positioned outside the room to record the relative humidity and outdoor temperature. Figure 5.4 shows the temperature profile of the vertical earth pipe cooling, standard room and outside the room.

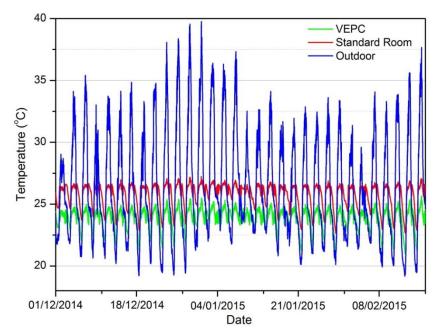


Figure 5.4: Temperature fields in the vertical earth pipe cooling and standard room close to the wall, and outdoor during summer 2014-2015.

Figure 5.4 shows that the daily indoor room temperature ranges from 20.95°C to 25.66°C in the vertical earth pipe cooling room and 22.62°C to 27.24°C in the standard room, while the outdoor temperature varies from 19.18°C to 39.77°C. Comparing the experimental results between these two rooms, it was found that the vertical earth pipe cooling technology contributes to reducing the room temperature to a maximum of 3.32°C (1.86°C on average) from the standard room. Moreover, the outdoor air temperature was found to be lower at night than the vertical earth pipe cooling and standard room temperatures. Due to cooler weather, the outdoor temperature gets comparatively lower than the indoor room temperatures during the night.

The relative humidity of air has also an impact on the thermal comfort. So, it is necessary to measure its impact on the room cooling performance in a hot and humid climate. Relative humidity distributions in both the vertical earth pipe cooling and standard rooms are shown in Figure 5.5. Table 5.1 summarises the indoor and outdoor air temperature and relative humidity of the VEPC and standard room.

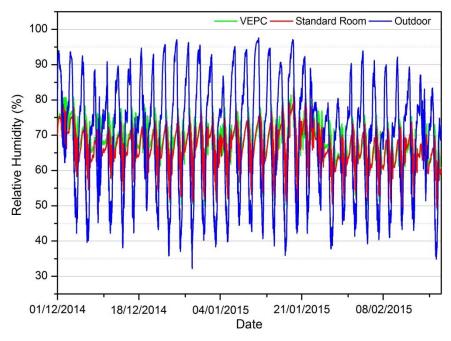


Figure 5.5: Relative humidity measured in the vertical earth pipe cooling, standard room and outdoor.

	Indoor temperature			Outdoor temperature			Relative humidity		
Modelled rooms	Min (°C)	Max (°C)	Avg (°C)	Min (°C)	Max (°C)	Avg (°C)	Min (%)	Max (%)	Avg (%)
VEPC	20.95	25.66	23.92	19.18	39.77	26.37	48.68	84.70	67.88
Standard Room	22.62	27.24	25.79				49.16	83.20	66.73

Table 5.1: Air temperature and relative humidity in the VEPC and standard room.

The relative humidity varies from 48.68% to 84.70% in the VEPC room, from 49.16% to 83.20% in the standard room, and from 32.18% to 97.6% outside the rooms as shown in Table 5.1. The standard room shows 66.73% relative humidity, while the VEPC room gives 67.88% average relative humidity which is 1.15% higher than that of the standard room. The air that passes through the pipes buried underground creates this additional relative humidity in the VEPC room (Thanu et al., 2001). When air goes through the buried pipes, air gets moisture and cannot evaporate under the ground.

Temperature and relative humidity measurements carried out for the VEPC system was compared with the ASHRAE standard 55-2010 using the centre for the built environment (CBE) thermal comfort tool. The measured average temperature and relative humidity in the vertical earth pipe cooling room shown in Table 5.1 complies with the ASHRAE standard 55-2010 (ASHRAE, 2004), Brown's bioclimatic chart (Brown, 1985) and Givoni's chart (Givoni, 1992).

Air temperature and velocity at the inlet and outlet of the pipe (inlet to the room) were also recorded to measure their impact on the performance of the VEPC system. The HOBO U23-001 Pro v2 data logger was positioned at the pipe inlet for measuring the inlet air temperature. At the same time, the HOBO U10-003 data logger was set at the pipe outlet to observe the outlet air temperature. Figure 5.6 shows a typical inlet and outlet temperature data recording over 24 hour duration.

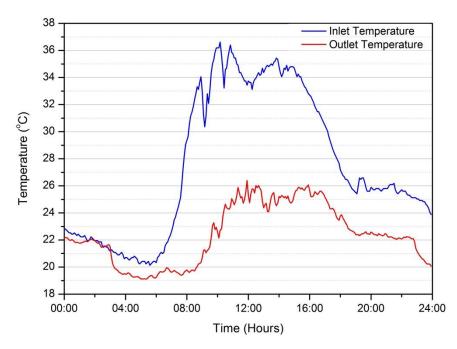


Figure 5.6: Temperature field at pipe inlet and outlet in VEPC system.

As seen from Figure 5.6, the inlet temperature was lower during the night and started to rise during the day reaching the peak temperature from around 10 am to 5 pm. From 2:20 am to 3:00 am the inlet temperature got quite lower than the outlet temperature. The outdoor temperature in Rockhampton falls at late night as mentioned earlier and when this cooler temperature goes through the buried pipes at night, it absorbs heat from the soil as the soil works as a heat source in cool

environment. Therefore, during this time, higher temperature arises at the outlet. The outlet air temperature varies from a low of 19.11°C at 4:40 am to a high of 26.40°C at 12:00 pm. The pipe inlet temperature showed a similar trend and it varied from 20.14°C to 36.62°C.

Data were collected over a period of 82 days and the average of these data gave a temperature reduction of 4.89°C at the pipe outlet. As observed from the figure, the temperature reduction is more during the warming hours from 10 am to 5 pm. A typical data recording for the inlet and outlet temperatures during this warming period is shown in Figure 5.7 which shows a big difference between the outlet and inlet temperature. When an average value of all the data collected for the warming hours was taken, a 9.98°C reduction was achieved. As the outdoor temperature got warmer during this period because of the sun light, the soil temperature remained cooler. The significant temperature differences between the inlet air temperature and the soil temperature shown in Figure 5.2 increase the cooling rate and thus show more temperature reduction.

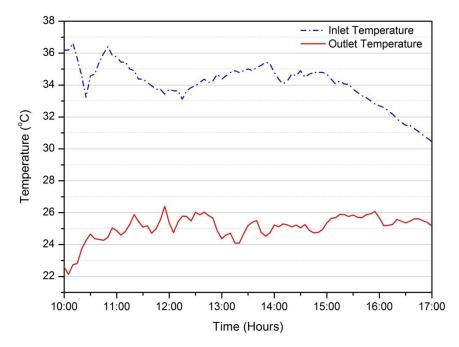


Figure 5.7: Temperature profile at pipe outlet during 10:00 am-5:00 pm in VEPC system.

As mentioned in the previous chapter, a 24 hour data collection and measurement were taken into account for assessing the overall thermal performance of the earth pipe cooling system during the whole summer though the pipe outlet temperature dropped more during the warming hours. The higher temperature reduction at the pipe outlet contributes to reduce more temperature in the room, and therefore more energy can be saved during the warming hours from 10:00 am to 5:00 pm. The temperature reduction at the pipe outlet also depends on the speed of air velocity. The velocity profiles at the pipe inlet and outlet is shown in Figure 5.8.

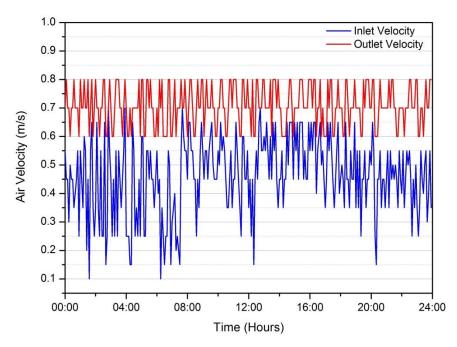


Figure 5.8: Velocity field at pipe inlet and outlet in VEPC system.

As seen in Figure 5.8, the air velocity varies from 0.1 m/s to 0.7 m/s at the pipe inlet, whereas the average gives 0.46 m/s. Meanwhile, the outlet (inlet to the room) velocity ranges from 0.6 m/s to 0.8 m/s, while the average velocity gets 0.71 m/s. The velocity at the pipe outlet grows higher due to the installed fan positioned just at the pipe outlet. The exhaust fan used in the VEPC system draws the cooler air from the buried pipe underground. As mentioned before, when the air passes through the buried pipes, it gets cooler by transferring heat to the soil due to convection.

5.4. Model Development for Vertical Earth Pipe Cooling System

All the buried pipes and room connected with the vertical earth pipe cooling system have been considered for the vertical earth pipe cooling model. For the simplicity of the model, the integrated model was divided into two parts - one involving all the pipes, called the pipe model, and the other includes the room only. Procedures for the development of the integrated model are described below.

5.4.1. Modelling Approaches

A thermal model for the vertical earth pipe cooling system involves a heat transfer process, where the air transfers excess heat as it passes through the buried pipes. The Realisable $k - \varepsilon$ turbulence model was used to analyse the heat transfer process of the system. The flow passing through the buried pipes was found to be turbulent which was calculated using the formula of Reynolds number described in section 2.7. Moreover, this model is reliable and provides more accurate results.

The model satisfies definite mathematical constraints, which is consistent with turbulent flow physics. The problem was solved numerically by using the CFD code "Fluent in ANSYS 15.0", which employs the finite volume method for discretisation of the computational domain. The relevant modelling equations and solver approaches described in chapter 4 were used for the vertical earth pipe cooling model development.

5.4.1.1. Geometry of the Model

Two 2D geometries were produced using DesignModeller in ANSYS 15.0; one is for the pipe model and the other is for the room model. The pipe model consists of 20 PVC pipes, each of length 6.0 m, diameter 20 mm and thickness 2 mm. These pipes were connected with two manifolds of thickness 4 mm. The room model geometry involves the vertical earth pipe cooling room of dimension 5.63 m x 2.26 m. The geometries are presented in Appendix 5.1.

5.4.1.2. Mesh Generation

A typical mesh for both the pipe and room model was generated using DesignModeller in ANSYS 15.0. Figure 5.9 and Figure 5.10 shows the meshing of the pipe and room model respectively. The element size of 0.01m was used for generating the mesh for both the model, which produced 41,510 and 127,373 elements in pipe and room model respectively. To check the influence of the grid variation and to establish the optimum mesh size, a study was completed for every mesh size as discussed in section 5.4.1.3.

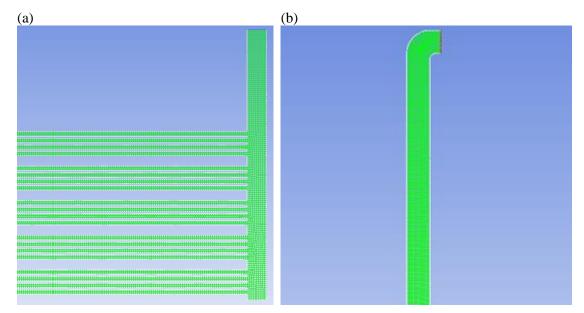


Figure 5.9: Mesh for VEPC pipe model. (a) Showing inlet. (b) Showing outlet (inlet to the room).

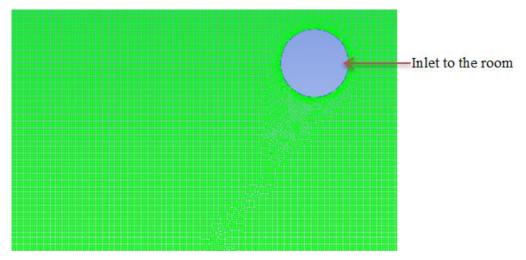


Figure 5.10: Mesh pattern for VEPC room model.

5.4.1.3. Grid Independence Study

Three grids were created for both the pipe and room model of the VEPC system using different element sizes as summarised in Table 5.2. The pipe model comprises 0.01m, 0.005m and 0.003m element sizes, where 0.01m was taken for generating the mesh of the pipe model. The Grid 2 and Grid 3 shows different mesh size, which was generated by changing 0.01m element size to 0.005m and 0.003m respectively. Likewise, the room model comprises 0.01m, 0.008m and 0.005m element sizes, where 0.01m element size was selected for generating the mesh for the room model.

The Grid 2 and Grid 3 denote different mesh size, which was obtained by changing 0.01m element size to 0.008m and 0.005m respectively.

Grid size	Element size (m)		No	des	Elements		
	Pipe	Room	Pipe	Room	Pipe	Room	
Grid 1	0.01	0.01	52982	128213	41510	127373	
Grid 2	0.005	0.008	160301	200515	136037	199472	
Grid 3	0.003	0.005	400228	510964	384122	509301	

Table 5.2: Different grid sizes for VEPC model.

Figure 5.11 shows the temperature fields at the outlet of the pipe model for different mesh sizes. Grid 1 shows the outlet temperature, which is consistent with the results using Grid 2 and Grid 3. The simulated outlet temperature using Grid 2 and Grid 3 lies within 1-2% of the values attained with the Grid 1 is seen in Figure 5.11. A similar result was also found for the room model referring to the Figure 5.12. This study was advanced with Grid 1 for simulating the models as Grid 1 takes less time for numerical computations.

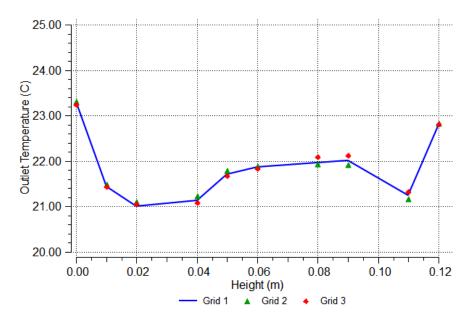


Figure 5.11: Temperature fields at the outlet of pipe model for different mesh size.

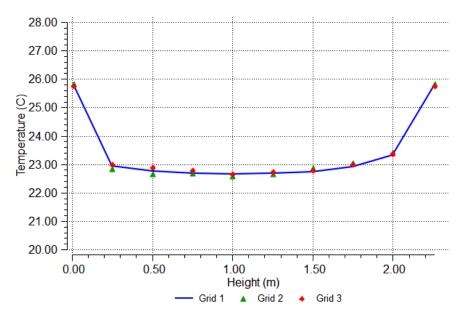


Figure 5.12: Temperature field at different heights of VEPC room model for different mesh size.

5.4.2. Simulation Results and Discussion

The earth pipe cooling performance was calculated numerically using simulation in ANSYS Fluent. The flow and thermal variables for the boundary and cell zone conditions were set on the boundaries of the models. No slip boundary conditions were applied on the pipe and room walls. The cell zone condition for the surface body was defined as fluid in both the pipe and room model.

Two simulations were run on an Intel Xeon CPU E3-1225 V3 @ 3.20 GHz processor computer of RAM 16.0GB (15.8 GB usable); one is for pipe model and the other is for the room model. The solutions were convergent at 182 and 223 iterations, which required a total CPU time of 57.87 seconds and 1 minute 10.91 seconds for the pipe and the room model respectively. It is noted that the total CPU time does not include any waiting time for communications or load imbalances. The following sections show the simulation results for both the models.

5.4.2.1. Simulation for VEPC Pipe Model

The results of pipe model simulations were achieved under the boundary conditions which are summarised in Table 5.3. Average air velocity of 0.46 m/s and the average air temperature of 26.37°C measured at the pipe inlet were set as the inlet velocity and inlet temperature respectively in the boundary conditions of the model. The

exhaust fan run in the vertical earth pipe cooling technology was set as the outlet of the pipe model. Soil temperatures at different depths (where the 20 PVC pipes were laid and aligned) were also used in the boundary conditions of the model.

Parameters	Value
Inlet velocity	0.46 m/s
Inlet temperature	26.37°C
Soil temperature at 0.60 m depth	21.08°C
Soil temperature at 0.73 m depth	21.01°C
Soil temperature at 0.85 m depth	20.88°C
Soil temperature at 0.97 m depth	20.76°C
Soil temperature at 1.10 m depth	20.65°C
Thermal conductivity of PVC pipe	0.16 W/m-K
Density of PVC pipe	1390 kg/m ³
Specific heat of PVC pipe	1000 J/kg-K
Air thermal conductivity	0.024 W/m-K
Air density	1.204 kg/m ³
Specific heat of air	1006.43 J/kg-K
Air viscosity	1.850387e-05 kg/m-s

Table 5.3: Parameters used in boundary conditions of the VEPC pipe model.

Figures 5.13, 5.14 and 5.15 show the temperature profile throughout the pipes, at the pipe inlet and pipe outlet respectively, while Figures 5.16, 5.17 and 5.18 represent the velocity profile throughout the pipes, at pipe inlet and pipe outlet respectively.

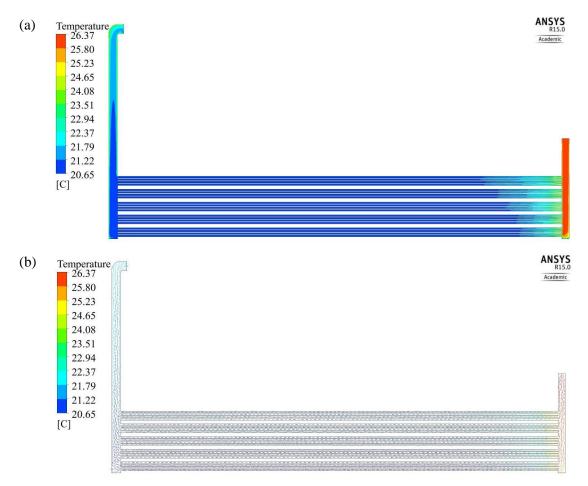


Figure 5.13: Temperature fields throughout the pipes in VEPC system. (a) Temperature magnitude. (b) Temperature velocity.

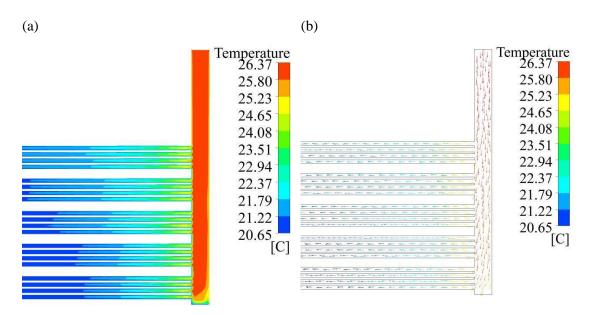


Figure 5.14: Temperature fields at the pipe inlet in VEPC system. (a) Temperature magnitude. (b) Temperature velocity.

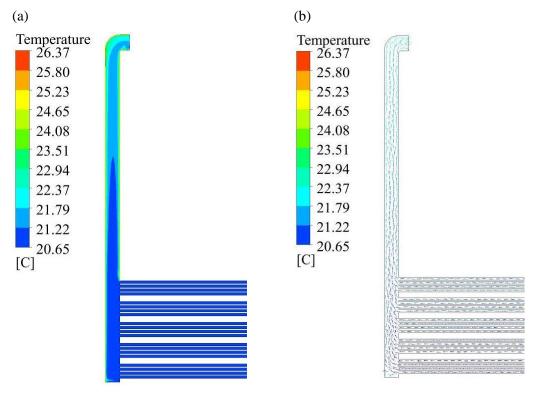


Figure 5.15: Temperature fields at the pipe outlet in VEPC system. (a) Temperature magnitude. (b) Temperature velocity.

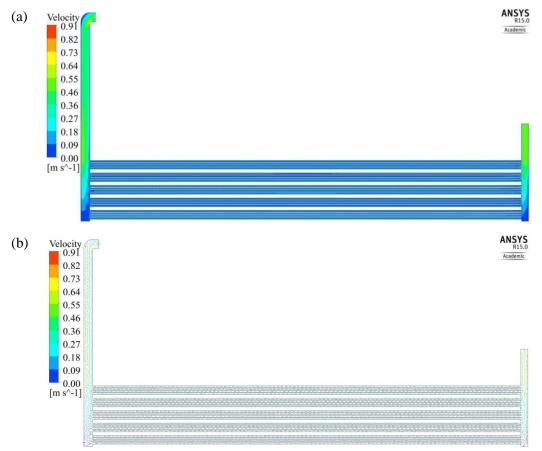


Figure 5.16: Velocity fields throughout the pipes in VEPC system. (a) Velocity magnitude. (b) Velocity vector.

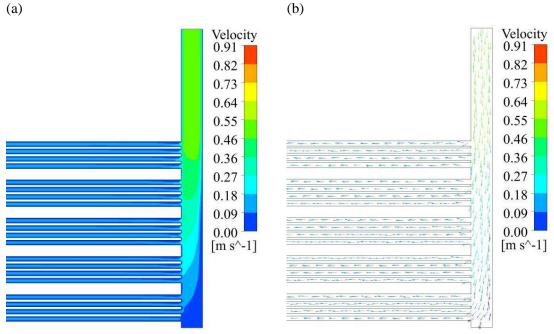


Figure 5.17: Velocity fields at the pipe inlet in VEPC system. (a) Velocity magnitude. (b) Velocity vector.

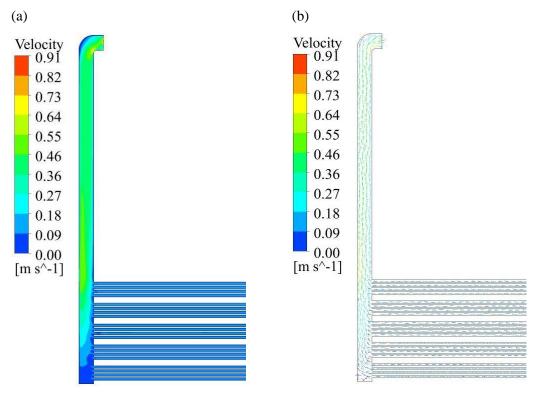


Figure 5.18: Velocity fields at the pipe outlet in VEPC system. (a) Velocity magnitude. (b) Velocity vector.

Figure 5.13 shows the air temperature inside the pipes that ranges from 20.65°C to 26.37°C, where the maximum and minimum occur at the pipe inlet and in the buried pipes. As discussed in the previous chapter, hot air comes from the atmosphere to the pipe inlet, moves down to the bottom of the buried pipes and transfers excess heat to the ground by conduction, finally the cooler air goes to the pipe outlet. Air gets more residential time inside the pipe to transfer heat to the soil as it passes through long buried pipes of 7.5 m in length.

As seen from Figure 5.15, the air temperature at the pipe outlet is higher than the buried pipes end. Heat is produced by the motor of the fan installed at the pipe outlet, and therefore this higher temperature arises at the pipe outlet. Another reason is that when the air moves from the buried pipes to the pipe outlet, the pipe absorbs heat from the atmosphere and thus the air gains heat.

An average outlet temperature of 21.85°C and air velocity of 0.63 m/s was found in the simulation result, which shows a good agreement with the measured average outlet temperature of 22.41°C and velocity of 0.71 m/s. These results represent that the average outlet temperature creates a 2.5% difference between the experimental and numerical results, while the average outlet velocity shows an 11.27% difference. The numerical results were also compared with the experimental results at the pipe outlet as shown in Table 5.4. These results are also shown in graphical form in Figure 5.19.

Height (m)	Experimental (°C)	Numerical (°C)	Differences (%)
0.12	22.79	24.67	8.25
0.10	21.25	21.75	2.35
0.09	22.01	22.31	1.36
0.08	21.96	22.42	2.09
0.06	21.87	21.77	0.46
0.05	21.71	21.25	2.12
0.04	21.13	21.36	1.09
0.02	21.00	21.69	3.29
0.01	21.43	22.55	5.23
0.00	23.31	24.31	4.29

Table 5.4: Comparison in temperature between experimental and numerical (simulation)results at pipe outlet.

Although some variations are found (Table 5.4) between the experimental and numerical results, the overall numerical results are in very good agreement with the corresponding experimental results as seen in Figure 5.19. The variations are due to the uncertainties and errors in the experiments and CFD simulations as mentioned in the section 4.4.2.1.

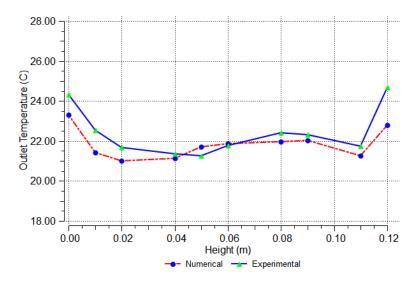


Figure 5.19: Numerical data plotted against experimental data at the pipe outlet.

5.4.2.2. Simulation for VEPC Room Model

The outlet of the VEPC pipe model was considered as the inlet of the VEPC room model. The average air temperature of 21.85°C and air velocity of 0.63 m/s at the pipe outlet (inlet to the room) of the pipe model was set as the inlet air temperature and velocity for the room model respectively. Average maximum room temperature recorded from the standard room was set as the room temperature of the model. The temperature and velocity profile in the vertical earth pipe cooling room are shown in Figure 5.20 and Figure 5.21 respectively. Table 5.5 summarises the boundary conditions used for the VEPC room model.

Parameters	Value
Inlet velocity	0.63 m/s
Inlet temperature	21.85°C
Standard room temperature	25.79°C
Air thermal conductivity	0.024 W/m-K
Air density	1.204 kg/m ³
Specific heat of air	1006.43 J/kg-K
Air viscosity	1.850387e-05 kg/m-s

Table 5.5: Parameters used in boundary conditions of the VEPC room model.

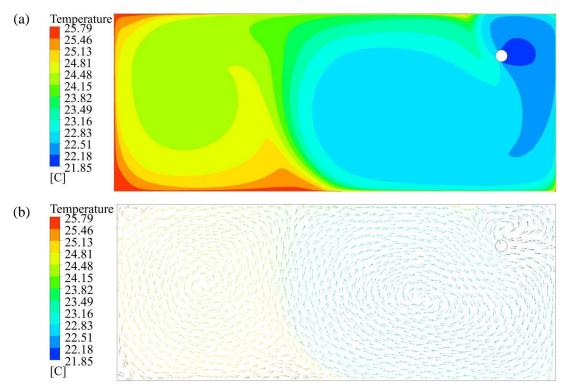


Figure 5.20: Temperature profile in VEPC room. (a) Temperature magnitude. (b) Temperature vector.

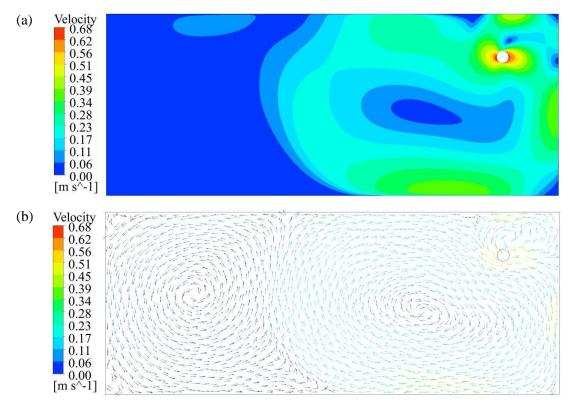


Figure 5.21: Velocity profile in VEPC room. (a) Velocity magnitude. (b) Velocity vector.

Figure 5.20 shows the VEPC room temperature that varies from 21.85°C to 25.79°C. Minimum temperatures are found at the inlet and its surroundings as the stronger velocity is seen at these points. Meanwhile, the maximum temperatures are observed at the points close to the room wall because of the zero wall velocity and weaker velocity close to the wall.

The average temperature in the VEPC room was found to be 23.43°C, which is 2.36°C lower than the standard room temperature. As the cooler air comes through the buried pipes, the VEPC room is cooled and hence the temperature reduction is achieved. The air is cooled by transferring heat to the soil when it passes via buried pipes as discussed in the previous chapter.

The VEPC room temperatures were calculated at different heights along the centre of the room wall using simulation and those were compared with the corresponding experimental results as summarised in Table 5.6. The simulation and experimental results are in very good agreement (Figure 5.22) and lie within 1.07%-6.06% limits in the vertical earth pipe cooling room.

Height (m)	Experimental (°C)	Numerical (°C)	Differences (%)
2.26	26.61	25.79	3.08
2.00	23.02	23.32	1.30
1.75	23.18	22.92	1.12
1.50	23.23	22.74	2.11
1.25	22.45	22.69	1.07
1.00	22.95	22.67	1.22
0.75	23.43	22.69	3.16
0.50	23.01	22.76	1.09
0.25	24.43	22.95	6.06
0.01	26.91	25.79	4.16

 Table 5.6: Comparison in room temperature between experimental and numerical results of the room model.

A 1.87°C temperature reduction was found through the experiment, while 2.36°C was obtained through the simulation works, which makes a 2.05% difference between these results. The numerical results show some deviations from the

experimental results because of the probable error of the measurements discussed in section 5.7.

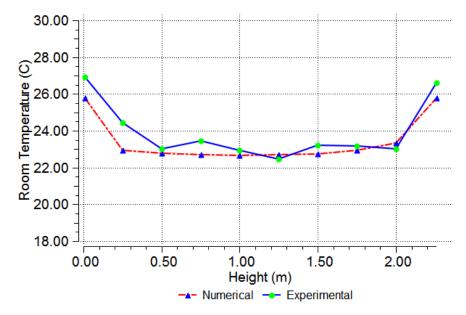


Figure 5.22: Numerical data plotted against experimental data along middle of the VEPC room.

5.5. Energy Savings Using Vertical Earth Pipe Cooling System

Vertical earth pipe cooling performance is evaluated in this section in terms of energy savings. As mentioned earlier, the VEPC system involves an 8 watt fan and an air conditioner. Figure 5.23 shows the energy used by the fan and the air conditioning unit in both vertical earth pipe cooling and standard room. The figure shows that the maximum energy was consumed at the hot peak hours of the day, whereas the minimum was consumed during off the peak hours at night. Hourly energy data were recorded during the summer from December 2014 to 18 February 2015 to measure the energy efficiency of the system.

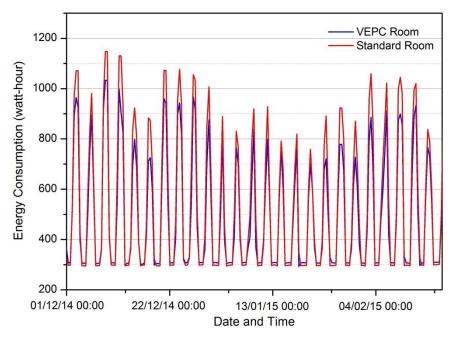


Figure 5.23: Energy consumption of VEPC and standard room.

Usually, air conditioning energy consumption depends on the outdoor air temperature. The VEPC room consumes less energy than the standard room during day time, and higher energy during midnight and early morning as shown in Figure 5.23. The outdoor air temperature gets cooler during the midnight and early morning. Table 5.7 shows the amount of energy consumed by the VEPC and standard room.

Modelled rooms	Hourly energy	Hourly energy savings					
	(watt-hour)		(watt-hour)				
	Min Max Avg			Min	Max	Avg	Max (%)
VEPC	292.71	1032.98	503.36	9.46	310.25	44.13	32.78
Standard Room	294.14	1147.59	547.49				

Table 5.7: Hourly energy savings using vertical earth pipe cooling technology.

An average hourly energy savings of 44.13 W was achieved using the VEPC system as shown in Table 5.7, while the hourly maximum and minimum savings are 310.25 watts and 9.46 watts respectively. These savings were calculated manually from the differences of the energy consumption by the VEPC and standard room. The VEPC system contributes an average energy savings of 84.73 kW, where the maximum savings was 685.03 kW during the summer from 1 December 2014 to 18 February 2015 (80 days). This is a noticeable energy savings that causes a noticeable reduction in the energy cost.

Several energy usage charging categories are used in Australian buildings. The residential customers use tariff 11, which is the most common charging category (EE, 2014). Table 5.8 shows the energy cost for tariff 11 that includes the cost of energy usage at a flat rate over 24 hours, plus a daily supply charge as a service fee.

Tariff 11 Residential	GST inclusive from 1 July 2015
All consumption (cents per kWh)	24.462
Daily supply charge (cents per day)	117.401

Table 5.8: Energy costs for residential customers.

Since the rate of energy consumption is varied with the energy consumers, all the energy consumption is a variable cost. Meanwhile, the daily supply charge in tariff 11 is a fixed cost as it remains the same for all the customers. Therefore, the total energy cost for a building can be calculated from the energy used in the building. According to the price of tariff 11, the total energy cost savings have been calculated during summer from 1 December 2014 to 18 February 2015, and are summarised in Table 5.9.

 Table 5.9: Energy cost savings using vertical earth pipe cooling system (costs in Australian Dollars (AUD)).

W	eekly		Monthly			Summer 2014-2015			
Min	Max	Avg	Min	Max	Avg	Min	Max	Avg	Max (%)
8.61	20.97	10.03	36.89	89.86	43.00	113.12	275.58	131.84	8.51

Table 5.9 illustrates that the VEPC system has the potential to save an average energy cost of \$131.84 (5.91%) and a maximum of \$275.58 (8.51%) in summer. The savings are achieved for a $27.23m^3$ room. A substantial amount of savings can be achieved using the vertical earth pipe cooling technology for a complete building. The efficiency of this technology is also measured by its cost effectiveness which is calculated using the payback period discussed in the following section.

5.6. Payback Period

It is essential to measure the total cost savings over the whole year to calculate the payback period. But this study calculated the savings for 3 months summer only, since the earth pipe cooling system performs better in summer. However, the savings in other seasons (autumn, winter, and spring) are also required to find the payback period. The interpolation method can be applied to find these using the monthly known average cost savings for corresponding average temperatures of summer. The polynomial interpolation (5.1) was used to predict the monthly average savings of the corresponding temperatures shown in Table 5.10. The predicted savings with its corresponding temperatures are also presented graphically in Fig. 5.24.

$$y = -0.0831x^2 + 7.55x - 117.47 \tag{5.1}$$

Where, x is the independent variable used as the monthly average temperature, and y is the dependent variable indicated as average savings cost.

The predicted energy cost savings for their corresponding temperatures are fitted best with the polynomial (5.1) as the goodness of the fit of regression, R^2 gives the value of 1. To predict the energy cost savings, the polynomial interpolation was used for autumn, winter, and spring, since the summer energy cost savings data were found as nonlinear.

Seasons	Months over	Average	Average energy cost
	2014-2015	Temperature (°C)	savings (AUD)
Autumn	March	30.1	35.80
	April	28.5	31.23
	May	25.8	26.05
Winter	June	24.7	24.85
	July	25	25.13
	August	27.4	28.73
Spring	September	30.9	38.50
	October	31.3	39.95
	November	32.1	43.07
Summer	December	33.1	47.42
	January	32.5	44.79
	February	31.2	39.63
Yearly			425.15

 Table 5.10: Predicted average energy cost savings during autumn, winter, and spring using the known savings of summer for VEPC.

As seen from Table 5.10, the maximum savings is obtained during the summer using the vertical earth pipe cooling system whereas the minimum is observed in winter. As mentioned earlier, the earth pipe cooling system works as a heat sink in summer and as a heat source in winter. Therefore, the system can cool a room more effectively in summer and the maximum saving is found. As shown in Table 5.10, a yearly saving of \$425.15 can be achieved using the VEPC system.

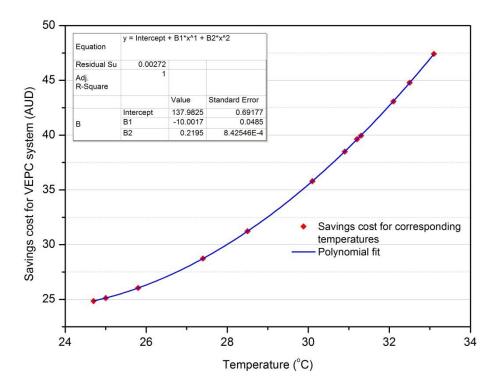


Figure 5.24: Average savings cost in each month throughout the year using VEPC system.

The initial investment for the VEPC system was calculated as \$1813.40 by summing all the costs consisting of pipe cost (\$382.72), excavator hiring (\$300), labour costs for installing the pipes underground (\$540), gardening (\$320.68), and the fan (\$270). The payback period of the VEPC system is calculated using the formula (4.6) and found as 4.27 years. Therefore the VEPC provides the maximum rate of return in 3.26 years.

5.7. Error Analysis

Errors and uncertainties can be produced by instrument selection, reading, observation, test planning, environment, condition and calibration. To measure the

accuracy of the experiment, an error analysis is required. The probable error and it's percentage of the parameters used for the VEPC study are calculated using the formula (4.7) as shown in Table 5.10.

Parameters		Mean	Standard Deviation	Probable	Percentage
			$\sigma = \sqrt{\frac{1}{N-1} \sum_{i=1}^{N} \left(x_i - \overline{x}\right)^2}$	Error $\gamma = 0.6745 \times \sigma$	Error (%)
Indoor air temperature	HEPC room	23.92	0.892	0.602	2.515
(°C)	Standard room	25.79	0.916	0.618	2.396
Relative Humidity (%)	HEPC room	67.88	7.139	4.815	7.094
	Standard room	66.73	3.978	2.683	4.021
	Outdoor	69.51	8.792	5.930	8.531
Active energy	HEPC room	503.36	36.051	24.316	4.831
(watt-hr)	Standard room	547.49	42.926	28.954	5.288
Outdoor air ter (°C)	mperature	26.37	3.018	2.036	7.720
Inlet air veloci	ty (m/s)	0.46	0.062	0.042	9.091
Outlet air velo	city (m/s)	0.71	0.083	0.056	7.885
Soil temperatu m depth (°C)	are at 0.6	21.08	0.621	0.419	1.987
Soil temperature at 0.73 m depth (°C)		21.01	0.756	0.510	2.427
Soil temperature at 0.85 m depth (°C)		20.88	0.583	0.393	1.883
Soil temperature at 0.97 m depth (°C)		20.76	0.557	0.376	1.810
Soil temperatu m depth (°C)	re at 1.10	20.65	0.434	0.293	1.418

Table 5.11: Parameters used in the VEPC experiment and their mean value, probable error, and the error in percentage.

Table 5.11 shows the probable error of each measurement of the VEPC system, which lie within 1.42% to 9.09%.

5.8. Performance comparison between VEPC and HEPC system

The vertical earth pipe cooling performance was compared with the horizontal earth pipe cooling system based on the data collected in April 2014. To compare the performance between these systems, data were collected from both the horizontal and vertical earth pipe cooling room at the same period. Air temperature and relative humidity were recorded inside and outside the rooms at 20 minutes interval. Meanwhile, the air velocity was also measured at the pipe inlet and outlet (inlet to the room) of the systems. Figure 5.25 and Figure 5.26 show the air temperature and relative humidity of the vertical and horizontal earth pipe cooling room, and outside the room.

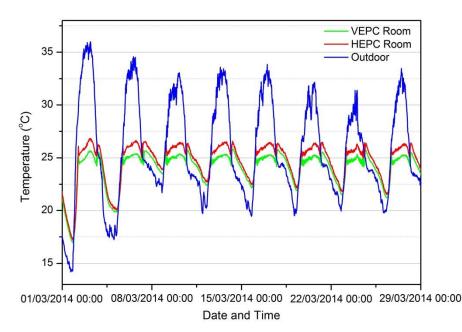


Figure 5.25: Air temperature in VEPC room, HEPC room and outside the room.

The indoor temperature varies from 16.98°C to 25.79°C in the VEPC room and from 17.19°C to 26.96°C in the HEPC room, while the outdoor temperature ranges from 14.19°C to 36.00°C as shown in Figure 5.25. The figure illustrates that the VEPC average room temperature gets 0.68 °C lower than the HEPC average room temperature. The buried pipes aligned in the VEPC system was in deeper ground than that for the HEPC system. As mentioned earlier, the air temperature in the buried pipes decreases with increasing depth. This cooler effect contributed to the

result. The air temperature and relative humidity in the VEPC and HEPC room are summarised in Table 5.12 for a comparison.

	Indoor temperature			Outdo	Outdoor temperature			Relative humidity		
Modelled rooms	Min (°C)	Max (°C)	Avg (°C)	Min (°C)	Max (°C)	Avg (°C)	Min (%)	Max (%)	Avg (%)	
VEPC	16.98	25.79	24.02	14.19	36.00	25.86	41.08	75.78	60.27	
HEPC	17.19	26.96	24.70				39.78	78.31	60.50	

Table 5.12: Air temperature and relative humidity in VEPC and HEPC room.

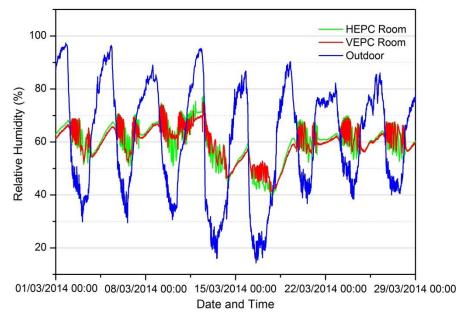


Figure 5.26: Relative humidity in HEPC room, VEPC room and outside the room.

As seen from Table 5.12, the average relative humidity of the VEPC room is close to the HEPC average relative humidity, where it ranges from 41.08% to 75.78% in the VEPC room and from 39.78% to 78.31% in the HEPC room. The HEPC room shows an average relative humidity of 60.50%, which is quite a lot higher than that of the VEPC room. The average air velocity at the outlet in the HEPC system (1.03 m/s) was greater than that of the VEPC system (0.76 m/s). This higher air velocity creates the additional humidity in the HEPC system.

As the VEPC average room temperature is 0.68°C lower than that for the HEPC system, and the VEPC average relative humidity of 60.27% is seen as acceptable for achieving thermal comfort as per Szokolay (2008), it can be concluded that the VEPC system has the potential to perform better than the HEPC system.

5.9. Conclusion

The thermal performance of the vertical earth pipe cooling system has been evaluated in this chapter by assessing the impact of air temperature, air velocity, soil temperature, and relative humidity on room cooling performance. In particular, the performance was measured in terms of temperature reduction achieved in the vertical earth pipe cooling system and the room due to deeper vertical pipe layout.

The experimental measurements were analysed and investigated. A thermal integrated model was developed for the vertical earth pipe cooling system. It was validated by comparing the numerical results extracted from the simulation in ANSYS Fluent and the experimental results obtained from the field work experiment. The vertical earth pipe cooling system contributed to a reduced average room temperature of 1.87°C. This temperature reduction saved a maximum energy of 685.03 kW (84.73 kW on average) during the summer 2014-2015 from 1 December 2014 to 18 February 2015. This translates to a maximum savings of \$275.58 (8.51%), while the average savings is \$131.84 (5.91%). The initial investment cost is returned in 4.27 years due to this energy savings.

The performance of the vertical earth pipe cooling system was compared with the horizontal earth pipe cooling system, and it was found that the vertical earth pipe cooling system shows better performance than the horizontal earth pipe cooling system. The buried pipes used in the vertical earth pipe cooling system were laid underground at greater depths than the horizontal earth pipe cooling system, which assisted in reducing the temperature by 0.68°C more than in the vertical earth pipe cooling system.

CHAPTER 6 : PARAMETRIC STUDIES OF EARTH PIPE COOLING SYSTEM

6.1. Introduction

The developed model of vertical earth pipe cooling is optimised in this chapter through a parametric investigation using ANSYS Fluent. The vertical earth pipe cooling system is selected for this parametric investigation due to its better performance between the two earth pipe cooling systems discussed in the previous chapters. The parameters, namely air velocity, pipe length, pipe diameter and thickness, pipe material, and pipe depth were considered for the parametric analysis. The data used for analysing the vertical earth pipe cooling system in chapter 5 were considered for this analysis. The following section describes the effect of the parameters on the performance of the earth pipe cooling system.

6.2. Air Velocity

The impact of different air velocities at the pipe inlet has been investigated in this section. For this air velocity investigation, the other variables such as pipe length, pipe diameter and thickness, pipe material, and pipe depth were kept constant. The average air velocities of 0.46 m/s, 1.0 m/s, 1.5 m/s and 5.0 m/s were considered for the investigation. The temperature fields for these air velocities are shown in Figure 6.1 at the pipe outlet (inlet to the room). The inlet average air velocity measured in the field work experiment was 0.46 m/s. The outlet temperature profile was calculated at different heights of the pipe outlet shown in Figure 3.22.

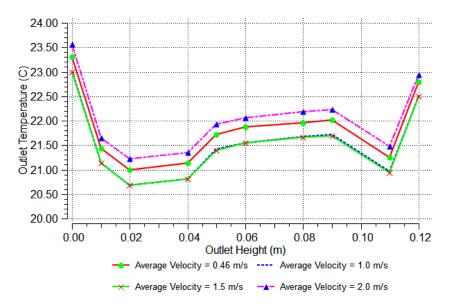


Figure 6.1: Parametric study using four different air velocities.

As seen from Figure 6.1, the temperature varies from 21.00°C to 23.3°C at various heights of the pipe outlet for the air velocity of 0.46 m/s. When the velocity is increased to 1.0 m/s, the outlet temperature is decreased and varied from 20.68°C to 23.02°C. The temperature is further decreased again when the velocity is increased to 1.5 m/s and varied from 20.68°C to 20.99°C. When the air velocity is increased to 2.0 m/s, the outlet temperature is increased and varied from 21.22°C to 23.56°C.

The temperatures at the lower and upper point of the pipe outlet (0.00 m and 0.12 m) are higher than that at the other points as shown in Figure 6.1. The maximum outlet temperature occurs at 0.12 m height, while the minimum is found at 0.02 m. No noticeable air velocity is observed at 0.12 m height (Figure 5.16) and hence the maximum temperature occurs at this point. Moreover, a good amount of air velocity occurs at the outlet height of 0.02 m (Figure 5.16), which contributes to providing a lower temperature.

This study shows that an air velocity of 1.5 m/s provides a better outcome whereas a higher air velocity shows less performance. This result is consistent with Khedari's thermal comfort chart as the chart demonstrated that thermal comfort can be achieved at 0.5 m/s, 1.0 m/s, or 1.5 m/s depending on the climate conditions (Khedari et al., 2000).

6.3. Pipe Length

The effect of different pipe lengths is analysed in this section to determine the most efficient length among the pipe lengths of 6.0m, 12.0m, 24.0m and 48.0m. The air velocity of 1.5 m/s was selected from the previous investigation for this analysis since it showed the best performance. The other variables such as pipe diameter and thickness, pipe material, and pipe depth were kept constant. Figure 6.2 shows the outlet temperatures for the different pipe lengths at the air velocity of 1.5 m/s.

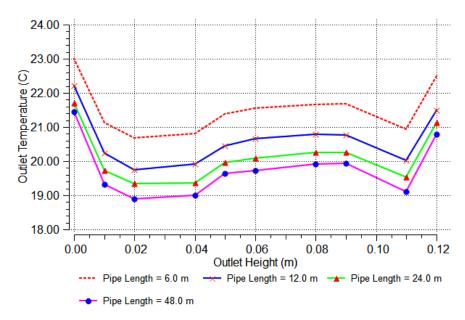


Figure 6.2: Parametric study using four different pipe lengths.

The results shown in Figure 6.2 illustrate that when the length of the buried pipe is halved or quartered, the average temperature at the pipe outlet increases (Table 6.1). When the length is increased, the temperature is reduced. For example, when the length is doubled to 48m long, the average outlet temperature is reduced and becomes more stable. These results indicate that for longer buried pipes, the heat transfer process becomes longer as the air flow stays for a longer period inside the pipe, which allows more time for the heat transfer to take place between the air and soil. Therefore, the 48m long buried pipe provides more of a cooling effect than by a shorter pipe length.

Pipe Length (m)	Outlet Temperature (°C)					
	Min	Max	Avg			
6.0	20.68	22.99	21.53			
12.0	20.03	22.21	20.62			
24.0	19.33	21.71	20.13			
48.0	18.90	21.44	19.78			

Table 6.1: Outlet temperature for different pipe lengths.

It should be noted that the parametric study for the earth pipe cooling system started with a 6.0 m long buried pipe, 125 mm diameter, 4 mm pipe thickness, and inlet air velocity of 0.46 m/s produced by a 8.0 W powered fan. But, this fan may not be capable to draw the air velocity of 1.5 m/s (the best air velocity found from previous parametric study) from the pipe inlet. Therefore, this parametric study (for different lengths) needs to take the fan power into consideration. For example, from Table 6.1 it is seen that a length of 48 m does give an average temperature of 19.78°C. However this would mean that a length of this size will need more fan power to produce the air velocity of 1.5 m/s. The effective fan power P_{ef} can be calculated using the following formula (CIBSE, 2001, Sanusi, 2012):

$$P_{ef} = \frac{\Delta P_t q v}{\eta_o}$$

(6.1)

where, P_{ef} is the effective fan power (W), ΔP_t is the pressure loss (Pa), qv is the volume air flow (m³/s), and η_o is the efficiency.

The pressure loss, ΔP_t is given by (CIBSE, 2001, Sanusi, 2012)

$$\Delta P_t = \frac{fl\rho v^2}{2D} \tag{6.2}$$

where f, D, l, ρ , v are the constant, pipe diameter, pipe length, air density, and air velocity respectively.

After substituting the value of ΔP_t in Equation 6.1, it becomes

$$P_{ef} = \frac{fl\rho v^2}{2D} \frac{qv}{\eta_o}$$
(6.3)

Let the effective fan power for the buried pipe length of 6.0 m with 0.46 m/s air velocity and the buried pipe length of 48.0 m with 1.5 m/s air velocity be P_{ef1} and P_{ef2} respectively. All the variables in the Equation 6.3 except the air velocity (v), pipe length (l) and diameter (D) are considered as constant. Then Equation 6.3 becomes

$$P_{ef} = \text{constant x } \frac{lv^2}{D}$$
(6.4)

Equation 6.4 can be written in terms of P_{ef1} and P_{ef2} as

$$\frac{P_{ef1}}{P_{ef2}} = \frac{l_1 D_2}{l_2 D_1} \left(\frac{v_1}{v_2}\right)^2$$
(6.5)

The variable D_1 and D_2 are calculated from the following formula (TET, 2012):

$$v_i = \frac{q_i}{A_i} \tag{6.6}$$

where q_i is the air flow (m³/s), and $A_i = \pi \left(\frac{D_i}{2}\right)^2$ is the area of the pipe (m²).

Assuming a constant flow, the following expression can be obtained from the above equation,

$$D_1 = \frac{4}{\pi} \sqrt{\frac{1}{v_1}}$$
 and $D_2 = \frac{4}{\pi} \sqrt{\frac{1}{v_2}}$

After substitution the values of D_1 and D_2 in Equation 6.5, the equation becomes

$$\frac{P_{ef1}}{P_{ef2}} = \frac{6}{48} \left(\frac{v_1}{v_2}\right)^{\frac{1}{2}} \left(\frac{v_1}{v_2}\right)^2$$
(6.7)

After substituting the values of V_1 and V_2 in Equation 6.7,

$$P_{ef2} = 153.85 \times P_{ef1}$$

It is found that the effective fan power, P_{ef2} is 153.85 times greater than P_{ef1} . This is equal to $8 \times 153.85 = 1230.77$ W. Therefore, a 1230.77W fan is required to generate 1.5 m/s air velocity at the pipe inlet for the length of 48.0 m pipe. Since the 48.0 m long pipe provides the lowest temperature at the pipe outlet, this pipe has been considered for the next parametric study to continue the analysis, although it is expensive to operate a 1230.77W fan in the earth pipe cooling system.

6.4. Pipe Diameter and Thickness

The third parametric study investigates the influence of different pipe size in terms of pipe diameter and thickness on the earth pipe cooling performance. Each pipe size has its own diameter, area and thickness as shown in Table 6.2. The most efficient dimensions from the previous investigations such as 1.5 m/s air velocity and 48.0m pipe length have been used in this study. The other variables, such as PVC pipe material and 1.1 m pipe depth, remain as constants.

Table 6.2: Different pipe sizes in terms of pipe diameter, area and thickness.

Pipe size	Pipe size-1		Pipe size -2		Pipe size -3		Pipe size -4	
	Manifold	Buried	Manifold	Buried	Manifold	Buried	Manifold	Buried
	(inlet)		(inlet)		(inlet)		(inlet)	
Diameter	0.062	0.01	0.125	0.02	0.200	0.040	0.400	0.08
(m)								
Inlet Area	0.003	0.0001	0.012	0.0003	0.031	0.001	0.126	0.005
(m ²)								
Thickness	0.003	0.002	0.004	0.002	0.008	0.003	0.012	0.005
(m)								

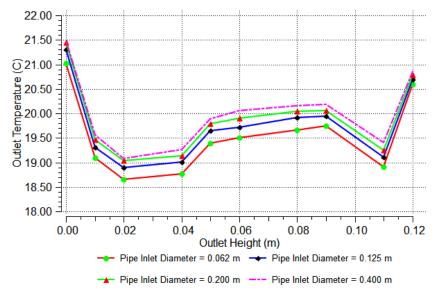


Figure 6.3: Parametric study for different pipe sizes.

Figure 6.3 shows the pipe outlet temperature profile along the height for various pipe diameters. As seen, the pipe outlet temperature increases with the increasing pipe inlet diameter. The outlet temperature varies from 18.65°C to 21.02°C for a 0.062 m

pipe inlet diameter. For an increased pipe inlet diameter of 0.125 m, the outlet temperature increases and varies from 18.90°C to 21.3°C. When the pipe diameter is increased further to 0.20 m, the outlet temperature is also increased and varies from 19.03°C to 21.45°C. The same result is also found for the inlet diameter of 0.40 m, where the outlet temperature ranges from 19.08°C to 21.49°C. The outlet temperature using a 0.062 m pipe inlet diameter provides the lower outlet temperature than that for the other pipe diameters used in this study. These results demonstrate that smaller diameters pipe can produce a better cooling effect.

In the case of small pipe diameter, air stays in the centre of the pipe, gets closer to the surrounding soil, the transfer of heat energy flows quickly, allowing more heat transfer to the soil and therefore the temperature gets close to the surrounding soil temperature. Another rationale behind this is the impact of the pipe thickness. PVC pipes come with the standard pipe sizes and thickness as the smaller pipes have less thickness. The 0.062 m pipe diameter has the lowest thickness of 3 mm (0.003m), which enables it to transfer more heat to the soil quickly. Therefore, this pipe size provides an efficient result for the earth pipe cooling system.

6.5. Pipe Material

The thermal performance of the earth pipe cooling system has been assessed for different pipe materials. PVC, polyethylene, concrete and clay were taken into account for this parametric study (Figure 6.4). The other parameters, air velocity (= 1.5 m/s), pipe length (= 48.0 m), pipe diameter and thickness (= 0.062 m and 0.003 m), and pipe depth were kept constant.

Typically, the performance of the earth pipe cooling depends on the thermal conductivity of the particular material. The higher the thermal conductivity, the more is the heat transfer. The pipes with different materials that are widely used for the earth pipe cooling system were considered. The thermal conductivity of each of the pipe materials considered in this study is summarised in Table 6.3.

Table 6.3: Thermal conductivity of different pipe materials.

Material	PVC	Polyethylene	Concrete	Clay
Thermal Conductivity, W/(m K)	0.19	0.42	0.70	1.80

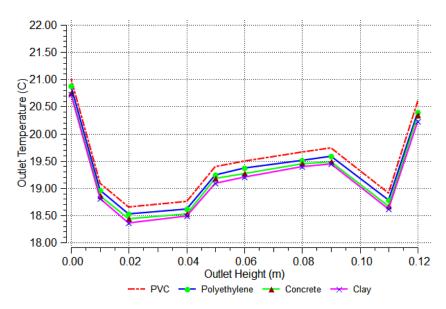


Figure 6.4: Parametric study for various pipe materials.

Table 6.3 shows the temperature profile for the different pipe materials of PVC, polyethylene, concrete and clay at different heights of the pipe outlet. The PVC pipe generates higher outlet temperature that ranges from 18.65°C to 21.02°C, which is greater than that for the other materials as shown in Table 6.4. The PVC pipe has the lowest thermal conductivity than the other materials while the pipe of clay material has the highest. Therefore the clay pipe produces the lowest average outlet temperature of 19.29°C as shown in Table 6.3 and therefore clay has been considered here. Similar result was observed in other studies, for example in the study by Sanusi (2012). The materials with high thermal conductivity assist in transferring more heat from the air inside the buried pipe to the soil, while the materials with low thermal conductivity transfer less heat. Therefore, the high thermal conductivity materials are seen as suitable for achieving an effective heat transfer (Chung, 2001).

Pipe Material	Outlet Temperature (°C)				
	Min	Max	Avg		
PVC	18.65	21.02	19.53		
Polyethylene	18.53	20.87	19.38		
Concrete	18.43	20.75	19.29		
Clay	18.36	20.72	19.23		

Table 6.4: Outlet temperature ranges for various materials.

Although it suggests that the pipe materials of high thermal conductivity can give more cooling effect, those have not been considered in this study as they are too expensive and not commonly used. Hence the cheaper pipe materials of PVC, polyethylene, concrete and clay have been considered. Furthermore, these four materials were used by other researchers as indicated before.

6.6. Pipe Depth

This study investigates the thermal performance of the earth pipe cooling system at different pipe depths. The buried pipe depths of 1.1 m, 2.0 m, 4.0 m and 8.0 m have been considered for this parametric study (Figure 6.5). The other parameters such as air velocity (1.5 m/s), pipe length (48.0 m), pipe diameter and thickness (0.062 m and 0.003 m), and pipe material (clay) were kept constant.

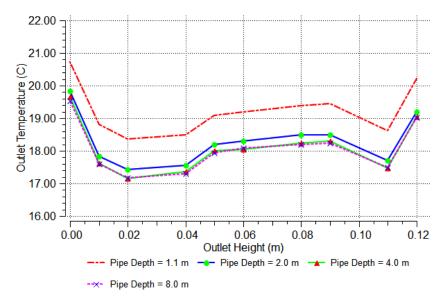


Figure 6.5: Parametric study for different depths.

The outlet temperature ranges from 18.36°C to 20.72°C for the buried pipe at a depth of 1.1 m as shown in Figure 6.5. When the depth of the buried pipes is increased to 2.0 m, the pipe outlet temperature is decreased and varies from 17.42°C to 19.82°C. For the depth of 4.0 m, the outlet temperature is decreased again and it ranges from 17.15°C to 19.65°C. The lowest average outlet temperature of 18.06°C was found at 8.0 m depth, which varies from 17.18°C to 19.65°C. The results show that the outlet temperature decreases with increasing depth, where 8.0 m pipe depth predicts to provide the best result. The outlet temperature relies on the soil temperature, and the

soil temperature is reduced with the increasing depths. Moreover, the outlet temperature range at the depths of 4.0 m and 8.0 m are nearly the same as the soil temperature is fairly constant and stable at 4.0 m depth (Santamouris et al., 1995). Furthermore, the laying of pipes at such depths can be expensive and operationally cumbersome.

6.7. Conclusion

The impact of the parameters affecting the earth pipe cooling performance was investigated by a parametric analysis using simulation in ANSYS Fluent. Air velocity flowing through the buried pipe, pipe length, pipe diameter and thickness, pipe material and pipe depth were taken into account for the parametric analysis. The vertical earth pipe cooling system was selected for the parametric analysis as it showed better performance in this study than the horizontal earth pipe cooling system.

The first parametric study was conducted for different air velocities of 0.46 m/s, 1.0 m/s, 1.5 m/s and 5.0 m/s, where other variables such as pipe length, pipe diameter and thickness, pipe material, and pipe depth were kept constant. The air velocity of 1.5 m/s showed the better performance than that for other velocities. The second study analysed the impact of different pipe lengths of 6.0m, 12.0m, 24.0m and 48.0m. The 48m long buried pipe provided the maximum performance for the inlet velocity of 1.5 m/s, while a smaller pipe length showed inferior performance. The effects of different pipe diameters (0.062 m, 0.125m, 0.200 m, and 0.400m) with different pipe thickness (0.01 m, 0.02 m, 0.04 m and 0.08 m) were investigated in the third parametric study. The smaller pipe diameter with smaller thickness showed the maximum performance.

Different pipe materials of PVC, polyethylene, concrete and clay were used in the fourth parametric study. It was found that the materials with high thermal conductivity provide better cooling performance. The last parametric study examined the impact of various pipe depths of 1.1 m, 2.0 m, 4.0 m and 8.0 m. The study illustrated that the deeper pipe depths provide more cooling effect and hence better performance. The parametric analysis with ANSYS Fluent showed a significant

effect of air velocity, pipe length and pipe diameter. However, the influence of the pipe length on the earth pipe cooling performance was more dominant among all the parameters.

Before undertaking the parametric analysis, the average pipe outlet temperature of the vertical earth pipe cooling was found as 21.53°C. The parametric analysis reduced this outlet temperature to 18.06°C, which is 3.50°C lower than the previous result. Although the parameters of 1.5 m/s air velocity, 48.0 m pipe length, 0.062 m pipe diameter, 0.003 m pipe thickness, clay pipe material, and 8.0 m depth are the most suitable, an optimum length and air velocity are required to be adopted for optimal performance in terms of energy savings.

CHAPTER 7 : CONCLUSIONS AND RECOMMENDATIONS

7.1. Major Findings and Conclusions

Thermal performance of a horizontal and a vertical earth pipe cooling system was evaluated in summer in a hot and humid subtropical climate, Rockhampton, Australia. The earth pipe cooling performance was measured in terms of room temperature reduction and its energy efficiency. The horizontal earth pipe cooling (HEPC) study showed an average temperature reduction of 1.13° C in a $27.23m^{3}$ room. This was achieved for 3.08° C temperature reduction at the pipe outlet. It was observed that the outlet temperature reduction can be increased to $5.45 \,^{\circ}$ C during the hot peak hours of the day from around 10:00 am to 5 pm, and hence more room temperature reduction can be achieved.

The room temperature reduction using the HEPC system contributed to a maximum energy savings of 420.49 kW in 3 months of summer 2013-2014, while the average was 60.57 kW. This converts to a maximum cost savings of 210.87 (7.23%), whereas the average cost savings was 122.82 (4.02%). This energy cost savings assists to return the initial investment cost in 4.59 years using the HEPC system.

In the vertical earth pipe cooling (VEPC) study, a temperature reduction of 1.87°C was found in the 27.23m³ room, where the reduction at the pipe outlet was 4.89°C. The outlet temperature reduction was increased to 9.98°C during the hot warming hours (10:00am - 5:00 pm). The room temperature reduction assisted to reduce the air conditioning load, and saved energy of 685.03 kW as a maximum and 84.73 kW as an average during the summer 2014-2015 from 1 December 2014 to 18 February 2015. This translates to a maximum savings of \$275.58 (8.51%) using this system, while the average savings was \$131.84 (5.91%) during this period. The maximum rate of return was calculated for the VEPC system as 4.27 years.

To justify the earth pipe cooling measurements, numerical investigations were made for both the HEPC and VEPC system by a 2D (two dimensional) thermal integrated model using the simulation program ANSYS Fluent. For simplicity, the integrated model was divided into two parts, one comprising all the pipes considered as the earth pipe model, and the other including the room only considered as the room model. The Realisable $k - \varepsilon$ model was used for developing the model. The numerical results obtained from the simulations were compared with the experimental results. The overall simulated results were in very good agreement with the corresponding experiments, and lie within 0.37%-5.30% and 0.46%-8.25% variation in the HEPC and VEPC system respectively.

In the numerical study of the HEPC system, an average outlet temperature of 22.65°C was found for the pipe model, which shows a good agreement with the measured average outlet temperature of 23.08°C. On the other hand, 24.74°C was calculated as an average temperature in the HEPC room using the simulation, while average room temperature of 24.64°C was observed through the experiment. These results show a 1.90% and 0.41% difference with the average temperature of the pipe model and the room model respectively.

The numerical results for the VEPC system provided an average outlet temperature of 21.85°C for the pipe model, which is consistent with the measured outlet temperature of 22.41°C. In the case of the room model, the simulation showed 23.43°C as an average room temperature, while the experimental results provided 23.92°C room temperature. These results give 2.5% and 2.05% variation with the average temperature for the pipe model and the room model respectively.

A parametric study was carried out in ANSYS Fluent to optimise the earth pipe cooling system, and to analyse the effect of the parameters that affect the earth pipe cooling performance. The vertical earth pipe cooling system was considered for the parametric analysis as it was found to be a better performing system compared to the horizontal earth pipe cooling system. Since the parameters, namely air velocity, pipe length, pipe diameter and thickness, pipe material, and pipe depth affect the earth pipe cooling performance, these parameters were considered for the parametric study. The parametric study shows that the length of the buried pipe has greater influence on the earth pipe cooling performance whereas the pipe material has the least impact. The best value of the parameters was calculated as 1.5 m/s air velocity, 48.0 m pipe length, 0.062 m pipe diameter, 0.003 m pipe thickness, clay pipe material, and 8.0 m depth. However, as found in the parametric study of the pipe length, a 1230.77 W powered fan is required for a 48.0 m long pipe to suck 1.5 m/s air velocity from the pipe inlet. This is not practical to use as the fan requires more energy for 48.0 m long buried pipe. Considering this, 12.0 m or 24.0 m pipe length can be considered for minimising the overall cost of the earth pipe cooling system.

The parametric analysis showed a 3.50°C reduction at the pipe outlet of the vertical earth pipe cooling system, which would reduce the room temperature of the earth pipe cooling system. In view of these findings, it can be concluded that the earth pipe cooling technique assists in saving energy in buildings, and has less negative and environmental effects compared to other existing techniques. It can significantly reduce the air-conditioning load of many buildings while producing virtually no greenhouse gas emissions. The findings of this study provide useful information for developing guidelines for use by the regulators, manufacturers and inhabitants for the deployment of passive cooling techniques in hot humid climates.

7.2. Recommendations

As this study deals with the thermal performance of the earth pipe cooling system, the following recommendations can be made for further enhancement of the passive cooling performance based on this study:

- Although some bioclimatic charts exist that indicate a few appropriate passive cooling techniques for particular locations, there is a need to develop a universal bioclimatic chart showing all existing and common passive cooling techniques. Using the universal bioclimatic chart, the building occupants would be able to choose a suitable technique for their local climate. Further study is needed to develop a universal chart.
- A combination of natural building materials such as timber, stone, rammed earth, dressed climate sheets, pigmented or natural cement render, etc. and the creative use of contemporary materials such as aluminium, steel, glass, and

metal profiles are to be encouraged. These materials supplement the overall vision for the domain by enabling fascinating and contemporary varieties in each building's character.

- Coloured and painted rendered surfaces of natural materials with metal varnishes are also encouraged. At the same time, work is still needed to select the full gamut of such high-potential resources and produce them for more extensive commercial use.
- Quantitative planting standards should be established in the earth pipe cooling systems, which will assist in optimising the vegetation cooling effect, particularly when applied in conjunction with conventional insulation and shading devices. Care should be taken with the use of vegetation to ensure the balancing of advantages from the reduction in temperature with the potentially deleterious effects from high humidity resulting from the evapotranspiration process. Optimisation of native plant usage should also be investigated.
- The parametric study carried out in this study shows that 8.0 m buried pipe depth provides the best performance rather than 1.1 m, 2.0 m and 4.0 m. The published literature suggests that the soil temperatures are fairly constant and stable at 4.0 m or deeper. Therefore, the 4.0 m pipe depth can be considered instead of 8.0 m to minimise the excavation and installation cost.
- Vent size and the distance between inlets and outlets should be optimised to improve the heat removal capability of earth pipe cooling systems. The heat removal process could be improved by precooling incoming air using low energy earth pipe cooling techniques.
- Further study should be carried out on the earth pipe cooling system in combination with various hybrid systems like green roof technology to increase the performance and efficiency of the system.

References

- ABSA 2010, Association of Building Sustainability Assessors. Complete House Plans, Energy Efficient Homes [cited on 16 April 2014]. Available from: <http://www.completehouseplans.com.au/sustainable.html> [Online].
- AG 2013, Australian Government. Australian weather and seasons a variety of climates [cited on 16 march 2015]. Available from: <http://www.australia.gov.au/about-australia/australian-story/austnweather-and-the-seasons> [Online].
- AHMED, A, KENNETH, I, MILLER, A & GIDADO, K 2009, Thermal performance of earth–air heat exchanger for reducing cooling energy demand of office buildings in the United Kingdom, *11th Conference of international building performance simulation association*, 2228-2235.
- AHMED, SF, KHAN, MMK, AMANULLAH, MTO & RASUL, MG 2014, Selection of suitable passive cooling strategy for a subtropical climate, *International Journal of Mechanical and Materials Engineering*, 9, 1-11.
- ANSYS 2006, FLUENT User's Guide [cited on 23 January 2015]. Available from: http://aerojet.engr.ucdavis.edu/fluenthelp/html/ug/node998.htm> [Online].
- ANSYS 2010, ANSYS FLUENT Theory Guide: Version 13.0, Ansys Inc., Canonsburg.
- ANTONOPOULOS, K & KORONAKI, E 2000, Thermal parameter components of building envelope, *Applied Thermal Engineering*, 20, 1193-1211.
- ANWAR, M, RASUL, M & KHAN, MMK 2013, Thermal Performance Analysis of Rooftop Greenery System in subtropical climate of Australia, 7th WSEAS International Conference on Renewable Energy Sources, 2-4.
- ASASUTJARIT, C, HIRUNLABH, J, KHEDARI, J, CHAROENVAI, S, ZEGHMATI, B & SHIN, UC 2007, Development of coconut coir-based lightweight cement board, *Construction and Building Materials*, 21, 277-288.

- ASHRAE 2004, Thermal environmental conditions for human occupancy, American Society of Heating, Refrigerating and Air-Conditioning Engineers, Standard 55-2004.
- ATG 2013, Australia Travel Guide. Map & Weather of Australia [cited on 16 March 2015]. Available from: ">http://www.finalword.com/map-weather-of-australia/.
- AYNSLEY, R 2007, Natural ventilation in passive design, *BEDP Environment* Design Guide Tec, 2.
- AZAD, AK, RASUL, MG, GIANNANGELO B & ISLAM R 2015, Comparative study of diesel engine performance and emission with soybean and waste oil biodiesel fuels, *International Journal of Automotive and Mechanical Engineering*, 12, 2866-2881.
- BAHADORI, MN 1985, An improved design of wind towers for natural ventilation and passive cooling, *Solar Energy*, 35, 119-129.
- BANKS, D 2012, An introduction to thermogeology: ground source heating and cooling, John Wiley & Sons.
- BANSAL, V, MISRA, R, AGRAWAL, GD & MATHUR, J 2010, Performance analysis of earth-pipe-air heat exchanger for summer cooling, *Energy and Buildings*, 42, 645-648.
- BAS 2014, Body and Soul. Why women feel the cold more than men [cited on 9 May 2014], Available from: <http://www.bodyandsoul.com.au/health/health+news/why+women+feel+the +cold+more+than+men,13259> [Online].
- BERGMAN, TL, INCROPERA, FP & LAVINE, AS 2011, Fundamentals of heat and mass transfer, John Wiley & Sons.
- BHATIA, A 2012, Alternatives to Active HVAC Systems [cited on 14 April 2014]. Available from: http://www.cedengineering.com/upload/Alternatives%20to%20Active%20 HVAC%20Systems.pdf>. [Online].

- BISONIYA, TS, KUMAR, A & BAREDAR, P 2013, Experimental and analytical studies of earth–air heat exchanger (EAHE) systems in India: a review, *Renewable and Sustainable Energy Reviews*, 19, 238-246.
- BLISS, RW 1959, The derivations of several "plate-efficiency factors" useful in the design of flat-plate solar heat collectors, *Solar Energy*, 3, 55-64.
- BOM 2014, Bureau of Meteorology. Rockhampton Weather [cited on 17 March 2015]. Available from: http://www.bom.gov.au/qld/rockhampton/ [Online].
- BOONMA, P, PHETHUAYLUK, S, WAEWSAK, J, KLOMPONG, N & SOMPECH, S 2005, Some physical properties of hollow concrete block mixed with oil palm fibers and bagass fibers, *Proceedings of the 1st Conference on Energy Network of Thailand, 2005 Chon Buri, Thailand.*
- BPEO 2012, BP energy outlook 2030. BP Statistical Review [cited on 12 March 2015]. Available from: http://www.old.cambridgeeprg.com/wp-content/uploads/2011/05/Keynote.pdf>.
- BRESCU 2000, Building Research Establishment, Sustainable Construction Unit. Energy consumption guide 19: Energy use in offices [cited on 27 February 2014]. Available from: < http://www.targ.co.uk/other/guide19.pdf>.
- BROWN, G 1985, Sun, wind, and light: Architectural design strategies, Canada, John Willey & Sons.
- BROWN, MJ 1990, Optimization of thermal mass in commercial building applications, *Journal of solar energy engineering*, 112, 273-279.
- BRUEL & KJAER 1982, Technical Review No. 2, Thermal Comfort.
- BULIAN, F & GRAYSTONE, J 2009, Wood coatings: Theory and practice, Elsevier.
- BURCH, D, MALCOLM, S & DAVIS, K 1984, The effects of wall mass on the summer space cooling of six test buildings, *ASHRAE transactions*, 90, 5-21.
- CÂNDIDO, C, DE DEAR, R, LAMBERTS, R & BITTENCOURT, L 2010, Air movement acceptability limits and thermal comfort in Brazil's hot humid climate zone, *Building and Environment*, 45, 222-229.

- CARSLAW, HS & JAEGER, JC 1959, Conduction of heat in solids, Oxford: Clarendon Press, 1959, 2nd ed., 1.
- CCA 2013, Climate Change Authority, Analysis of electricity consumption, electricity generation emissions intensity and economy-wide emissions [cited on 4 April 2014]. Available from: http://climatechangeauthority.gov.au/node/155>.
- CENGEL, YA, BOLES, MA & KANOĞLU, M 2002, *Thermodynamics: an engineering approach*, McGraw-Hill New York.
- CENGEL, YA, KLEIN, S & BECKMAN, W 1998, *Heat transfer: a practical approach*, WBC McGraw-Hill Boston.
- CHENVIDYAKARN, T 2007, Passive Design for Thermal Comfort in Hot Humid Climates, *Journal of Architectural/Planning Research and Studies*, 5, 3-27.
- CHUNG, D 2001, Materials for thermal conduction, *Applied Thermal Engineering*, 21, 1593-1605.
- CIBSE 2001, CIBSE Guide B: Heating, Ventilating, Air Conditioning and Refrigeration, *Chartered Institution of Building Services Engineers*.
- CIBSE, GA 2006, Environmental design, The Chartered Institution of Building Services Engineers, London.
- CINQUEMANI, V, OWENBY JR, J & BALDWIN, R 1978, *Input data for solar systems*, National Climatic Center, Asheville, NC (USA).
- CLARK, G & ALLEN, C 1978, The estimation of atmospheric radiation for clear and cloudy skies, *Proc. 2nd National Passive Solar Conference (AS/ISES)*, 675-678.
- CLEAR 2013, Comfortable Low Energy Architecture Factsheet: Climatic Design [Online].
- COOK, J 1989, Passive cooling, Arizona State Univ., Tempe, AZ (USA).
- COT 2014, Climate & Temperature. Rockhampton, Queensland climate and temperature [cited on 17 March 2015]. Available from: <http://www.rockhampton.climatemps.com/> [Online].

- COV 2009, City of Vancouver, Passive Design Toolkit [cited on 8 May 2014]. Available from: http://vancouver.ca/files/cov/passive-design-large-buildings.pdf>.
- CSIRO 2009, *The Science of tackling climate change* [cited on 2 April 2014]. Available from: <http://www.csiro.au/Outcomes/Climate/Understanding/Tackling-climatechange.aspx> [Online].
- DEWHA 2008, Department of the Environment, Water, Heritage and the Arts. *Energy use in the Australian residential sector 1986-2020* [cited on 4 April 2014]. Available from: <http://ee.ret.gov.au/sites/default/files/documents/04_2013/energy-useaustralian-residential-sector-1986-2020-part1.pdf>.
- DRET 2012, Department of Resources, Energy and Tourism, *Energy in Australia* [cited on 15 September 2014]. Available from: <http://www.industry.gov.au/industry/Office-of-the-Chief-Economist/Publications/Documents/energy-in-aust/energy-in-australia-2012.pdf>.
- DTI 2003, Department of Trade and Industry, Renewables innovation review [cited on 26 Febriary 2014]. Available from: <http://webarchive.nationalarchives.gov.uk/+/http://www.berr.gov.uk/files/fil e21955.pdf> [Online].
- DU 2011, Democratic Underground. They need something like wind towers to cool warehouses, [cited on 24 April 2014]. Available from: <http://www.democraticunderground.com/discuss/duboard.php?az=show_me sg&forum=102&topic_id=5050352&mesg_id=5050375>. [Online].
- ECEFAST 2015, Data Logger for Universal Thermocouple Types LU-BTM-4208SD [cited on 6 April 2015]. Available from: <http://www.ecefast.com.au/data-logger-for-universal-type-thermocoupleslu-btm-4208sd?industry=14> [Online].
- ECI 2008, European Copper Institute, Passive Home Training Module for Architects and Planners [cited on 13 May 2014]. Available from:

<http://www.slideshare.net/sustenergy/passive-home-training-module-forarchitects-and-planners> [Online].

- EE 2014, Ergon energy, General supply tariffs, Tariff 11 Residential [cited on 26 November 2014]. Available from: https://www.ergon.com.au/retail/residential/tariffs-and-prices/general-supply-tariffs> [Online].
- EIA 2013, Energy Information Administration. International Energy Outlook [cited on 25 March 2014]. Available from: http://www.eia.gov/forecasts/ieo/pdf/0484%282013%29.pdf>.
- EPA 2007, Environmental Protection Agency, Buildings and the environment: A statistical summary [cited on 26 February 2014]. Available from: http://www.epa.gov/greenbuilding/pubs/gbstats.pdf> [Online].
- ESCOMBE, AR, OESER, CC, GILMAN, RH, NAVINCOPA, M, TICONA, E, PAN, W, MARTÍNEZ, C, CHACALTANA, J, RODRÍGUEZ, R & MOORE, DA 2007, Natural ventilation for the prevention of airborne contagion, *PLoS medicine*, 4, e68.
- FANGER, PO 1970, Thermal comfort, Denmark, McGraw-Hill.
- FORD, B, SCHIANO-PHAN, R & ZHONGCHENG, D 2007, The Passivhaus standard in European warm climates: Design guidelines for comfortable low energy homes [cited on 13 May 2014]. Available from: http://www.passive-on.org/CD/1.%20Technical%20Guidelines/Part%203/Part%203.pdf>.
- GAMBOC, J 2012, Passive Cooling Techniques [cited on 24 April 2014]. Available from: http://www.academia.edu/6241302/Passive_Cooling_Techniques>.
- GARDE, F, MARA, T, LAURET, A, BOYER, H & CELAIRE, R 2001, Bringing simulation to implementation: presentation of a global approach in the design of passive solar buildings under humid tropical climates, *Solar Energy*, 71, 109-120.
- GEIGER, R, ARON, RH & TODHUNTER, P 2009, *The climate near the ground*, Rowman & Littlefield.

- GHOSAL, M & TIWARI, G 2006, Modeling and parametric studies for thermal performance of an earth to air heat exchanger integrated with a greenhouse, *Energy conversion and management*, 47, 1779-1798.
- GHOSAL, M, TIWARI, G & SRIVASTAVA, N 2004, Thermal modeling of a greenhouse with an integrated earth to air heat exchanger: an experimental validation, *Energy and Buildings*, 36, 219-227.
- GIVONI, B 1976, *Man, Climate and Architecture* (2nd edn.), London: Elsevier Science Ltd.
- GIVONI, B 1992, Comfort, climate analysis and building design guidelines, *Energy and buildings*, 18, 11-23.
- GIVONI, B 1994, *Passive low energy cooling of buildings*, Canada, John Willey & Sons.
- GIVONI, B 1998, *Climate considerations in building and urban design*, John Wiley & Sons.
- GIVONI, B 2007, Cooled soil as a cooling source for buildings, *Solar energy*, 81, 316-328.
- GIVONI, B & HOFFMAN, M 1968, Effect of building materials on internal temperatures.
- GOI 2010, Government of Ireland, Energy efficiency in traditional buildings [cited on 13 May 2014]. Available from:
 http://www.dublincity.ie/Planning/HeritageConservation/Conservation/Doc uments/Energy%20Efficiency%20in%20Traditional%20Buildings.pdf
 [Online].
- GÓMEZ, EV, MARTÍNEZ, F & GONZÁLEZ, AT 2010, The phenomenon of evaporative cooling from a humid surface as an alternative method for airconditioning, *International Journal of Energy & Environment*.
- GOSWAMI, D & BISELI, K 1993, Use of underground air tunnels for heating and cooling agricultural and residential buildings, Fact Sheet EES 78 [cited on 28 February, 2014]. Available from: < http://infohouse.p2ric.org/ref/08/07683.pdf>. *Fact Sheet EES*.

- GOSWAMI, D, SINHA, R & KLETT, D 1981, Theoretical and Experimental Analysis of Passive Cooling Using Underground Air Pipe, *Proceedings of ISES Meeting, Brighton, England.*
- HAN, J, ZHANG, G, ZHANG, Q, ZHANG, J, LIU, J, TIAN, L, ZHENG, C, HAO, J, LIN, J & LIU, Y 2007, Field study on occupants' thermal comfort and residential thermal environment in a hot-humid climate of China, *Building* and Environment, 42, 4043-4050.
- HANBY, VI, LOVEDAY, D & AL-AJMI, F 2005, The optimal design for a ground cooling tube in a hot, arid climate, *Building Services Engineering Research and Technology*, 26, 1-10.
- HEIMO STALLER, AT, IFZ 2010, New technical solutions for energy efficient buildings; [cited on 13 May 2014]. Available from: .
- IEA 2012, International Energy Agency 2012 [cited on 12 march 2015]. Available from: <http://www.iea.org/publications/freepublications/publication/IEA_Annual_ Report_publicversion.pdf>.
- JACOVIDES, C, MIHALAKAKOU, G, SANTAMOURIS, M & LEWIS, J 1996, On the ground temperature profile for passive cooling applications in buildings, *Solar energy*, 57, 167-175.
- JOHNSTON, S 2011, Using the Earth's Heat [cited 29 January 2014]. Available from: http://www.homepower.com/articles/home-efficiency/project-profiles/using-earths-heat. [Online].
- KHEDARI, J, SUTTISONK, B, PRATINTHONG, N & HIRUNLABH, J 2001, New lightweight composite construction materials with low thermal conductivity, *Cement and Concrete Composites*, 23, 65-70.
- KHEDARI, J, WATSANASATHAPORN, P & HIRUNLABH, J 2005, Development of fibre-based soil–cement block with low thermal conductivity, *Cement and Concrete Composites*, 27, 111-116.

- KHEDARI, J, YAMTRAIPAT, N, PRATINTONG, N & HIRUNLABH, J 2000, Thailand ventilation comfort chart, *Energy and Buildings*, 32, 245-249.
- KOENIGSBERGER, OH 1975, Manual Of Tropical Housing & Building, Orient Blackswan.
- KOTEY, N, WRIGHT, JL & COLLINS, M 2009a, Determining Off-Normal Solar Optical Properties of Drapery Fabrics, *ASHRAE Transactions*, 115.
- KOTEY, NA, WRIGHT, JL & COLLINS, MR 2009b, A Detailed Model to Determine the Effective Solar Optical Properties of Draperies, ASHRAE Transactions, 115.
- KOTEY, NA, WRIGHT, JL & COLLINS, MR 2009c, Determining Off-Normal Solar Optical Properties of Insect Screens, *ASHRAE Transactions*, 115.
- KOTEY, NA, WRIGHT, JL & COLLINS, MR 2009d, Determining Off-Normal Solar Optical Properties of Roller Blinds, *ASHRAE Transactions*, 115.
- KRARTI, M, CLARIDGE, D & KREIDER, J 1993, Energy Calculations for Basements, Slabs, and Crawl Space, *Final Report ASHRAE TC*, 4.
- KRARTI, M & KREIDER, JF 1996, Analytical model for heat transfer in an underground air tunnel, *Energy conversion and management*, 37, 1561-1574.
- KRARTI, M, LOPEZ-ALONZO, C, CLARIDGE, D & KREIDER, J 1995, Analytical model to predict annual soil surface temperature variation, *Journal* of Solar Energy Engineering, 117, 91-99.
- KREITH, F, MANGLIK, R & BOHN, M 2010, *Principles of heat transfer*, Cengage learning.
- KUSUDA, T & BEAN, J 1981, Comparison of calculated hourly cooling load and indoor temperature with measured data for a high mass building tested in an environmental chamber, *ASHRAE Transactions*, 87, 1232-1240.
- LA ROCHE, PM 2011, Carbon-neutral architectural design, CRC Press.
- LAOPANITCHAKUL, V, SUNAKORN, P & SRISUTAPAN 2007, A Climbingplants on solid wall reducing energy in tropical climate, *International Conference on Sustainable Building As Seoul.*

- LEAURUNGREONG, V 2004, Vetiver grass technology for architecture, Proceedings of the 1st Professional and Academic Collaborative Symposium, Bangkok.
- LEAURUNGREONG, V, ORANRATMANEE, R, SIHALARTH, P & INSISIENGMAY, S 2005, The local intelligence for a dwellings comfort living in Chiang Mai & Luang Prabang, *Journal of Energy Research*, 2, 17-38.
- LEE, KH & STRAND, RK 2008, The cooling and heating potential of an earth tube system in buildings, *Energy and Buildings*, 40, 486-494.
- LIN, T-P & MATZARAKIS, A 2008, Tourism climate and thermal comfort in Sun Moon Lake, Taiwan, *International Journal of Biometeorology*, 52, 281-290.
- LIPING, W & HIEN, WN 2007, The impacts of ventilation strategies and facade on indoor thermal environment for naturally ventilated residential buildings in Singapore, *Building and Environment*, 42, 4006-4015.
- LUTRON 2011, 12 channels TEMPERATURE RECORDER + SD Card data recorder [cited on 5 April 2015]. Available from: <http://www.lutron.com.tw/ugC_ShowroomItem_Detail.asp?hidKindID=3& hidTypeID=157&hidCatID=&hidShowID=1186&hidPrdType=&txtSrhData => [Online].
- LUXMOORE, DA, JAYASINGHE, M & MAHENDRAN, M 2005, Mitigating temperature increases in high lot density sub-tropical residential developments, *Energy and buildings*, 37, 1212-1224.
- MAJUMDAR, M 2001, Energy-efficient buildings in India, TERI Press.
- MALLICK, FH 1996, Thermal comfort and building design in the tropical climates, *Energy and buildings*, 23, 161-167.
- MANI, M & NAGARAJAN, G 2009, Influence of injection timing on performance, emission and combustion characteristics of a DI diesel engine running on waste plastic oil, *Energy*, 34, 1617-1623.
- MDH 2010, Minnesota Department of Health, Geothermal Heating and Cooling Systems [cited on 6 May 2014]. Available from: <http://www.health.state.mn.us/divs/eh/wells/geothermal.html> [Online].

- MENG, Q & ZHANG, L 2006, The rooftop shading system of the Humanities Building at SCUT, *Energy and buildings*, 38, 1356-1359.
- MICRODAQ 2015, Vane Anemometer Meter w/ SD Card Slot for Data Logging [cited on 5 April 2015]. Available from: <http://www.microdaq.com/reed/vane-anemometer-datalogger.php> [Online].
- MIHALAKAKOU, G, SANTAMOURIS, M, ASIMAKOPOULOS, D & PAPANIKOLAOU, N 1994, Impact of ground cover on the efficiencies of earth-to-air heat exchangers, *Applied Energy*, 48, 19-32.
- MIHALAKAKOU, G, SANTAMOURIS, M, ASIMAKOPOULOS, D & TSELEPIDAKI, I 1995, Parametric prediction of the buried pipes cooling potential for passive cooling applications, *Solar Energy*, 55, 163-173.
- MIHALAKAKOU, G, SANTAMOURIS, M, LEWIS, J & ASIMAKOPOULOS, D 1997, On the application of the energy balance equation to predict ground temperature profiles, *Solar Energy*, 60, 181-190.
- MINGOZZI, A & BOTTIGLIONI, S 2005, Logical use of traditional technologies for housing passive cooling in hot humid Italian climate areas, *Proceedings* of International Conference: Passive and Low Energy Cooling for the Built Environment. Santorini, Greece, 579-584.
- MOSTREL, M & GIVONI, B 1982, Windscreens in radiant cooling, *Passive Sol. J*, (United States), 1.
- NICOL, F 2004, Adaptive thermal comfort standards in the hot-humid tropics, Energy and Buildings, 36, 628-637.
- NYUK HIEN, W, PUAY YOK, T & YU, C 2007, Study of thermal performance of extensive rooftop greenery systems in the tropical climate, *Building and Environment*, 42, 25-54.
- OMER, A 2012, The Energy Crisis, the Role of Renewable and Global Warming Greener, *Journal of Environment Management and Public Safety*, 1, 38-70.
- OMER, AM 2008, Energy, environment and sustainable development, *Renewable and sustainable energy reviews*, 12, 2265-2300.

ONSET 2010, *HOBO® Pro v2 (U23-00x) Manual* [cited on 6 April 2015]. Available from: http://wpc.306e.edgecastcdn.net/80306E/onsetcomp_com/files/manual_pdfs

/10694-K-MAN-U23.pdf> [Online].

- ONSET 2015a, HOBO U10 Temperature Relative Humidity Data Logger U10-003 [cited on 3 April 2015]. Available from: <http://www.onetemp.com.au/p/1077/hobo-u10-temperature-relativehumidity-data-logger-u10-003> [Online].
- ONSET 2015b, HOBO U23 Pro v2 Temperature/Relative Humidity Data Logger -U23-001 [cited on 3 April 2015]. Available from: <http://www.onsetcomp.com/products/data-loggers/u23-001> [Online].
- ORIGIN 2013, *Heating and Cooling* [cited on 9 April, 2014]. Available from: http://www.originenergy.com.au/2673/Heating-and-cooling [Online].
- OVACEN 2014, The orientation energy certification or any project [cited on 13 May 2014]. Available from: http://ovacen.com/la-orientacion-en-la-certificacion-energetica/> [Online].
- PAKUNWORAKIJ, T, PUTHIPIROJ, P, OONJITTICHAI, W & TISAVIPAT, P 2006, Thermal resistance efficiency of building insulation material from agricultural waste, *Journal of Architectural/Planning Research and Studies*, 4, 2-13.
- PARKER, J 1983, The effectiveness of vegetation on residential cooling, *Passive Solar Journal*, 2, 123-132.
- PARKER, JH 1987, The use of shrubs in energy conservation plantings, *Landscape Journal*, 6, 132-139.
- PARKER, JH 1989, The impact of vegetation on air conditioning consumption, Conference on Controlling the Summer Heat Island, Berkeley.
- PASILO, A, HANCHAIYUNGWA, N & TEEBOONMA 2007, UA study of particle board properties manufactured from straw rise and rise husk, *Proceedings of the 3rd Conference on Energy Network of Thailand, Bangkok.*

PENMAN, HL 1963, Vegetation and hydrology, Soil Science, 96, 357.

- PFROMMER, P, LOMAS, K & KUPKE, C 1996, Solar radiation transport through slat-type blinds: a new model and its application for thermal simulation of buildings, *Solar Energy*, 57, 77-91.
- REEA 2012, Regional Energy and Environmental Agency, Cooling Demand management [cited on 15 April 2014]. Available from: http://raee.org/climatisationsolaire/gb/cooling.php. [Online].
- REYES, V, MOYA, S, MORALES, J & SIERRA-ESPINOSA, F 2013, A study of air flow and heat transfer in building-wind tower passive cooling systems applied to arid and semi-arid regions of Mexico. *Energy and Buildings*, 66, 211-221.
- ROSENBERG, M 2014, *Current World Population* [cited on 18 August, 2014]. Available from: <http://geography.about.com/od/obtainpopulationdata/a/worldpopulation.htm> [Online].
- ROSENFELD, J, PLATZER, W, VAN DIJK, H & MACCARI, A 2001, Modelling the optical and thermal properties of complex glazing: overview of recent developments, *Solar Energy*, 69, 1-13.
- RUUD, M, MITCHELL, J & KLEIN, S 1990, Use of building thermal mass to offset cooling loads, ASHRAE Transactions (American Society of Heating, Refrigerating and Air-Conditioning Engineers);(United States), 96.
- SADINENI, SB, MADALA, S & BOEHM, RF 2011, Passive building energy savings: A review of building envelope components, *Renewable and Sustainable Energy Reviews*, 15, 3617-3631.
- SAMUEL, D, NAGENDRA, S & MAIYA, M 2013, Passive alternatives to mechanical air conditioning of building: A review, *Building and Environment*.
- SANTAMOURIS, M 2007, Advances in passive cooling, Earthscan.
- SANTAMOURIS, M & ASIMAKOPOULOS, D 1996, *Passive cooling of buildings*, UK, James & James (Science Publishers) Ltd.
- SANTAMOURIS, M, MIHALAKAKOU, G, BALARAS, C, ARGIRIOU, A, ASIMAKOPOULOS, D & VALLINDRAS, M 1995, Use of buried pipes for

energy conservation in cooling of agricultural greenhouses, *Solar Energy*, 55, 111-124.

- SANUSI, ANZ 2012, Low Energy Ground Cooling System for Buildings in Hot and Humid Malaysia, PhD, De Montfort University.
- SAWHNEY, R, BUDDHI, D & THANU, N 1998, An experimental study of summer performance of a recirculation type underground airpipe air conditioning system, *Building and Environment*, 34, 189-196.
- SE 2013, Solar & Electrics, Global Scenario [cited on 31 August 2014]. Available from: http://solarpvworcester.co.uk/sample-page-2/global-scenario/. [Online].
- SHAHIDUZZAMAN, M 2012, Energy Consumption, Economic Growth and CO₂ Emissions in Australia: The Potential for Energy Conservation, PhD Thesis, University of Southern Queensland.
- SHAVIV, E, YEZIORO, A & CAPELUTO, IG 2001, Thermal mass and night ventilation as passive cooling design strategy, *Renewable Energy*, 24, 445-452.
- SODHA, M, BUDDHI, D & SAWHNEY, R 1991, Thermal performance of underground air pipe: different earth surface treatments, *Energy Conversion and Management*, 31, 95-104.
- SODHA, M, KAUR, J & SAWHNEY, R 1992, Effect of storage on thermal performance of a building, *International Journal of Energy Research*, 16, 697-707.
- SUPREME 2014, Elspec G4400 Blackbox Fixed Power Quality Analyzer [cited on 7 April 2015]. Available from: ">http://www.supremetechnology.com.au/product/elspec-g4400-blackbox-fixed-power-quality-analyzer.aspx?Id=23>">http://www.supremetechnology.com.au/product/elspec-g4400-blackbox-fixed-power-quality-analyzer.aspx?Id=23>">http://www.supremetechnology.com.au/product/elspec-g4400-blackbox-fixed-power-quality-analyzer.aspx?Id=23>">http://www.supremetechnology.com.au/product/elspec-g4400-blackbox-fixed-power-quality-analyzer.aspx?Id=23>">http://www.supremetechnology.com.au/product/elspec-g4400-blackbox-fixed-power-quality-analyzer.aspx?Id=23>">http://www.supremetechnology.com.au/product/elspec-g4400-blackbox-fixed-power-quality-analyzer.aspx?Id=23>">http://www.supremetechnology.com.au/product/elspec-g4400-blackbox-fixed-power-quality-analyzer.aspx?Id=23>">http://www.supremetechnology.com.au/product/elspec-g4400-blackbox-fixed-power-quality-analyzer.aspx?Id=23>">http://www.supremetechnology.com.au/product/elspec-g4400-blackbox-fixed-power-quality-analyzer.aspx?Id=23>">http://www.supremetechnology.com.au/product/elspec-g4400-blackbox-fixed-power-quality-analyzer.aspx?Id=23>">http://www.supremetechnology.com.au/product/elspec-g4400-blackbox-fixed-power-quality-analyzer.aspx?Id=23>">http://www.supremetechnology.com.au/product/elspec-g4400-blackbox-fixed-power-quality-analyzer.aspx?Id=23>">http://www.supremetechnology.com.au/product/elspec-g4400-blackbox-fixed-power-quality-analyzer.aspx?Id=23>">http://www.supremetechnology.com.au/product/elspec-g4400-blackbox-fixed-power-quality-analyzer.aspx?Id=23>">http://www.supremetechnology.com.au/product/elspec-g4400-blackbox-fixed-power-quality-analyzer.aspx?Id=23>">http://www.supremetechnology.com.au/product/elspec-g4400-blackbox-fixed-power-quality-analyzer.aspx?Id=23>">http://www.supremetechnology.com.aspx?Id=23>""
- SZOKOLAY, SV 2008, Introduction to architectural science: the basis of sustainable design, Routledge.
- TAN, X-H, ZHU, D-S, ZHOU, G-Y & ZENG, L-D 2012, Experimental and numerical study of convective heat transfer and fluid flow in twisted oval tubes, *International Journal of Heat and Mass Transfer*, 55, 4701-4710.

- TANTASAVASDI, C 2002, CFD approach towards natural ventilation design: Guidelines for houses in Thailand, *Journal of Architectural Research and Studies*, 1, 45-63.
- TANTASAVASDI, C, JAREEMIT, D, SUWANCHAISKUL, A & NAKLADA, T 2007, Natural ventilation: Evaluation and design of houses in Thailand, 3rd Conference on Energy Network, Bangkok, Thailand.
- TANTASAVASDI, C, SREBRIC, J & CHEN, Q 2001, Natural ventilation design for houses in Thailand, *Energy and Buildings*, 33, 815-824.
- TET 2012, The Engineering Toolbox, Duct Velocity in Imperial Units [cited on 14 May 2015], available from: http://www.engineeringtoolbox.com/ductwork-equations-d_883.html [Online].
- THANU, N, SAWHNEY, R, KHARE, R & BUDDHI, D 2001, An experimental study of the thermal performance of an earth-air-pipe system in single pass mode, *Solar Energy*, 71, 353-364.
- THONGKAMSAMUT, C 2003, Development of walls from local materials for thermal comfort improvement: Case study of non air-conditioned schools in North-eastern Thailand, *Journal of the Faculty of Architecture*, 2, 39-48.
- UNEP 2009, Buildings and climate change: a summary for decision-makers, Sustainable Buildings and Climate Initiative [cited on 10 November 2014]. Available from : < http://www.unep.org/sbci/pdfs/SBCI-BCCSummary.pdf>.
- UOI 2014, University of Iowa, Acclimatization: Adjusting to the Temperature [cited on 9 May 2014]. Available from: <http://www.uihealthcare.org/2column.aspx?id=237259> [Online].
- VAN DIJK, D & GOULDING, J 1996, WIS Advanced Windows Information System: WIS Reference Manual, TNO Building and Construction Research, Delft.
- WEC 2009, World Energy Consumption 1990-2030, 2009 [cited on 4 April 2014]. Available from: http://rainforests.mongabay.com/energy/energy.html. [Online].

- WIKIPEDIA 2015, World Energy Consumption [cited on 13 March 2015]. Available from: http://en.wikipedia.org/wiki/World_energy_consumption#cite_note-BP-Review-2013-4>. [Online].
- WONG, NH, CHEN, Y, ONG, CL & SIA, A 2003, Investigation of thermal benefits of rooftop garden in the tropical environment, *Building and environment*, 38, 261-270.
- YAHODA, DS & WRIGHT, JL 2004, Methods for Calculating the Effective Longwave Radiative Properties of a Venetian Blind Layer, ASHRAE Transactions, 110.
- YAHODA, DS & WRIGHT, JL 2005, Methods for Calculating the Effective Solar-Optical Properties of a Venetian Blind Layer, *ASHRAE Transactions*, 111.
- YANG, L & LI, Y 2008, Cooling load reduction by using thermal mass and night ventilation. *energy and buildings*, 40, 2052-2058.
- YELLOWHOUSE 2013, *Principles of eco-design* [cited on 23 April 2014] Available from: http://www.theyellowhouse.org.uk/eco-prin/princip.html [Online].
- ZAKI, AK, AMJAD, A-M. & ALMSSAD, A 2007, Cooling by underground earth tubes, 2nd PALENC Conference and 28th AIVC Conference on Building Low Energy Cooling and Advanced Ventilation Technologies in the 21st Century, Crete island, Greece.

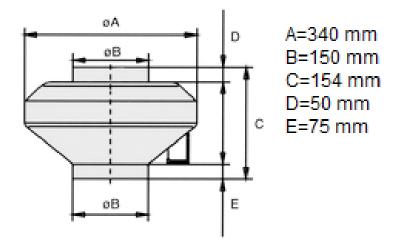
ZWILLINGER, D & KOKOSKA, S 1999, CRC standard probability and statistics tables and formulae, United States, Taylor & Francis Inc.

Appendices

Appendix 2.1: Clo-value of different clothing (Bruel and Kjaer, 1982).

Clothing	Clo-value	
Naked	0.0	
Briefs	0.06	
T-shirt	0.09	
Long underwear upper	0.35	
Long underwear lower	0.35	
Shirt: light, short sleeve (5% would be added for tie or	0.14	
turtleneck)		
Shirt: heavy, long sleeve (5% would be added for tie or	0.29	
turtleneck)		
Skirt	0.22-0.70	
Trousers	0.26-0.32	
Sweater	0.20-0.37	
Socks	0.04-0.10, 0.02-0.08	
Light summer outfit	0.3	
Working clothes	0.8	
Typical indoor winter clothing combination	1.0	
Heavy business suit	1.5	

Appendix 3.1: Dimensions of the fan used in this study (Vent-Axia of model MAN1503).



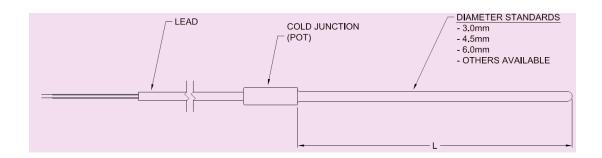
Operation range	Internal sensors: -40°-70°C (-40°- 158°F)
Accuracy	±0.2°C over 0°C-50°C (0.36°F over 32°-122°F)
Resolution	±0.02°C at 25°C (0.04°F at 77°F)
Response time	40 minutes in air moving 1 m/sec
Stability (drift)	< 0.1°C (0.18°F) per year
Operation range	0-100% RH, -40°-70°C (-40°-158°F)
Accuracy	±2.5% from 10 to 90% typical, to a maximum of
	±3.5%
Resolution	0.03%
Response time	40 minute in air moving 1 m/sec with protective cap
(typical to 90%)	
Stability (drift)	< 1% per year typical; hysteresis 1%
Operation range	-40°-70°C (-40°-158°F)
Real-time clock	± 1 minute per month 0°-50°C (32°-122°F)
Battery	1/2 AA, 3.6 Volt lithium, user-replaceable
Battery life	3 years
(typical use)	
Memory (non-	64 Kilobytes memory (approx. 21,000 temperature and
volatile)	RH measurements)
	Accuracy Resolution Response time Stability (drift) Operation range Accuracy Accuracy Resolution Resolution Resolution Resolution Stability (drift) Operation range Stability (drift) Operation range Real-time clock Battery Battery Battery Memory (non-

Appendix 3.2: Specifications of HOBO U23-001 Pro v2 (Onset, 2015b).

Appendix 3.3: Specifications of HOBO U10-003 (Onset, 2015a).

Measurement range	Temperature: -20°-70°C (-4°-158°F)				
	RH: 25%-95%				
Accuracy	Temperature: $\pm 0.4^{\circ}$ C over 0° - 40° C ($\pm 0.72^{\circ}$ F over 32° - 104° F),				
	RH: \pm 3.5% from 25% to 85% over the range of 15° to 45°C				
	(59° to 113°F), \pm 5% from 25% to 95% over the range of 5° to				
	55°C (41° to 131°F)				
Resolution	Temperature: $0.1^{\circ}C$ at $25^{\circ}C$ ($0.2^{\circ}F$ at $77^{\circ}F$)				
	RH: 0.07% @ 25°C and 30% RH				
Drift	Temperature: 0.1°C per year (0.2°F per year)				
	RH: <1% per year typical				
Response time in	Temperature: 10 minutes, typical to 90%				
airflow of 1 m/s (2.2	RH: 6 minutes, typical to 90%				
mph)					
Time accuracy	Approximately ± 1 minute per month at 25°C (77°F)				
Operating range	Logging: -20°-70°C (-4°-158°F); 0-95% RH (non-condensing)				
Battery life	1 year typical use				
Memory	64 Kilobytes (52,000 10-bit measurements)				
Dimensions	45 x 60 x 20 mm (1.8 x 2.38 x 0.77 inches)				

Appendix 3.4: Custom sized stainless steel tip probe.



Appendix 3.5: Mini plug connected to the thermocouple wire.



Appendix 3.6: Specification of the adapter connected with Lutron 12 channel thermometer (MicroDAQ, 2015):

- Input Voltage: 100-240 Volts AC; 50 Hz
- Output Voltage: 9 Volts DC/ 1 Amp Output
- Round Plug with 2.5 mm Diameter

Circuit	Custom	one-chip of microprocessor LSI circuit.	
Display	LCD size: 82 mm x 61 mm.		
Channels	12 channels : Type		
	T1, T2, T3, T4, T5, T6, T7, T8, T9, T10, T11 and T12.		
Sensor type	Type J/K/T/E/R/S thermocouple probe.		
Data logger	Auto	1 second to 3600 seconds	
sampling time		1 second can be set for sampling time, but there is a	
setting range		change to loss memory data.	
	Manual	One sample data will be saved once the data logger	
		button is pushed.	
Memory Card	SD card.	Memory: from 1 GB to 16 GB.	
Advanced	* Set clock time (Year/Month/Date, Hour/		
setting	Minute/	Second)	
	* Auto power OFF management		
	* Decimal point of SD card setting		
	* Set temperature unit to °C or °F		
	* Set beep Sound ON/OFF		
	* SD memory card Format		
	* Set sampling time		
Temperature	Automatic temperature compensation for the type K/J/T/E/R/S		
compensation	thermometer.		
Linear compensation	Linear Compensation for the full range.		
Offset adjustment	To adjust the zero temperature deviation value.		
Probe input socket	2 pin thermocouple socket.		
Data hold	Freeze the display reading.		
Memory recall	Minimum & Maximum value.		
Sampling time of	Approximate 1 second.		
display			
Data output	RS 232/U	USB PC computer interface.	

Appendix 3.7: Specification of Lutron 12 channel thermometer (Lutron, 2011).

Appendix 3.8: Specification of Reed Vane Anemometer (MicroDAQ, 2015).

Air velocity measurement using low friction ball vane wheels for better accuracy

Velocity and wind speed range from 0.4 to 30 m/s with $\pm 2\%$ accuracy

Recorded data saves to the SD card

Battery-powered data logging and AC/DC adapter can be powered for long time data logging

Backlight LCD display gives current, min and max readings as well as battery status

Sampling rate can be selected by the user from 1 second to 1 hour

Data logs directly to the SD card and software is not required

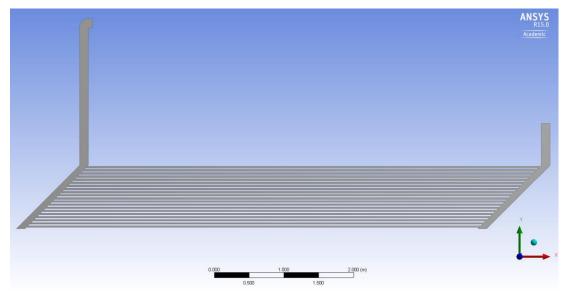
Includes vane sensor, hard carrying case and 4gb SD card

Type K or type J thermocouple probe is required

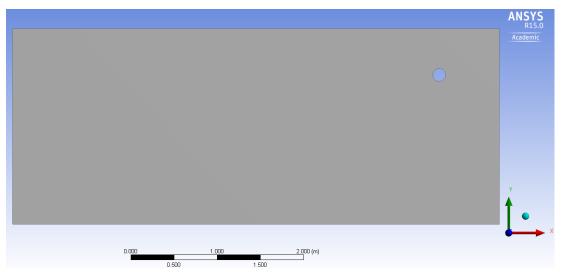
Power and Energy	Measurement Range Resolution		Accuracy
Active power	± 5kW x CT ratio x PT ratio	10 mW	± 0.2%
Reactive power	\pm 5kVAr x CT ratio x PT ratio	10 mVAr	± 2%
Apparent power	\pm 5kVA x CT ratio x PT ratio	10 mVA	± 0.2%
Active energy	± 5kW x CT ratio x PT ratio	10 mWh	$\pm 0.2\%$
Reactive energy	\pm 5kVArh x CT ratio x PT ratio	10 mVArh	± 2%
Apparent energy	± 5kVAh x CT ratio x PT ratio	10 mVAh	$\pm 0.2\%$

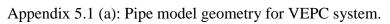
Appendix 3.9: Specifications of G4400 Blackbox power quality analyser.

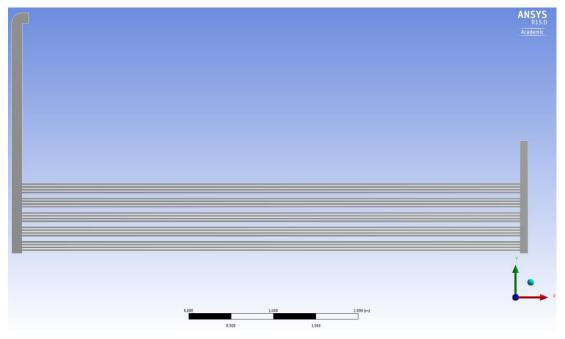
Appendix 4.1 (a): Pipe model geometry for HEPC system.



Appendix 4.1 (b): Room model geometry for HEPC system.







Appendix 5.1 (b): Room model geometry for VEPC system.

